~~~.	์ครงการวิจัยMR	05400007	F:1	D
ว.เถง.เห	ัผวงแบวเขาสถเทษเ	G5180227	Finai	Report

(รายงานในช่วงตั้งแต่วันที่	15 พ.ค. 2551	ถึงวันที่	14 พ.ค. 2553	)
โครงการ การศึกษ (String Theory)	¥าสมบัติของสสารนิวเคลียร์โดยการปร	ะยุกต์ใช้หลักค	าวามสมมูล AdS/CFT จากทฤษฎีสตริง	
	ปิยบุตร บุรีคำ	จุฬาลงกรณ์ม	มหาวิทยาลัย	
ดร. อภิ	เิสิทธิ์ อึ้งกิจจานุกิจ	จุฬาลงกรณ์ม	งหาวิทยาลัย	

สนับสนุนโดยสำนักงานคณะกรรมการการอุดมศึกษา และสำนักงานกองทุนสนับสนุนการวิจัย

เราศึกษาสมบัติของสสารหิวเคลียร์โดยใช้ความสมมูล AdS/CFT เราเสหอโครงรูปสตริงอันชัดเจนของ สถานะมัลติควาร์กในควาร์กกลูออนพลาสม่าเมื่อกลูออนเป็นอิสระแต่สมมาตรไครัลยังคงสลายอยู่ แม้ว่าสสารค วาร์กอิสระจะไม่เสถียรเชิงความร้อนแต่สสารแบบมัลติควาร์กซึ่งเกิดจากการแลกเปลี่ยนกลูออนระหว่างควาร์ก อิสระจะมีเสถียรภาพเชิงความร้อนหช่วงอุณหภูมิปานกลางและความหนาแน่นสูงมากพอ นี่หมายความว่า สถานะมัลติควาร์กนิวเคลียร์มีเสถียรภาพเชิงความร้อนมากกว่าสถานะนิวเคลียร์อื่น ๆเมื่อความหนาแน่นสูง ๆ มากพอ จากนั้นสมบัติเชิงแม่เหล็กของสถานมัลติควาร์กนิวเคลียร์จึงถูกศึกษา เราพบว่าสนามแม่เหล็กภายนอก ความแรงสูงจะทำให้โครงรูปมัลติควาร์กสองรูปแบบมีเสถียรภาพขึ้นได้ มัลติควาร์กหนึ่งในสองโครงรูปนี้ไม่มี ้ เสถียรภาพในกรณีที่ไม่มีสนามแม่เหล็ก สนามความแรงสูงและอุณหภูมิสูง ๆทำให้โครงรูปทั้งสองแบบลู่เข้าหากัน ้ เมื่อถึงสนามหรืออุณหภูมิค่าวิกฤตที่มัลติควาร์กทั้งสองผสานเป็นโครงรูปเดียวกัน มัลติควาร์กก็จะกลายเป็นไม่ เสถียร เมื่อความหนาแน่นถูกกำหนดให้คงที่ มัลติควาร์กจะเปลี่ยนไปมัลติควาร์กที่มีประจุเชิงรงค์ต่ำลงหรือ ละลายไปในควาร์กกลูออนพลาสม่าที่สมมาตรไครัลถูกอนุรักษ์คืนมา สถานะทางนิวเคลียร์อื่น ๆภายใต้ สนามแม่เหล็กถูกพิจารณาศึกษาในกรณีทั่วไปที่สุดของแบบจำลองแบบซาไกกับซึกิโมโตะ ในช่วงอุณหภูมิปาน กลาง สถานะมัลติควาร์กภายใต้สนามแม่เหล็กจะมีเสถียรภาพเชิงความร้อนมากกว่าสถานะอื่น ๆ เช่น สถานะพื้น ภายใต้สนามแม่เหล็ก สถานะไพออนเกรเดี่ยน และสถานะควาร์กกลูออนพลาสม่าภายใต้สนามแม่เหล็กที่ สมมาตรไครัลอนุรักษ์ หากความหนาแน่นสูงมากพอและสนามแม่เหล็กไม่แรงจนเกินไป สุดท้าย เราพิจารณา สมบัติเชิงความร้อนของสถานะมัลติควาร์กหิวเคลียร์และผลกระทบของมันต่อฟิสิกส์ของดาวอุ่นเล็ก ๆความ หนาแน่นสูง ๆ การศึกษาเชิงตัวเลขแสดงให้เห็นว่าอัตราเร็วเสียงในสสารมัลติควาร์กนิวเคลียร์มีค่าต่ำกว่า อัตราเร็วแสงในสุญญากาศและดังนั้นมันจึงสามารถถูกกดอัดได้แม้แต่ที่สภาวะความหนาแน่นสูง ๆเช่นนั้น

We study the properties of nuclear matter using the AdS/CFT correspondence. We propose rigorous string configurations of the multiquark states in the quark-gluon plasma when the gluons are deconfined but the chiral symmetry is still broken. Even though the pure quark matter is unstable thermodynamically, the multiquark matter resulted from the gluon exchanges between quarks are thermodynamically stable for intermediate temperatures and sufficiently large densities. This implies that the multiquark nuclear phase is thermodynamically preferred over other phases provided that the density is sufficiently large. The magnetic properties of the multiquark nuclear phase are then investigated. We found that the strong external magnetic fields stabilize two possible multiquark configurations. One of the configurations was unstable in the zero field situation. Strong field and large temperature converge the two configurations together. Around the critical field or temperature where the two configurations merge, the multiquarks become unstable. At a fixed density, the multiquarks either change into multiquarks with smaller colour charges or melt away into the chiral-symmetric quark-gluon plasma phase (QGP). The other

possible magnetic nuclear phases are explored in the most general case of Sakai-Sugimoto model. In the intermediate range of temperature, the magnetized multiquark phase is thermodynamically preferred over other phases such as the magnetized vacuum, the pion-gradient phase, and the magnetized chiral-symmetric QGP, provided that the density is sufficiently high and the magnetic field is not too strong.

Lastly, we consider the thermodynamical properties of the multiquark nuclear phase and its implications to the physics of densed warm compact star. Numerical studies reveal that the sound speed within the multiquark nuclear matter does not exceed the speed of light in the vacuum and thus the multiquark matter is compressible even at extremely large nuclear densities.

## ข้อเสนอโครงการวิจัย (Executive Summary)

1. ชื่อโครงการ (ภาษาไทย) .....การศึกษาสมบัติของสสารหิวเคลียร์โดยการประยุกต์ใช้หลักความสมมูล
AdS/CFT จากทฤษฎีสตริง (String Theory)

(ภาษาอังกฤษ) ......Study of the properties of nuclear matter via the applications of

### AdS/CFT correspondence from string theory

#### 2. คณะนักวิจัย

#### 2.1. หัวหน้าโครงการ:

ชื่อ-สกุล ไทย: ปิยบุตร บุรีคำ

ชื่อ-สกุล อังกฤษ: Piyabut Burikham ตำแหน่งวิชาการปัจจุบัน: อาจารย์

สถานที่ทำงาน: ภาควิชาฟิสิกส์ คณะวิทยาศาสตร์ จุฬาลงกรณ์มหาวิทยาลัย กทม. 10330

โทรศัพท์: 02-2187550, email: piyabut@gmail.com

## ผู้ช่วยวิจัย (Research Assistant) ที่คาดไว้:

ชื่อ-สกุล ไทย: เอกพงษ์ หิรัญสิริสวัสดิ์

ชื่อ-สกุล อังกฤษ: Ekapong Hirunsirisawat

ตำแหน่งวิชาการปัจจุบัน: prospect graduate student

สถานที่ทำงาน: ภาควิชาฟิสิกส์ คณะวิทยาศาสตร์ จุฬาลงกรณ์มหาวิทยาลัย กทม. 10330

โทรศัพท์: 02-2187550, email: ekapong.hirun@gmail.com

## 2.2. เวลาที่ใช้ในโครงการวิจัย: 2 ปี

ความจำเป็นที่ต้องใช้ผู้ช่วยวิจัยและหน้าที่: การจ้างผู้ช่วยวิจัยเป็นสิ่งธรรมดาที่เห็นได้ทั่วไปในกลุ่มวิจัยที่มีผลงานวิจัย เป็นรูปธรรมเด่นชัด โดยเฉพาะในประเทศอย่างสหรัฐอเมริกา กลุ่มประเทศในยุโรป และ ญี่ปุ่น โดยจะทำการจ้างนักศึกษา หรือคนที่มีความสนใจและมีความสามารถในการวิจัยมาเข้าร่วม นักศึกษาที่ถูกว่าจ้างมาเป็นผู้ช่วยวิจัยก็มักจะเป็นนักศึกษา ปริญญาเอกในกลุ่มวิจัยที่มีความรู้ความสามารถเพียงพอต่อหัวข้อวิจัยที่จะทำ ในที่นี้ เอกพงษ์ หิรัญสิริสวัสดิ์ ซึ่งได้รับ ปริญญาโทสาขาฟิสิกส์ทฤษฎีจากกลุ่มวิจัยนี้ ได้เข้าร่วมศึกษาใน study group มาตั้งแต่ต้นและได้ช่วยทำการคำนวณได้ผล ลัพธ์เป็นที่น่าพอใจซึ่งทำให้เห็นได้ว่าผลที่ได้จากบางกลุ่มวิจัยในต่างประเทศที่ตีพิมพ์มาแล้วนั้นมีความผิดพลาด เขาจึงเป็น คนที่เหมาะสมที่สุดในการช่วยทำงานวิจัยชิ้นนี้

หน้าที่ของผู้ช่วยวิจัยรวมถึงการเตรียมคอมพิวเตอร์และโปรมแกรมที่ใช้คำนวณ การสืบค้น เอกสารอ้างอิงที่เกี่ยวข้อง การตรวจเช็คผลการคำนวณ การริเริ่มหัวข้อใหม่ ๆที่เกี่ยวข้องในงานวิจัย อีกทั้งยังรวมถึงการไป นำเสนอผลงานยังที่ประชุมวิชาการต่าง ๆ ในขณะที่กำลังเขียนเอกสารนี้ ผู้ช่วยวิจัยเอกพงษ์ก็มีกำหนดการไปเสนอผลงาน บางส่วนที่ Siam Physics Congress 2008 ที่จังหวัดนครราชสีมาอีกด้วย 3. **สาขาวิชาที่ทำการวิจัย:** การศึกษาสมบัติของสสารนิวเคลียร์โดยการประยุกต์ใช้หลักความสมมูล AdS/CFT จาก ทฤษฎีสตริง (String Theory)

## 4. ความสำคัญและที่มาของปัญหาที่ทำการวิจัย:

การประยุกต์ใช้ทฤษฎีสตริงในการศึกษาอันตรกิริยาอย่างเข้ม (strong interaction) เป็นพัฒนาการทางทฤษฎีที่น่า จับตามองที่สุดในวงการทฤษฎีฟิสิกส์ในปัจจุบัน เพราะอันตรกิริยาที่ควาร์ก และกลูออนยึดเหนี่ยวกันอยู่ในสสาร นิวเคลียร์ เช่น ฮาดรอน (hadron) และภายในแก่นกลางของดาวความหนาแน่นสูงอย่างดาวนิวตรอนหรือแม้กระทั่ง ภายในหลุมดำ เป็นอันตรกิริยาที่มีความแรงสูงมากจนกระทั่งการศึกษาโดยใช้กระบวนวิธีแบบ perturbation theory หรือ perturbative expansion ไม่มีความแน่นอนที่เชื่อถือได้ การศึกษาโดยใช้ทางเลือกทางทฤษฎีอื่น ๆจึงมีความสำคัญ และสามารถให้ผลที่มีประโยชน์ต่อความรู้ความเข้าใจของสสารนิวเคลียร์เหล่านี้อย่างมาก

ทางเลือกหนึ่งก็คือการใช้หลักความสมมูล AdS/CFT [1] ที่ได้จากทฤษฎีสตริง โดยใช้ความสมมูลระหว่างทฤษฎี อันตรกิริยาอย่างเข้มที่มีความแรงมากกับทฤษฎีสตริงในอวกาศโค้งแบบ Anti de Sitter (AdS) ที่มีความแรงน้อยซึ่งทำ ให้เราทำการใช้ perturbation theory คำนวณได้ เราสามารถคำนวณปริมาณหลาย ๆปริมาณที่บอกสมบัติทางฟิสิกส์ของ ควาร์ก-กลูออน พลาสม่า (quark-gluon plasma) เช่น ค่าความหนืด [2] ค่าความเร็วเสียง drag force [3,4]ที่ควาร์กรับรู้ ขณะวิ่งผ่านควาร์ก-กลูออน พลาสม่า ศักย์ (potential) ทางอันตรกิริยาอย่างเข้มที่ยึดเหนี่ยวควาร์กและกลูออนที่อยู่ในพลาสม่า [5,6,7] และ screening length [4,5,6,7]

ในแง่ของทางทฤษฎี การประยุกต์ใช้ทฤษฎีสตริงในการศึกษาทฤษฎีเกจ (gauge theory) ที่มีความแรงมากยัง นับเป็นพัฒนาการที่น่าตื่นตาตื่นใจ ในปัจจุบัน ความสัมพันธ์ระหว่างทฤษฎีเกจอย่างแรง (strongly coupled gauge theory) และทฤษฎีความโน้มถ่วงอย่างอ่อน (weakly coupled gravity) ที่ได้จากความสมมูลนี้ยังเป็นหัวข้อที่มีการศึกษา กันอย่างแพร่หลายและยังคงให้ผลที่ช่วยให้ความรู้ความเข้าใจของเราต่ออันตรกิริยาทั้งสองเพิ่มพูนขึ้นอย่างมากมาย นักฟิสิกส์ชั้นนำหลาย ๆคนเชื่อว่าความรู้ใหม่ ๆที่ได้จากความสมมูลนี้จะช่วยให้เราสร้างทฤษฎีควอนตัมความโน้มถ่วงที่ ถูกต้องได้ในอนาคต งานวิจัยในเรื่องนี้จึงเกี่ยวพันกับปัญหาที่ยิ่งใหญ่ที่สุดปัญหาหนึ่งในฟิสิกส์ นั่นก็คือการสร้างทฤษฎี ควอนตัมสนามความโน้มถ่วงที่ถูกต้องและปราศจากปริมาณอนันต์ (infinity)

# 5. วัตถุประสงค์ของโครงการ

- 1.) ประยุกต์ใช้ความสมมูล AdS/CFT ในการศึกษาสมบัติของควาร์ก-กลูออน พลาสม่าที่อุณหภูมิสูงกว่า 175 MeV ซึ่งเป็นอุณหภูมิการเปลี่ยนสถานะจากสภาพที่ควาร์กและกลูออนถูกกักขังในฮาดรอนไปสู่สถานะที่มันกลายเป็นพลาสม่าร้อนที่ควาร์กและกลูออนเป็นอิสระ ศึกษาปริมาณ transport coefficients ในพลาสม่านี้โดยใช้ dual string theory ในอวกาศโค้งชนิดต่างๆ
- 2.) ศึกษาสมบัติของสสารนิวเคลียร์ที่สภาวะสุดโต่งอื่นๆ เช่น เมื่อความหนาแน่นสูงมากๆ เช่น ภายในดาว นิวตรอนโดยใช้สมมูล AdS/CFT
- 3.) ศึกษาสมบัติของทฤษฎีเกจและทฤษฎีความโน้มถ่วงจากมุมมองของความสมมูล AdS/CFT ศึกษาอันตรกิริยา ใหม่ ๆที่อาจจะมีได้จากสมมูลของอันตรกิริยาของสตริงแบบเปิดและแบบปิด (open-closed string duality) [8]
  - 4.) ศึกษาสมบัติของโพเมอรอน (pomeron) [9,10]ในอันตรกิริยาแบบเข้มโดยใช้มุมมองของทฤษฎีสตริง

เปรียบเทียบผลกับผลที่ได้จากทฤษฎี S-matrix [11]และที่ได้จากการคำนวณใน Quantum Chromodynamics (QCD) [12]

# 6. ระเบียบวิธีวิจัย ให้แสดงการวางแผนการวิจัย และลำดับขั้นตอนการวิจัย (ถ้ามี)

- 1.) พิจารณาวัตถุทางคณิตศาสตร์ที่เรียกว่า baryon vertex [13]ของทฤษฎีสตริงในอวกาศโค้งแบบ Anti de Sitter และ แบบ Sakai-Sugimoto [14]ที่สมมูลกับฮาดรอน (hadronic bound state) ในทฤษฎีแบบเกจ คำนวณ Nambu-Goto action เพื่อศึกษาศักย์ระหว่างควาร์กเมื่อมันอยู่ในสถานะของควาร์ก-กลูออน พลาสม่าและดูว่ามีความเปลี่ยนแปลงไป ตามอุณหภูมิอย่างไร เปรียบเทียบความแตกต่างระหว่างแบบจำลองที่มาจาก dual string theory แบบต่างๆ ใช้การ คำนวณเชิงตัวเลข (numerical methods) ในการศึกษาเปรียบเทียบผลที่ได้จากการประมาณเชิง analytic ขยายผลไปสู่ กรณีที่ฮาดรอนมีโมเมนตัมเชิงมุมและเปรียบเทียบผลกับฮาดรอนที่อยู่ที่สถานะพื้นที่ไม่มีโมเมนตัมเชิงมุม ศึกษาการขึ้น ของศักย์ต่อมวลของฮาดรอนโดยใช้ asymptotic expansion ของศักย์
- 2.) ศึกษาปริมาณอื่นๆที่คำนวณได้จากสมมูล AdS/CFT เช่น ความหนืดและ transport coefficient ต่างๆของ สสารนิวเคลียร์ที่อุณหภูมิที่สูงมากๆเช่นที่ LHC หาลักษณะจำเพาะของสถานะทางนิวเคลียร์ที่จะยืนยันผลที่ทำนายได้ จากทฤษฎีสตริง เช่น การขึ้นกับอุณหภูมิของ jet quenching (การตรวจพบ jet ที่น้อยลงมากกว่าปกติ) และ charmonium suppression (การตรวจพบ charmonium ที่น้อยลงกว่าปกติ)
- 3.) ศึกษาฟิสิกส์ของควาร์ก-กลูออนพลาสม่าเมื่อความหนาแน่นของมันมีค่าสูงมาก ๆ เช่นในดาวนิวตรอนโดยการ คำนวณโดยใช้สมมูล AdS/CFT เปรียบเทียบผลกับที่ได้จากสมบัติที่ได้จากการสังเกตการณ์ของดาวนิวตรอน
- 4.) ใช้สมมูลของสตริงแบบเปิดและแบบปิดพิจารณาหาอันตรกิริยาแบบใหม่ที่เกิดจากการแลกเปลี่ยน open-string singlet ที่มีมวลซึ่ง dual ของมันคือ massive gravitons [10]ในมุมมองของทฤษฎีสตริงในอวกาศที่โค้งซึ่งนำไปบรรยาย โพเมอรอนในอันตรกิริยาอย่างเข้มได้ เราสามารถใช้ข้อมูลของ total cross section [15]และ diffractive scattering ใน การศึกษาฟิสิกส์ของโพเมอรอนและเปรียบเทียบกับที่บรรยายโดยอันตรกิริยาที่มาจาก open-string singlet

#### 7. ขอบเขตของการวิจัย

ศึกษาการประยุกต์ใช้ทฤษฎีสตริงต่อฟิสิกส์ของสสารนิวเคลียร์ เช่น ควาร์ก-กลูออน พลาสม่า และฟิสิกส์ ใหม่ ๆที่ได้จากสมมูล AdS/CFT ในทฤษฎีสตริง

# 8. การเชื่อมโยงกับนักวิจัยที่เป็นผู้เชี่ยวชาญในสาขาวิชาที่ทำการวิจัย

ดร. อรรถกฤต ฉัตรภูติ เป็นอาจารย์ที่กลุ่มวิจัยฟิสิกส์ทฤษฎีเกี่ยวกับฟิสิกส์พลังงานสูงและมีความรู้ความ เชี่ยวชาญเกี่ยวกับทฤษฎีสตริงและเอกภพวิทยาเป็นอย่างดี และยังมีความสนใจในการศึกษาการประยุกต์ใช้ ความ สมมูล AdS/CFT ในการศึกษาสมบัติของควาร์กและกลูออนในควาร์ก-กลูออน พลาสม่า รวมถึงคำทำนายของทฤษฎี สตริงในทางเอกภพวิทยาและสมบัติของสสารนิวเคลียร์ในยุคแรกเริ่มของเอกภพอีกด้วย

ในปัจจุบัน ตัวผู้เสนอโครงการ ดร. อรรถกฤต และ ดร. อภิสิทธ์ อึ้งกิจจานุกิจ ได้สร้างกลุ่มศึกษา (study

group) เกี่ยวกับเอกภพวิทยาและทฤษฎีฟิสิกส์พลังงานสูงขึ้นและมีการพบปะอภิปรายกันสัปดาห์ละสองครั้งเพื่อศึกษา และต่อยอดงานวิจัยที่น่าสนใจ กลุ่มศึกษาประกอบไปด้วยนักศึกษาที่สนใจที่จุฬาลงกรณ์มหาวิทยาลัยหลายคนและ อาจารย์บางท่านจากมหาวิทยาลัยอื่น อาทิเช่น อาจารย์กุลพันธ์ พิมพ์สมาน จากมหาวิทยาลัยเกษตรศาสตร์ ทุกคนมี ความเป็นไปได้ที่จะเข้าเป็นส่วนหนึ่งของงานวิจัยที่เสนอนี้

## 9. ผลงานวิจัยที่เกี่ยวข้อง (literature review) และเอกสารอ้างอิง

# ดูข้อ 4, 5, 6 สำหรับงานวิจัยที่เกี่ยวข้อง

อนึ่ง เกี่ยวกับความสัมพันธ์ของสมมูล AdS/CFT ต่ออวกาศที่มีมิติเพิ่มเติม (extra dimensions) แบบRandall-Sundrum [16] นั้นอยู่ที่การที่อวกาศส่วน Anti de Sitter (AdS) ใน 5 มิติที่อยู่ใน 10 มิติของทฤษฎีสตริงนั้น ถก

ใช้เป็นอวกาศที่บรรยายแบบจำลองที่ความโน้มถ่วงมีสเกลระดับ TeV (10³ GeV) ซึ่งต่ำกว่าแพลงค์สเกล (10¹⁹ GeV) ที่เป็น สเกลของความโน้มถ่วงในสี่มิติดั้งเดิมอยู่มาก ในแบบจำลองของเอกภพแบบมี extra dimensions พวกนี้ extra dimensions จะเป็นมิติทางกายภาพที่มีอยู่จริง ต่างกับการประยุกต์ใช้สมมูล AdS/CFT ในการศึกษาสมบัติของสสาร นิวเคลียร์ที่ไม่ได้สมมติการมีอยู่จริงของextra dimensions ในเอกภพของเรา เพียงแต่ใช้การคำนวณของทฤษฎีสตริงใน อวกาศ 10 มิติแบบ AdS₅xS⁵ เพื่อคำนวณปริมาณทางกายภาพบางปริมาณของสสารนิวเคลียร์ในทฤษฎีเกจอย่างแรงในสี่ มิติ ที่มีความสมมูลกับทฤษฎีสตริงในสิบมิตินี้

ดังนั้นจึงกล่าวได้ว่า การศึกษาสมมูล AdS/CFT เป็นแรงบันดาลใจให้มีการสร้างแบบจำลองเอกภพแบบมี extra dimensions เช่นแบบจำลองของ Randall และ Sundrum แต่ไม่ได้หมายความว่าการประยุกต์ใช้AdS/CFT ในด้าน ต่างๆรวมถึงการศึกษาสมบัติของสสารนิวเคลียร์จะต้องเกี่ยวข้องกับแบบจำลอง Randall-Sundrum แต่อย่างใด

# References: (ชื่อของนักวิจัยในวงการฟิสิกส์พลังงานสูงเรียงตามลำดับของตัวอักษรของนามสกุล*)

- 1. J. Maldacena, Adv. Theor. Math. Phys. 2, 231 (1998) [hep-th/9711200].
- P. Kovtun, D. T. Son, A. O. Starinets, *Phys. Rev. Lett.* 94, 111601 (2005) [hep-th/0405231];
   P. Kovtun, D. T. Son, A. O. Starinets, *Phys. Rev. Lett.* 87, 081601 (2001) [hep-th/0104066].
  - 3. Steven Gubser, Phys. Rev. D74, 126005 (2006) [hep-th/0605182].
  - 4. Piyabut Burikham and Jun Li, JHEP 03, 067 (2007) [hep-ph/0701259].
  - Soo-Jong Rey and Jung-Tay Yee, Eur. Phys. J. C22, 379 (2001) [hep-th/9803001]; J. Maldacena, Phys. Rev. Lett. 80, 4859 (1998) [hep-th/9803002].
  - 6. Soo-Jong Rey, S. Theisen, Jung-Tay Yee, Nucl. Phys. B527, 171 (1998) [hep-th/9803135].
  - 7. Oleg Antipin, Piyabut Burikham, Jun Li, JHEP 06, 046 (2007) [hep-ph/0703105].
  - 8. Piyabut Burikham, Int. J. Mod. Phys. A22, 29 (2007)
  - 9. C. Csaki, H. Ooguri, Y. Oz, J. Terning, JHEP 01, 017 (1999) [hep-th/9806021].
  - 10. R. C. Brower, J. Polchinski, M. J. Strassler, Chung-I Tan, [hep-th/0603115].

- 11. G. F. Chew and S. Frautschi, Phys. Rev. Letts. 7, 394 (1961).
- E. A. Kuraev, L. N. Lipatov, V. S. Fadin, Sov. Phys. JETP 45, 199-204 (1977); I. I. Balitsky and L. N. Lipatov, Sov. J. Nucl. Phys. 28, 822-829 (1978).
- Edward Witten, JHEP 07, 006 (1998) [hep-th/9805112]; D. Gross and H. Ooguri, Phys. Rev. D58, 106002 (1998) [hep-th/9805129].
- T. Sakai and S. Sugimoto, *Prog. Theo. Phys.* 113, 843 (2005) [hep-th/0412141]; T. Sakai and S. Sugimoto, *Prog. Theo. Phys.* 114, 1083 (2006) [hep-th/0507073.
- 15. A. Donnachie and P. V. Landshoff, *Phys. Lett.* **B296**, 227-232 (1992) [hep-ph/9209205].
- Lisa Randall and Raman Sundrum, Phys. Rev. Lett. 83,3370 (1999) [hep-ph/9905221]; Lisa Randall and Raman Sundrum, Phys. Rev. Lett. 83,4690 (1999) [hep-th/9906064].

## 10. อุปกรณ์ที่ใช้ในการวิจัย

- 10.1. เครื่องคอมพิวเตอร์ Notebook ขนาดหน่วยความจำ RAM มากกว่า 1,024 MB และ หน่วยความจำ harddisk มากกว่า 100 GB เพื่อการใช้ศึกษาทางตัวเลข (numerical analysis) เตรียม presentation และตีพิมพ์งาน paper ทางวิชาการ
- 10.2. เครื่อง printer สำหรับพิมพ์งานและเอกสารที่จำเป็น
- 10.3. เอกสารอ้างอิงและอุปกรณ์สำนักงาน ได้แก่ กระดาษพิมพ์งาน กระดาษทด สมุดบันทึก เครื่องเขียน
- 10.4. โปรแกรม Antivirus และ AntiSpyware โปรแกรม Mathematica โปรแกรม Microsoft Offices

# 11. แผนการดำเหินงานตลอดโครงการ และผล (output) ที่จะได้ (ให้ระบุผลงานคาดว่าจะตีพิมพ์ได้ด้วย)

แผนการดำเนินการจะประกอบด้วยวัฏจักรที่มีความยาวประมาณ 6 เดือนประมาณ 4 ครั้ง ดังต่อไปนี้

- 11.1. เดือนแรกจะเป็นการศึกษางานที่เกี่ยวข้องรวมถึงความเป็นไปได้ในการขยายผลสู่หัวข้อที่น่าสนใจ
- 11.2. สองเดือนถัดมาจะเป็นการศึกษาและคำนวณหัวข้อที่น่าสนใจและสามารถต่อยอดความรู้ได้และสรุป เป็น ผลการวิจัย
- 11.3. สามเดือนถัดมาจะเป็นการเขียนเป็นเอกสารตีพิมพ์ (paper) การส่งเพื่อการตีพิมพ์ และการติดต่อ อภิปรายกับ Referees ของ journal ที่ส่งตีพิมพ์

# ผลงานที่คาดว่าจะตีพิมพ์ได้

- ปีที่ 1: 1. Properties of baryon in quark gluon plasma from gravity dual models, จะส่งตีพิมพ์ต่อ Journal of High Energy Physics (impact factor ปี 2006 5.393)
- ปีที่ 2: 2. Transport coefficients in extreme nuclear states by gravity dual models, จะส่งตีพิมพ์ต่อ Journal of High Energy Physics
  - 3. Description of pomeron by open-string singlet interactions, จะส่งตีพิมพ์ต่อ Journal of High Energy Physics

## 12. ประโยชห์ที่คาดว่าจะได้รับ

คาดได้ว่าจะมีงานตีพิมพ์ 2-3 paper ในระยะเวลาสองปี ความรู้ที่ได้จะทำให้เรามีความเข้าใจในสมบัติของสสาร นิวเคลียร์มากขึ้น รวมถึงความรู้ความเข้าใจทางทฤษฎีต่อความสัมพันธ์ระหว่างทฤษฎีเกจและความโน้มถ่วงที่ลึกซึ้งยิ่งขึ้น ซึ่งอาจนำไปสู่ความเข้าใจต่อธรรมชาติของความโน้มถ่วงทางควอนตัมที่เป็นปัญหาที่สำคัญที่สุดปัญหาหนึ่งในฟิสิกส์ยุค ปัจจุบัน

## 14. จดหมายรับรอง (recommendation) ในกรณีที่นักวิจัยที่ปรึกษาอยู่ต่างประเทศ

**หมายเหตุ** ให้จัดทำรายละเอียดตามหัวข้อต่างๆ ข้างต้นนี้ พร้อมประวัติผลงาน (CV) ของผู้สมัครขอรับทุน ส่งพร้อมกับ แบบสมัครขอรับทุนพัฒนาศักยภาพในการทำงานวิจัยของอาจารย์รุ่นใหม่ (จำนวน 5 ชุด)

## Output งานตีพิมพ์ 3 ชิ้น ในวารสาร Journal of High Energy Physics (JHEP) ได้แก่

1. Exotic Multi-quark States in the Deconfined Phase from Gravity Dual Models.

P. Burikham, Auttakit Chatrabhuti, E. Hirunsirisawat, (Chulalongkorn U.)

Published in JHEP 0905:006,2009.

e-Print: arXiv:0811.0243 [hep-ph]

2. Magnetic properties of holographic multiquarks in the quark-gluon plasma.

Piyabut Burikham, (Chulalongkorn U.)

Published in JHEP 1004:045,2010.

e-Print: arXiv:0909.0614 [hep-th]

3. Thermodynamic Properties of Holographic Multiquark and the Multiquark Star.

P. Burikham, E. Hirunsirisawat, S. Pinkanjanarod

e-Print: arXiv:1003.5470 [hep-ph]

To be published in JHEP.

งานทั้งสามชิ้นได้มีการนำไปเสนอผลงานที่ SPC 2009, SPC 2010 นอกจากนี้สำหรับตัวหัวหน้าโครงการเองแล้วได้มี ผลงานตีพิมพ์ในวารสาร JHEP อีกหนึ่งชิ้นที่ไม่ได้เป็นส่วนหนึ่งของโครงการนี้แต่ได้รับการสนับสนุนจากสกว.เช่นกันใน โครงการ MRG5180225



RECEIVED: November 11, 2008
REVISED: March 4, 2009
ACCEPTED: April 13, 2009
PUBLISHED: May 5, 2009

# Exotic multi-quark states in the deconfined phase from gravity dual models

#### P. Burikham, A. Chatrabhuti and E. Hirunsirisawat

Theoretical High-Energy Physics and Cosmology Group, Department of Physics, Faculty of Science, Chulalongkorn University, Bangkok 10330, Thailand E-mail: piyabut@gmail.com, auttakit.c@chula.ac.th, ekapong.hirun@gmail.com

ABSTRACT: In the deconfined phase of quark-gluon plasma, it seems that most of the quarks, antiquarks and gluons should be effectively free in the absence of the linear confining potential. However, the remaining Coulomb-type potential between quarks in the plasma could still be sufficiently strong that certain bound states, notably of heavy quarks such as  $J/\psi$  are stable even in the deconfined plasma up to a certain temperature. Baryons can also exist in the deconfined phase provided that the density is sufficiently large. We study three kinds of exotic multi-quark bound states in the deconfined phase of quark-gluon plasma from gravity dual models in addition to the normal baryon. They are k-baryon,  $(N + \bar{k})$ -baryon and a bound state of j mesons which we call "j-mesonance". Binding energies and screening lengths of these exotic states are studied and are found to have similar properties to those of mesons and baryons at the leading order. Phase diagram for the exotic nuclear phases is subsequently studied in the Sakai-Sugimoto model. Even though the exotics are less stable than normal baryons, in the region of high chemical potential and low temperature, they are more stable thermodynamically than the vacuum and chiral-symmetric quark-gluon plasma phases ( $\chi$ S-QGP).

Keywords: Brane Dynamics in Gauge Theories, D-branes

C	ontents	
1	Introduction	1
2	Some classes of multi-quark states	3
3	Force conditions	5
4	Binding energy and the screening length	7
5	Dependence on the free quark mass	11
6	Phase diagram	13
7	Discussions	19
8	Conclusion	20
$\mathbf{A}$	Force condition at the D8-branes	22

#### 1 Introduction

Contonto

The discovery of AdS/CFT correspondence [1, 2] provides a new tool for studying the strongly coupled gauge theories. Although the original setup and most of the systems that string theorists have been investigating so far are highly supersymmetric and conformal, a lot of progress has been made in constructing more realistic models. Now we have examples of QCD-like gauge theory with known gravity dual that share most of the qualitative features of QCD. These holographic models allow us to perform analytic calculations in the regimes which are too difficult to implement for the real QCD even for lattice calculations. The properties of quark-gluon plasma from Relativistic Heavy Ion Collisions and QCD at finite baryon density are two examples of such regimes.

The gravity dual of baryons can be described via baryon vertex [3, 4], a D-brane wrapping higher dimensional sphere in 10-dimensional curved background with N strings attached to it and ending at the boundary. These strings are required to cancel an N charge in the world-volume of the wrapped brane due to the presence of RR flux in the background. The endpoint of fundamental string that ends on D-brane is electrically charged with respect to world-volume U(1) gauge field. Its charge is +1 or -1 depending on the orientation of the string and D-brane. Moreover, strings stretching from the baryon vertex to the boundary of AdS or the corresponding background spacetime (e.g. in Sakai-Sugimoto model) behave as fermions, giving antisymmetricity of the baryon vertex. This fact allows us to construct an SU(N) gauge-invariant combination of N quarks as

required by the group theory. Baryon configurations were investigated further in [5]–[7]. The authors in [8] extended the consideration in confining background where it was found that the binding energy is linear in N and in the size of the baryon on the boundary. And furthermore, they found that in  $\mathcal{N}_{\text{SUSY}} = 4$  theory there are stable configurations for baryons which are made of k quarks, or "k-baryon", if  $5N/8 < k \le N$ . Such configurations can be realized by considering the usual baryon vertex with k strings stretched up to the boundary and the rest N-k strings stretched down to the horizon. These baryons are not colour singlet and transform as  $\frac{N!}{k!(N-k)!}$  representation under SU(N) gauge group, for example the case k = N-1 gives rise to a baryonic configuration in the anti-fundamental representation. In a confining theory we do not expect to find such a bound state. It was proposed in [9, 10] that the k < N bound states can exist in a deconfined phase.

In general, we could imagine that there would be more exotic baryon states in the deconfined phase where bound states of quarks need not be the colour singlet. Some attempts have been made in constructing holographic description of exotic multi-quarks bound states [9]-[12]. The author in [12] considered exotic quark configurations formed by combining two or more baryon vertices together. However, it might be possible to construct an exotic baryon from a single baryon vertex which should be more energetically preferable. One useful observation is that there are infinite combinations of string charges that can cancel the charge from the background RR flux. Hence, the total number of strings attached to the baryon vertex need not to be equal to N. For example, if the orientation of D-branes is fixed in such a way that there is +N units of charge on its world-volume, we can attach N+k strings, each with -1 charge and k strings with +1 charge to make the total charge vanishes. As long as the conservation of charge is concerned, k could be any integer. In this case, we can construct a k > N baryon. Such baryon could be the lightest bound state in some irreducible representation of the underlying gauge theory, thus it may be stable and can be observed in the deconfined phase. We would like to investigate this possibility further in this paper.

It is also interesting to study exotic baryons in more realistic model such as Sakai-Sugimoto model [13, 14]. This model is based on Witten's model [15] which uses the D4-brane wrapping a Scherk-Schwarz circle and adds a stack of  $N_f$  probe D8-branes and a stack of  $N_f$  probe anti-D8-branes transverse to the circle. This model contains massless chiral fermions and the flavour symmetry. The most striking feature of this model is that it introduces geometrical mechanism for spontaneous chiral symmetry breaking. Using the fact that the circle vanishes at a finite radial coordinates in the near horizon limit, D8-branes and anti-D8-branes are connected in a U-shaped configuration. At low temperature the model describes a confining gauge theory with broken chiral symmetry. Above a deconfinement temperature, gluons become effectively free. However, both the connected U-shape D8-branes configuration and the separated parallel brane-anti-brane configuration are possible in the intermediate temperature. The chiral symmetry is still broken even though the gluons are already deconfined. At higher temperature the chiral symmetry is restored, which is illustrated geometrically by the separation of the D8-branes and anti-D8-branes [16]. This corresponds to the branes being in parallel configuration.

The model also has an interesting phase structure. Finite baryon density in the Sakai-Sugimoto model has been studied in [17, 18] and extended to the full parameter space in [19] where baryon matter is represented by D4-branes in the D8-brane (nuclear matters) or by strings stretched from the D8-brane down to the horizon (quark matters). It was shown that the former configuration is always preferred to the latter and quark matters are unstable to density fluctuations. In the deconfined phase there are three regions corresponding to the vacuum, quark-gluon plasma, and nuclear matter, with a first-order and a second-order phase transition separating these three phases. The author in [19] found that for a large baryon number density, and at low temperatures, the dominant phase has broken chiral symmetry in agreement with QCD at high density. It is interesting to see how exotic baryon states fit into the phase structure.

This paper is organized as the following. In section 2, we discuss some classes of exotic baryon configurations and investigate their static configurations in section 3. Binding energy and screening length of the configurations are calculated in section 4. The dependence on free quark mass of exotic baryon configuration is discussed in section 5. The phase diagram of Sakai-Sukimoto model with exotic baryons is investigated in section 6. We discuss our results in section 7 and conclude in section 8.

#### 2 Some classes of multi-quark states

In the deconfined phase of QGP, coloured states of a number of quarks and antiquarks can exist in the medium as long as it is energetically more favoured than the free quarks and antiquarks or other mesonic states. We will call these multi-quark states as "baryons" in this article. In the confined phase, the only allowed baryons are those with colour singlet combinations such as nucleons and pentaquarks. For the deconfined phase, baryons can have colour and thus can have more varieties than the situation in the confined phase.

In general, a D(8-p)-brane wrapping the subspace  $S_{8-p}$  of the background spacetime sources the gauge field  $A_{(1)}$  on its world volume. This gauge field will couple with the antisymmetric (8-p)-form field strength  $G_{(8-p)}$  and induce the charge upon the wrapping D(8-p)-brane. If the background is generated by a stack of N Dp-branes, then the charge being induced upon the wrapping D(8-p)-brane will be exactly N. This charge needs to be cancelled by external charges brought about by strings. Each of the strings stretching out from the wrapping brane to the spacetime boundary or probe branes carries -1 unit of charge. Therefore it is required that the total number of "quark" strings stretching out from the wrapping brane must be N. The configuration of wrapping D(8-p)-brane with totally N strings stretching out is called a baryon vertex [3, 4].

For the confined phase, since quarks cannot exist as free-quark strings with one end falling behind the horizon, therefore they can only start from the baryon vertex and go to the probe branes. On the other hand, in the deconfined phase, a radial string configuration lying along the radial coordinate is also a classical solution of the Nambu-Goto action [20] and it represents the free (anti)quark state in the QGP medium. A string can either start from the baryon vertex and go radially to the horizon of the background spacetime or it can

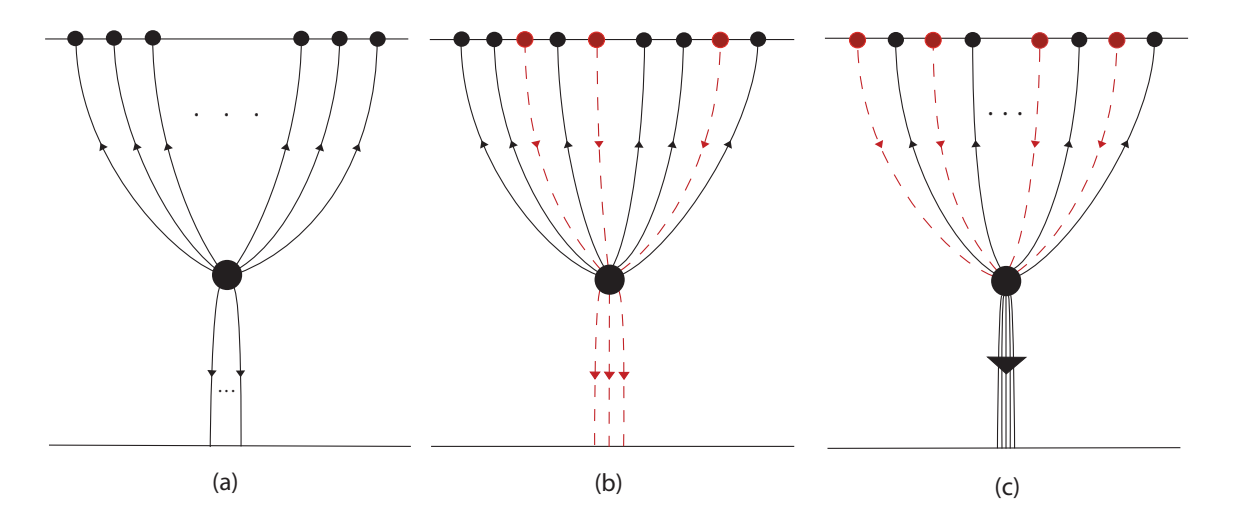


Figure 1. The gravity dual configurations of the hypothetical exotic states (a) k-baryon with the number of hanging strings  $k_{\rm h}=k< N$  and the number of radial strings  $k_{\rm r}=N-k$ . (b)  $(N+\bar k)$ -baryon with  $k_{\rm h}=N+\bar k$  and  $k_{\rm r}=\bar k$ . (c) j-mesonance with  $k_{\rm h}=2j$  and  $k_{\rm r}=N$ .

come from the horizon and end at the baryon vertex. We will call this string configuration which is allowed in the deconfined phase as the "radial string".

In the deconfined phase of QGP, it is possible to have  $k_h$  strings hanging from the spacetime boundary down to the baryon vertex and another  $k_r$  strings stretching radially from the baryon vertex down to the horizon. The total number  $k_h + k_r = N$  is the charge conservation constraint on the configuration. This configuration is known as "k-baryon" [8].

Another possible configuration is when there are N quark-strings and  $\bar{k}$  antiquark-strings hanging down to the vertex from the probe branes. To conserve the charge, there are additional k quark-strings hanging from the vertex down to the horizon. We will call this configuration " $(N + \bar{k})$ -baryon" (e.g. pentaquark could be represented by one of this kind).

An even more interesting configuration allowed in the deconfined phase is when there are j pairs of quark and antiquark strings hanging from the probe branes down to the vertex. Again, to conserve charges, we need N radial strings stretching from the vertex down to the horizon. This configuration obviously can decay into j mesons when it is less energetically favoured. Therefore we will call this state, a "j-mesonance", representing a binding state of j mesons in the QGP.

In summary, the charge conservation constraint for each case can be expressed as the following.

For k-baryon,

$$k_{\rm h} + k_{\rm r} = N; \quad k_{\rm h} = k.$$
 (2.1)

For  $(N + \bar{k})$ -baryon,

$$k_{\rm h} - k_{\rm r} = N; \quad k_{\rm h} = N + \bar{k}.$$
 (2.2)

For j-mesonance,

$$k_{\rm h} = 2j; \qquad k_{\rm r} = N. \tag{2.3}$$

Note that  $k_h$  is the number of strings hanging from the boundary down to the baryon vertex and  $k_r$  is the number of strings hanging from the vertex down to the horizon. The value of  $\bar{k}$  and j can be as large as  $N \times N_f$ . However, in this article, we will take this number to be large and ignore the upper bound on  $\bar{k}$  and j. Each configuration of exotic baryons is illustrated in figure 1.

#### 3 Force conditions

In this section, we will consider the force condition for each exotic configuration of the quarks and antiquarks in a deconfined phase. The calculation will be performed in the gravity background similar to those of Sakai and Sugimoto's [13]. Even though the chiral symmetry restoration can be addressed within this model, we will not consider the aspect in this section but rather focus our attention on the high temperature phase where quarks and antiquarks are effectively free in the absence of the linear confining potential. The positions of  $D8/\overline{D8}$  will be taken to be large and we will approximate it to be infinity in this section as well as in the discussion of binding energy and screening length in section 4. Analysis in this heavy-quark limit provides us with valuable physical understanding of certain essential features of the exotic states. Generalized results for a near-horizon background metric of the Dp-branes solution and its dependence on positions of the probe branes will be given in section 5.

Even in the deconfined phase, quarks and antiquarks feel effective (screened) potential from other constituents. Therefore, a number of population of them will exist in various forms of bound states, some of which are exotic in the sense that they cannot be formed in the confined phase at low temperature.

Start with the following background metric

$$ds^{2} = \left(\frac{u}{R_{D4}}\right)^{3/2} \left(f(u)dt^{2} + \delta_{ij}dx^{i}dx^{j} + dx_{4}^{2}\right) + \left(\frac{R_{D4}}{u}\right)^{3/2} \left(u^{2}d\Omega_{4}^{2} + \frac{du^{2}}{f(u)}\right)$$

$$F_{(4)} = \frac{2\pi N}{V_{4}}\epsilon_{4}, \qquad e^{\phi} = g_{s}\left(\frac{u}{R_{D4}}\right)^{3/4}, \qquad R_{D4}^{3} \equiv \pi g_{s}Nl_{s}^{3},$$

$$(3.1)$$

where  $f(u) \equiv 1 - u_T^3/u^3$ ,  $u_T = 16\pi^2 R_{\mathrm{D}4}^3 T^2/9$ . Note that the compactified  $x_4$  coordinate ( $x^4$  transverse to the probe D8 branes), with arbitrary periodicity  $2\pi R$ , never shrinks to zero. The volume of the unit four-sphere  $\Omega_4$  is denoted by  $V_4$  and the corresponding volume 4-form by  $\epsilon_4$ .  $F_{(4)}$  is the 4-form field strength,  $l_s$  is the string length and  $g_s$  is the string coupling. The dilaton in this background has u-dependence and its value changes along the radial direction u. This is a crucial difference in comparison to the AdS-Schwarzschild metric case where dilaton contribution is constant.

The action of the baryon configuration is given by

$$S = S_{\rm D4} + k_{\rm h} S_{\rm F1} + k_{\rm r} \tilde{S}_{\rm F1}, \tag{3.2}$$

where  $S_{D4}$  represents the action of the D4-brane.  $S_{F1}$  is the action of a stretched string from the boundary down to the baryon vertex and  $\tilde{S}_{F1}$  is the action of a radial string hanging from the baryon vertex down to the horizon. Recall that  $S_{D4}$  can be obtained from the Dirac-Born-Infeld action.¹ After some calculations, we obtain

$$S_{\rm D4} = \frac{\tau N u_c \sqrt{f(u_c)}}{6\pi\alpha'}, \quad S_{\rm F1} = \frac{\tau}{2\pi\alpha'} \int_0^L d\sigma \sqrt{u'^2 + f(u) \left(\frac{u}{R}\right)^3}, \quad \tilde{S}_{\rm F1} = \frac{\tau}{2\pi\alpha'} (u_c - u_{\rm T}), \tag{3.3}$$

where  $\tau$  is the total time over which we evaluate the action and  $u_c$  is the position where the D4-brane vertex is located.

The variation of the action with respect to u gives the volume term and the surface term. The volume term leads to the usual Euler-Lagrange equation for the classical configuration of strings. As an approximation, we assume the baryon vertex to be a point (not being distorted by the connecting strings) located at a fixed value of  $u = u_c$  as in ref. [8]. Under this assumption, the surface terms provide additional zero-force condition on the configuration,

$$\frac{N}{3}G_0(x) - k_h B + k_r = 0 (3.4)$$

where

$$G_0(x) \equiv \frac{1 + \frac{x^3}{2}}{\sqrt{1 - x^3}}, \quad x \equiv \frac{u_T}{u_c} < 1, \text{ and } B \equiv \frac{u_c'}{\sqrt{u_c'^2 + f(u_c)(\frac{u_c}{R_{\rm D4}})^3}}.$$
 (3.5)

Notice that these conditions occur at the location of the vertex at  $u = u_c$ , at which there exists the balance between the pull-up force (toward the direction of increasing u) due to the tension of hanging strings and the pull-down force due to the "weight" of D4-brane plus the tension of radial strings.

Since  $B \leq 1$ , we obtain

$$k_{\rm h} \ge \frac{N}{3} G_0(x) + k_{\rm r},$$
 (3.6)

which expresses the lower bound of the number of hanging strings. In other words, the number of hanging strings cannot be less than this critical value, otherwise the no-force condition is not satisfied. The equality of (3.6) is held only when all hanging strings are stretched straight, otherwise we require more hanging strings to balance the pull-down force. Let us now consider each class of the multi-quark states.

In the case of k-baryon, plugging the condition (2.1) into (3.6), we obtain

$$k_{\rm h} = k \ge \frac{N}{6} \left( G_0(x) + 3 \right).$$
 (3.7)

 $S_{\text{DBI}} = \int dx^0 d\xi^p T_p; \quad T_p = \left(e^{-\phi} (2\pi)^p {\alpha'}^{(p+1)/2}\right)^{-1} \sqrt{-\det(g)}$ 

²This is not exactly the weight in the usual sense since the direct gravitational force on Dbrane is already balanced by the force from the RR-flux, but it is the force originated from minimization of self-energy due to the brane tension caused by the background metric and the gauge interaction. This is very similar to the self-energy of a spring under gravity where the spring potential energy changes with the tidal force from gravity in the background. The DBI action of the D4~  $u_c\sqrt{f(u_c)}$  which is positive for  $u_c > u_T$  and becomes zero (minimum) at  $u_c = u_T$  and thus it represents the "weight" on D4 towards the horizon.

Apart from the lower bound, we also have the upper bound,  $k \leq N$ , therefore  $G_0(x)$  cannot be larger than 3, resulting in

$$x \lesssim 0.922. \tag{3.8}$$

Notice that this restriction on x is a result from the conditions of the force balance and conservation of string charges. This shows that there is an upper-bound on the temperature, over which the horizon is too near to the point vertex that the pull-down force always overcomes the pull-up one.

In the case of  $(N + \bar{k})$ -baryon, in the same way as the preceding case, plugging the condition of charge conservation (2.2) into (3.6), we have the following condition,

$$k_{\rm h} = N + \bar{k} \ge \frac{N}{3}G_0(x) + \bar{k}.$$

Unlike the case of k-baryon, the upper-bound of the number of hanging strings does not exist. However, we still obtain the same condition  $G_0(x) \leq 3$ , hence  $x \leq 0.922$ .

Finally, in the case of j-mesonance, similarly, eq. (2.3) results in

$$j \ge \frac{N}{6} \left( G_0(x) + 3 \right). \tag{3.9}$$

The lower-bound of the value of j is 2N/3 at zero temperature (x = 0) and it will be larger as the temperature grows. Nevertheless, the upper-bound of the limit on j does not exist.

Finally, we would like to comment on the limits on the value of  $k, \bar{k}, j$  when the temperature is zero. In terms of  $n \equiv 7-p$  (of the spacetime background generated by Dp-branes), the condition (3.6) becomes

$$k_h \ge \frac{N}{n} + k_r \tag{3.10}$$

which leads to

$$\frac{k}{N}, \frac{j}{N} \ge \frac{n+1}{2n},\tag{3.11}$$

and no conditions on  $\bar{k}$ . This critical numbers are 5/8,2/3 for n=4,3 (the AdS-Schwarzschild and Sakai-Sugimoto model) respectively. It is an interesting coincidence that the critical numbers are the same for both k-baryon and j-mesonance. Even though it appears from eq. (3.10) that there should also be a constraint on the  $(N+\bar{k})$  configuration, it turns out that there is none.

#### 4 Binding energy and the screening length

In this section we will calculate the binding energies of the k-baryon,  $(N + \bar{k})$ -baryon, and j-mesonance in the deconfined phase. These binding energies are taken to be the differences between the total energies of each configuration and the corresponding energies of the free strings configuration which represents the free quarks and/or antiquarks state. The number of free strings in the free quarks state is determined solely by the total number of strings hanging from the boundary,  $k_h$ .

The total energy of each configuration is given by  $E = S/\tau$  of the corresponding action S for each configuration. The binding energy for each hanging string is consequently,

$$E_{\rm F1} = \frac{1}{2\pi} \int_0^L d\sigma \sqrt{u'^2 + \left(\frac{u}{R_{\rm D4}}\right)^3 f(u)} - \frac{1}{2\pi} \int_{u_T}^{\infty} du.$$
 (4.1)

Due to the no-force condition in the surface term, we impose eq. (3.4) and eq. (3.5), or

$$u_c^{\prime 2} = \frac{f(u_c)B^2}{1 - B^2} \left(\frac{u_c}{R_{\rm D4}}\right)^3 \tag{4.2}$$

where the tension of each hanging string at  $u_c$  is constrained by

$$B = B(k_{\rm h}, k_{\rm r}, x) = \frac{N}{3k_{\rm h}}G_0(x) + \frac{k_{\rm r}}{k_{\rm h}}.$$
 (4.3)

Since the Lagrangian  $\mathcal{L}$  does not depend on  $\sigma$  explicitly, the conserved Hamiltonian can be defined to be

$$\mathcal{H} \equiv \mathcal{L} - u' \frac{\partial \mathcal{L}}{\partial u'} = \text{const},$$
 (4.4)

leading to

$$\frac{f(u_c)(\frac{u_c}{R_{\rm D4}})^3}{\sqrt{u_c'^2 + f(u_c)(\frac{u_c}{R_{\rm D4}})^3}} = \frac{f(u)(\frac{u}{R_{\rm D4}})^3}{\sqrt{u_c'^2 + f(u)(\frac{u}{R_{\rm D4}})^3}}.$$
(4.5)

Then substituting eq. (4.2) into this equation, we obtain

$$u'^{2} = \frac{f(u)^{2} (\frac{u}{R_{D4}})^{6}}{f(u_{c})(\frac{u_{c}}{R_{D4}})^{3} (1 - B^{2})} - f(u) \left(\frac{u}{R_{D4}}\right)^{3}.$$
 (4.6)

This gives the size (radius) of the baryon as seen on the gauge theory side,

$$L = \frac{R_{\rm D4}^{3/2}}{u_{\rm c}^{1/2}} \int_{1}^{\infty} dy \sqrt{\frac{(1-x^3)(1-B^2)}{(y^3-x^3)(y^3-x^3-(1-x^3)(1-B^2))}}.$$
 (4.7)

Note that  $u_c \approx \frac{R_{\rm D4}^3}{L^2}$  at the leading order.

Using eq. (4.6) and let  $y \equiv u/u_c$ , the regulated binding energy now becomes

$$E_{\rm F1} = \frac{u_c}{2\pi} \left\{ \int_1^\infty dy \left[ \sqrt{\frac{y^3 - x^3}{(y^3 - x^3) - (1 - x^3)(1 - B^2)}} - 1 \right] - (1 - x) \right\}. \tag{4.8}$$

Hence, we obtain the total energy of the configurations as

$$E = \frac{Nu_T}{2\pi} \left( \frac{\sqrt{1-x^3}}{3x} + \left(\frac{k_h}{N}\right) \frac{\mathcal{E}}{x} + \left(\frac{k_r}{N}\right) \frac{1-x}{x} \right)$$
(4.9)

$$\sim \frac{N^2}{L^2} \tag{4.10}$$

where  $\mathcal{E}$  represents the terms within the brace of (4.8).

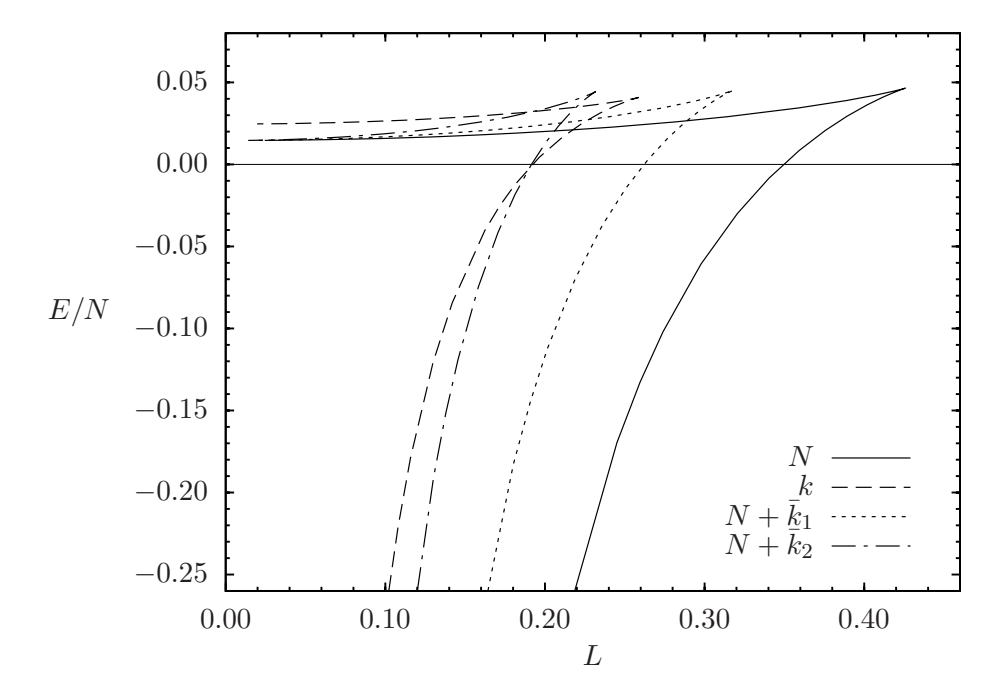


**Figure 2.** Comparison of the potential per N between N-baryon, k-baryon, and  $(N + \bar{k})$ -baryon for  $k/N = 0.8, \bar{k_1}/N = 2/3, \bar{k_2}/N = 2$  at temperature T = 0.25.

To obtain the relations between the total energy of the configurations E(x) and L(x), we eliminate the parameter  $x = u_T/u_c$ . By numerical calculations, the results are shown in figure 2, 3. The binding energy of N-baryon is the deepest, suggesting that it is the most tightly bound state. For  $(N+\bar{k})$ -baryon, increasing  $\bar{k}$  makes the binding energy smaller and the bound state is less tightly bound. The case of j-mesonance is quite similar. Generically, a j-mesonance has shallower binding potential than the total energy of j mesons. However, as j grows, the difference gets smaller and smaller.

The screening radius or screening length of exotic multi-quark state is defined to be the value of radius  $L^*$  at which the binding energy becomes zero from negative values at smaller distances. This screening radius is therefore one-half of the usual definition of screening length in the discussion of mesonic state where it is defined as the zero-potential distance between quark and antiquark.

Numerical results suggest that the screening length of baryons and mesonance decrease as the temperature increases, i.e.  $L^* \sim 1/T$  for a fixed value of  $k, \bar{k}, j$  as is shown in figure 4-6. This is the generic form for the screening length in both the AdS-Schwarzschild and Sakai-Sugimoto models because it is the quantity which does not depend on the 't Hooft coupling at the leading order [21]. It is also an increasing function of k and j. Interestingly,  $(N+\bar{k})$ -baryon has the opposite tendency with the screening length decreases as  $\bar{k}$  grows. On the other hand, the screening length of j-mesonance has a saturation value  $L_{j-mesonance}^* \to L_{\rm meson}^*$  as  $j \to \infty$ .

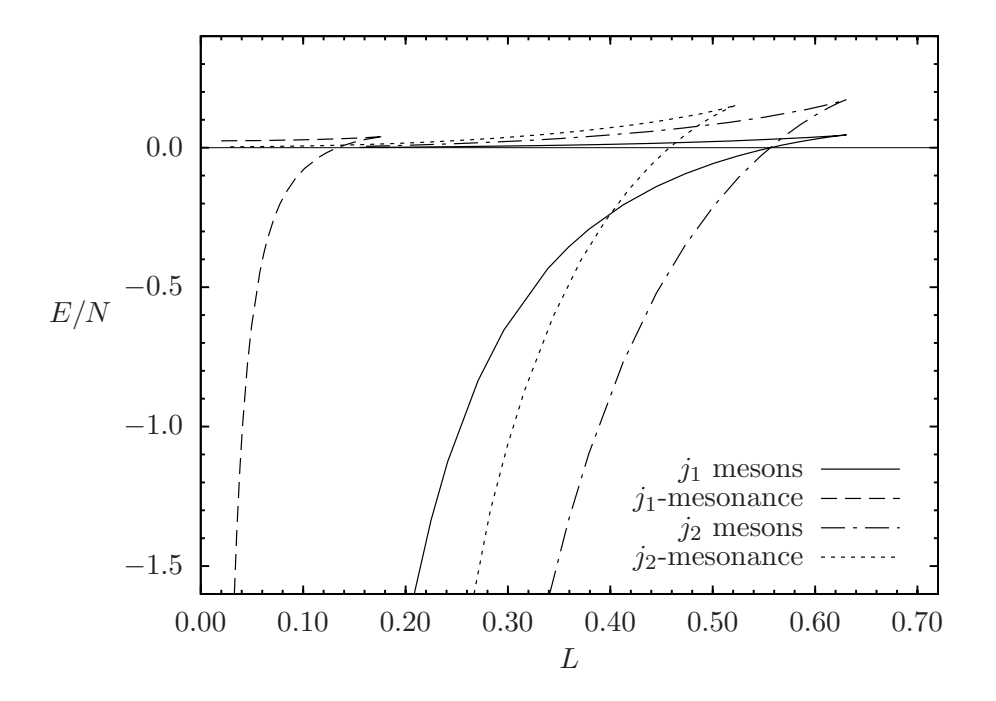


**Figure 3**. Comparison of the potential per N between j-mesonance and j mesons for  $j_1/N = 0.8, j_2/N = 3$  at temperature T = 0.25.

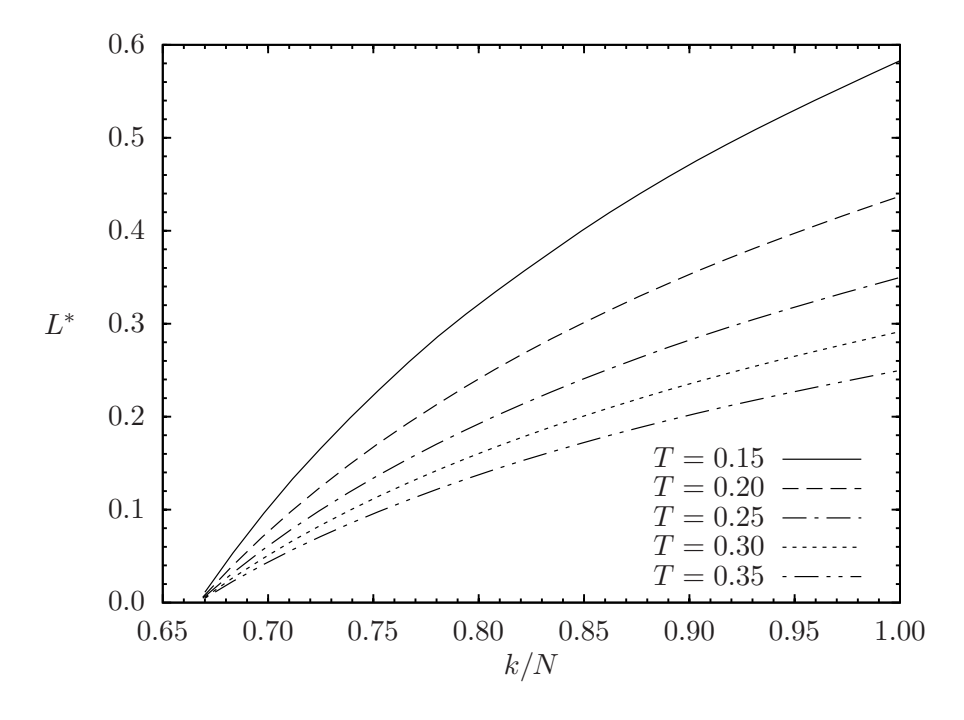


Figure 4. Screening length with respect to k for the temperatures in 0.15 - 0.35 range.

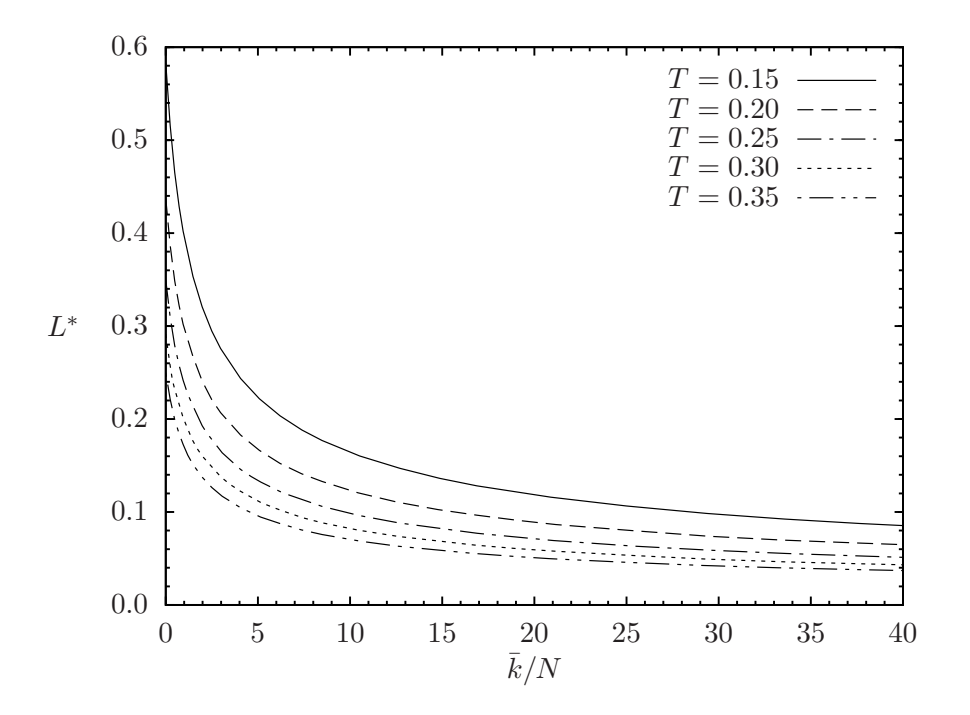
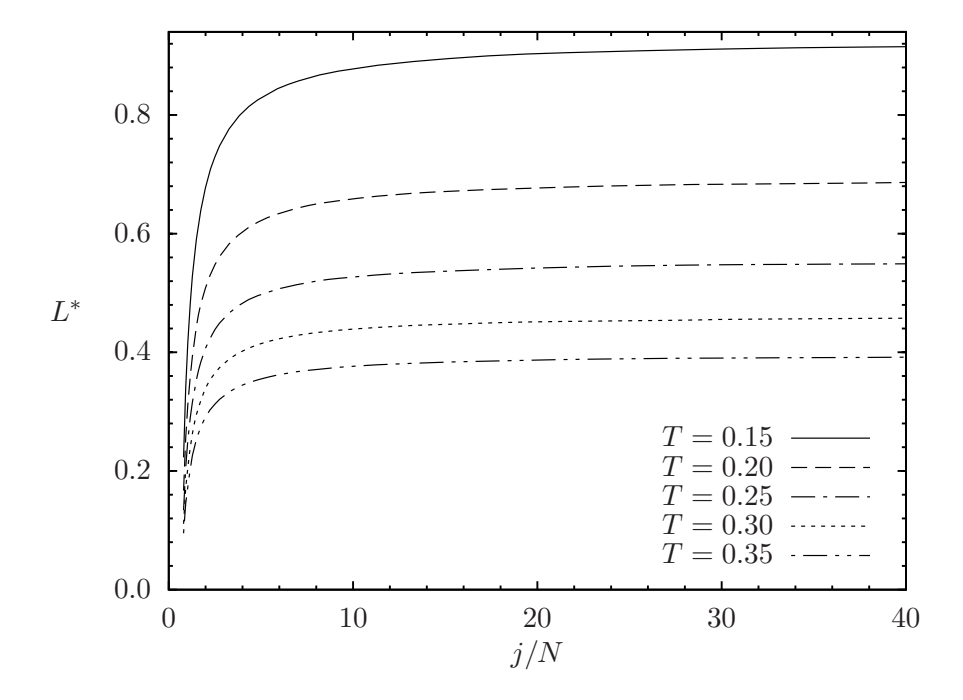


Figure 5. Screening length with respect to  $\bar{k}$  for the temperatures in 0.15-0.35 range.



**Figure 6.** Screening length with respect to j for the temperatures in 0.15 - 0.35 range.

#### 5 Dependence on the free quark mass

In this section, we will study dependence of the binding potential on the position of the probe branes. This is useful when position of the probe branes are at finite distance from

the black hole horizon and the corresponding quarks have finite mass. For example, the probe branes are D8 and  $\overline{D8}$  flavour branes in the Sakai-Sugimoto model.

The calculation of binding energy as a function of the radius L of the multi-quark states in the previous sections can be generalized to the case where the background metric is generated by a stack of Dp-branes as the following. Start with the energy of a hanging fundamental string with n = 7 - p,

$$E_{F1} = \frac{u_c}{2\pi} \left\{ \int_1^\infty dy \left[ \sqrt{\frac{y^n - x^n}{(y^n - x^n) - (1 - x^n)(1 - A(n)^2)}} - 1 \right] - (1 - x) \right\}$$
 (5.1)

and the radius,

$$L = \frac{R^{n/2}}{u_c^{(n-2)/2}} \int_1^\infty dy \, \sqrt{\frac{(1-x^n)(1-A(n)^2)}{(y^n-x^n)(y^n-x^n-(1-x^n)(1-A(n)^2))}}.$$
 (5.2)

The total regulated binding energy of the configuration then becomes

$$E_{\text{tot}} = \frac{Nu_h}{2\pi} \left\{ \frac{\sqrt{1 - x^n}}{nx} + \left(\frac{k_h}{N}\right) \frac{\mathcal{E}}{x} + \left(\frac{k_r}{N}\right) \frac{1 - x}{x} \right\}$$
 (5.3)

where

$$\mathcal{E} = \int_{1}^{\infty} dy \left[ \sqrt{\frac{y^{n} - x^{n}}{(y^{n} - x^{n}) - (1 - x^{n})(1 - A(n)^{2})}} - 1 \right] - (1 - x), \tag{5.4}$$

and

$$A(n) = \frac{u_c'}{\sqrt{u_c'^2 + f(u_c)(\frac{u_c}{R_{Dp}})^n}} = \frac{N}{nk_h} \left( \frac{1 + \frac{n-2}{2}x^n}{\sqrt{1 - x^n}} \right) + \frac{k_r}{k_h}.$$
 (5.5)

The parameter x is again given by

$$x = \frac{u_T(n)}{u_c}, \quad u_T(n=3,4) = \frac{16}{9}\pi^2 R^3 T^2, \pi R^2 T.$$
 (5.6)

Note that the case n=3 and n=4 corresponds to the case of Sakai-Sugimoto and AdS-Schwarzschild gravity dual model respectively.

Introduction of quark masses into the configuration can be done by terminating hanging strings at certain radial distance  $u_{\text{max}} < \infty$ . The universal behaviour of heavy-quark potential comes from the limit  $u_{\text{max}} \to \infty$ . We can split the total binding potential of the string into two parts. The first part is the binding potential in the  $u_{\text{max}} \to \infty$  limit and the second part is the mass dependent potential. Therefore, the mass dependence part of the binding potential,  $E_{F1}(u_{\text{max}})$  ( $m = u_{\text{max}}/2\pi$ ), can be expressed as

$$E_{\rm F1}(\text{finite mass}) = E_{\rm F1}(u_{\rm max} \to \infty) + E_{\rm F1}(u_{\rm max}), \tag{5.7}$$

$$E_{\text{F1}}(u_{\text{max}}) = -\frac{u_c}{2\pi} \int_{u_{\text{max}}/u_c}^{\infty} dy \left[ \sqrt{\frac{y^n - x^n}{(y^n - x^n) - (1 - x^n)(1 - A(n)^2)}} - 1 \right]$$
(5.8)

$$= -\frac{u_{\text{max}}(1 - A(n)^2)}{4\pi(n-1)} \left(\frac{u_c^n - u_T^n}{u_{\text{max}}^n}\right) + O(u_{\text{max}}^{1-2n}).$$
 (5.9)

Eliminate  $u_c$  by using

$$L = \frac{R^{n/2}}{u_c^{(n-2)/2}} \int_1^{u_{\text{max}}/u_c} dy \sqrt{\frac{(1-x^n)(1-A(n)^2)}{(y^n-x^n)(y^n-x^n-(1-x^n)(1-A(n)^2))}}.$$
 (5.10)

The result involves complicated functions of A which can be cast in the following form,

$$E_{F1}(u_{\text{max}}) \sim -u_{\text{max}}^{1-n} \left( R^{n^2/(n-2)} f_1(A) + u_T^n f_2(A) \right),$$
 (5.11)

where  $f_{1,2}(A)$  are some functions of A.

Interestingly, the mass dependence of multiquark potentials has similar form as the mass dependence of mesonic state  $\sim m^{1-n}$  in ref. [20]. This is natural due to the fact that most of the mass of constituent quarks come from the tail part of strings which extend to the large-u region. The mass dependence of the binding potential at the leading order is therefore determined only by the contribution of the hanging strings from the large-u region. As long as the background spacetime of the gravity dual is asymptotically similar to the background considered here in the large-u limit, we would expect the same mass dependence as the form we obtained in this section.

### 6 Phase diagram

A natural question to ask is whether we have a phase where the exotic multiquark states are preferred over the normal nuclear matter (namely the gas of N-baryons), vacuum, and the chiral-symmetric quark-gluon plasma phase. To consider a realistic model where these three phases are distinct, we focus our consideration on the Sakai-Sugimoto model with n=3. To calculate the phase diagram involving exotic states, it is necessary to consider the contribution from D8 and  $\overline{D8}$ -branes in the Sakai-Sugimoto model in addition to the contributions from strings and D4-branes. We will assume that the characteristic distance between D8 and  $\overline{D8}$  in  $x^4$  direction is  $L_0$ . The relevant scales of the model therefore depend on both  $u_T$  and  $L_0$ .

When there is no radial string pulling the vertex down towards the horizon, it was demonstrated in ref. [7] by numerical method that the vertex will be pulled all the way up to the position of the flavour branes if the temperature is not very high. Addition of radial strings to the vertex would pull the vertex and the flavour branes towards the horizon. As temperature rises, the radial strings pull the vertex down with stronger force since they are closer to the horizon. It is possible that the vertex then starts to separate from the flavour branes and we might need to consider the configuration where vertex and flavour branes are separated. However, we can see that the difference between the two configurations should be relatively small (namely, only the force conditions will be slightly different) and we should be able to approximate the situation by considering the configuration where the vertex is not separated from the flavour branes. It is also shown in the appendix that this configuration satisfies the force condition and thus is allowed. Therefore, it will be assumed that the vertex is always in the flavour branes for the discussion in this section. Moreover, the vertex will be treated as a static configuration and any distortion caused by the strings attached to it will be ignored.

The calculations presented in this section are adapted from ref. [19] except that we add radial strings hanging from the vertex down to the horizon for the consideration of exotic nuclear phase. We also use position of the D4,  $u_c$ , instead of  $u_0$  (where  $x_4'(u_0) \rightarrow \infty$ ) in our calculation concerning the exotics. This approach allows us to deal with the contribution from radial strings more conveniently. As is shown in figure 7, the vacuum phase with broken chiral symmetry corresponds to the configuration where D8 and  $\overline{D8}$  are connected into a curve in the  $x_4-u$  projection. The chiral-symmetric phase of quark-gluon plasma ( $\chi$ S-QGP) corresponds to the configuration with the parallel D8 and  $\overline{D8}$  stretching from the spacetime boundary down to the horizon. Finally, the nuclear (including exotics) phase corresponds to the configuration where the D4 vertex is located at the D8- $\overline{D8}$  curve, pulling it down towards the horizon by its "weight" in the background. Each vertex has radial strings attached to it, pulling it further towards the horizon. When there is no radial strings attached, the nuclear phase is of normal N-baryons. The chiral symmetry is also broken in this phase.

Under the above assumptions, the contribution from the strings hanging down from the spacetime boundary to the vertex is negligible. The only contribution of strings is from the radial strings hanging down from the vertex to the horizon. The total action of the configuration is given by

$$S = S_{D8} + S_{D4} + \tilde{S}_{F1}. (6.1)$$

Generically, the DBI action of the D8-branes is given by

$$S_{D8} = -\mu_8 \int d^9 X e^{-\phi} \text{Tr} \sqrt{-\det(g_{MN} + 2\pi\alpha' F_{MN})}$$
(6.2)

where the field strength of the flavour group  $U(N_f)$  is

$$\mathcal{F} = d\mathcal{A} + i\mathcal{A} \wedge \mathcal{A}. \tag{6.3}$$

The flavour branes provide "global" quantum numbers such as baryon number to the string and subsequently to the strings-brane configuration dual to baryon in the gauge theory side. The diagonal part of the representation matrix of  $\mathrm{U}(N_f)$  is the  $\mathrm{U}(1)$  subgroup which induces baryon number to the end of string attached to the flavour branes. Redefine the  $\mathrm{U}(1)$  part so that

$$\mathcal{A} = \mathcal{A}_{SU(N_f)} + \frac{1}{\sqrt{2N_f}}\hat{\mathcal{A}} \tag{6.4}$$

with  $\hat{A}$  represents the U(1) piece of the gauge field. The DBI action of the D8-brane coupled to the diagonal gauge field is then given by

$$S_{D8} = \mathcal{N} \int du \ u^4 \sqrt{f(u)(x_4'(u))^2 + u^{-3}(1 - (\hat{a}_0'(u))^2)}$$
 (6.5)

where the constant scales linearly with  $N_f$  as

$$\mathcal{N} = \frac{\mu_8 \tau N_f \Omega_4 V_3 R^5}{g_s},\tag{6.6}$$

and the rescaled U(1) diagonal field,

$$\hat{a} = \frac{2\pi\alpha'\hat{\mathcal{A}}}{R\sqrt{2N_f}}. (6.7)$$

The action does not depend on  $\hat{a}_0(u)$  explicitly and therefore a constant of motion can be defined as

$$d = \frac{u\hat{a}_0'(u)}{\sqrt{f(u)(x_4'(u))^2 + u^{-3}(1 - (\hat{a}_0'(u))^2)}}.$$
(6.8)

We will see below that the constant d can be interpreted as the baryon number density sourced by the D4-branes once we introduce the Chern-Simon action of the gauge field. Note that d plays the role of the electric displacement field [19]. In the confined phase, the only possible source for d is the D4-brane wrapped on  $S^4$  in the D8-branes. In the deconfined phase, either D4-brane or strings which stretch from the D8-brane down to the horizon can serve as the sources for d. Here, in the study of exotic baryons, we consider the case where both D4-brane and strings are present as the sources. This possibility was not investigated in [19].

Similarly, the constant of motion with respect to  $x_4(u)$  leads to

$$(x_4'(u))^2 = \frac{1}{u^3 f(u)} \left[ \frac{f(u)(u^8 + u^3 d^2)}{f(u_0)(u_0^8 + u_0^3 d^2)} - 1 \right]^{-1}$$
(6.9)

where  $u_0$  is the position when  $x'_4(u_0) = \infty$ .

Instead of using  $u_0$  as the reference position, the radial position of the D4 on the D8-branes,  $u_c$ , can be used to calculate  $x'_4(u)$ ,

$$(x_4'(u))^2 = \frac{1}{u^3 f(u)} \left[ \frac{f(u)(u^8 + u^3 d^2)}{F^2} - 1 \right]^{-1}$$
(6.10)

where

$$F = \frac{f(u_c)\sqrt{u_c^8 + u_c^3 d^2}}{\sqrt{f(u_c)(x_4'(u_c))^2 + u_c^{-3}}} x_4'(u_c)$$

$$= \frac{\sqrt{u_c^3 f(u_c)}}{3} \left[ 1 + \frac{1}{2} \left( \frac{u_T}{u_c} \right)^3 + 3n_s \sqrt{f(u_c)} \right] \sqrt{\frac{9(u_c^5 + d^2)}{1 + \frac{1}{2} (\frac{u_T}{u_c})^3 + 3n_s \sqrt{f(u_c)}} - \frac{d^2}{f(u_c)}}.$$
(6.11)

The number of radial strings  $n_s$  represents the number of strings hanging down from D4-branes to the horizon in unit of 1/N. For k,  $(N+\bar{k})$ -baryon and j-mesonance, the values of  $n_s$  are 1-k/N,  $\bar{k}/N$ , 1 respectively. Calculation of  $x_4'(u_c)$  is performed by minimizing the action with respect to the variation of  $u_c$  (see appendix). For a fixed  $L_0$ , increasing the number of strings  $n_s$  results in D4-D8 configuration being pulled down more towards the horizon.

The  $U(N_f)$  gauge field A also generates Chern-Simon term,

$$S_{\rm CS} = \frac{N}{24\pi^2} \int_{M^4 \times R} \omega_5(\mathcal{A}). \tag{6.12}$$

For  $\mathcal{A} = \mathcal{A}_{\mu}dx^{\mu} + \mathcal{A}_{u}du$ , the 5-form field strength is given by

$$\omega_5(\mathcal{A}) = Tr\left(\mathcal{A}\mathcal{F}^2 - \frac{1}{2}\mathcal{A}^3\mathcal{F} + \frac{1}{10}\mathcal{A}^5\right). \tag{6.13}$$

Only the first term contains non-vanishing contribution from the U(1) part which would be identified with the number density of baryon. We will assume a uniform distribution  $n_4$ of the gas of D4-branes in  $\mathbb{R}^3$  at  $u = u_c$  in the radial direction. This leads to the relation between the number density of D4-branes,  $n_4$ , and baryon number density d [19],

$$n_4 = \frac{2\pi\alpha' R^2 \mathcal{N}}{\tau V_3 N} d. \tag{6.14}$$

Phase transition for a system where the number of particles varies is most conveniently described by the grand canonical ensemble. The grand canonical potential of each phase can be defined using the corresponding action of the D8-branes as

$$\Omega(\mu) = \frac{1}{N} S_{D8}[x_4(u), \hat{a}_0(u)]_{cl}.$$
(6.15)

The baryon chemical potential is given by the U(1) diagonal field at the boundary,

$$\mu = \hat{a}_0(\infty), \tag{6.16}$$

from which the baryon number density is determined,

$$d = -\frac{\partial \Omega(\mu)}{\partial \mu}. (6.17)$$

This justifies the association of grand canonical potential with the D8 action. When additional sources of the baryon number are introduced, the free energy,  $\mathcal{F}_E$ , from the sources will also contribute to the baryon chemical potential,

$$\mu = \frac{\partial}{\partial d} \frac{1}{\mathcal{N}} \left( \tilde{S}_{D8}[x_4(u), d(u)]_{cl} + S_{\text{source}}(d, u_c) \right) \equiv \frac{\partial \mathcal{F}_E}{\partial d}, \tag{6.18}$$

where the Legendre-transformed action  $\tilde{S}_{D8}$  is given by

$$\tilde{S}_{D8} = S_{D8} + \mathcal{N} \int_{u_*}^{\infty} d(u)\hat{a}_0' du,$$
(6.19)

$$= \mathcal{N} \int_{u_c}^{\infty} du \ u^4 \sqrt{f(u)(x_4'(u))^2 + u^{-3}} \sqrt{1 + \frac{d^2}{u^5}}.$$
 (6.20)

In our case, the additional sources are D4 and radial strings. These relations can also be applied to the vacuum phase (with broken chiral symmetry) where  $u_c$  is replaced with  $u_0$ .

Setting  $L_0 = 2 \int_{u_i=u_0,u_c}^{\infty} x_4'(u) du = 1$ , the expressions for the grand canonical potential and the chemical potential for each phase are given by

vacuum phase, d = 0:

$$\Omega_{\text{vac}} = \int_{u_0}^{\infty} du \frac{u^{5/2} \sqrt{f(u)}}{\sqrt{f(u) - \frac{u_0^8}{u^8} f(u_0)}},$$
(6.21)

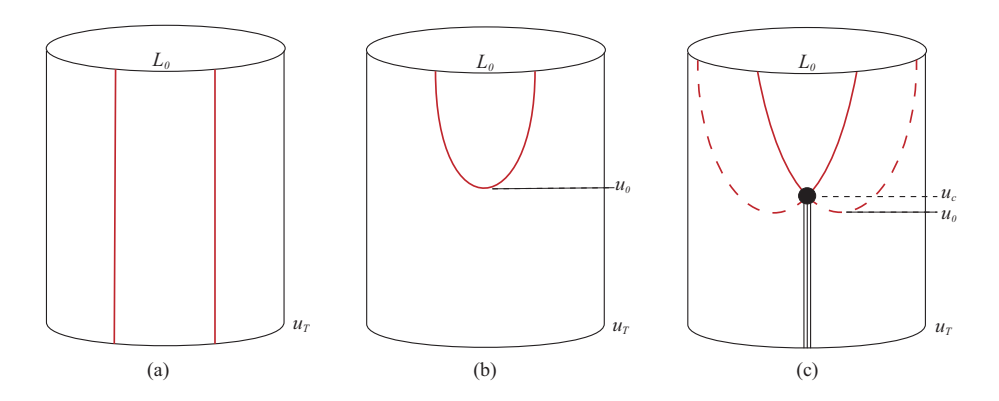


Figure 7. Configurations of  $\chi$ S-QGP (a), vacuum (b) and exotic nuclear phase (c) in  $x^4 - u$  projection.

 $\chi$ S-QGP phase,  $x'_4(u) = 0$ :

$$\Omega_{\rm qgp} = \int_{u\pi}^{\infty} du \frac{u^5}{\sqrt{u^5 + d^2}},\tag{6.22}$$

$$\mu_{\rm qgp} = \int_{u_T}^{\infty} du \frac{d}{\sqrt{u^5 + d^2}},\tag{6.23}$$

nuclear (including exotics) phase:

$$\Omega_{\text{nuc}} = \int_{u_c}^{\infty} du \left[ 1 - \frac{F^2}{f(u)(u^8 + u^3 d^2)} \right]^{-1/2} \frac{u^5}{\sqrt{u^5 + d^2}},$$
(6.24)

$$\mu_{\text{nuc}} = \int_{u_c}^{\infty} du \left[ 1 - \frac{F^2}{f(u)(u^8 + u^3 d^2)} \right]^{-1/2} \frac{d}{\sqrt{u^5 + d^2}} + \frac{1}{3} u_c \sqrt{f(u_c)} + n_s (u_c - u_T).$$
(6.25)

At a fixed temperature T and chemical potential  $\mu$ , a first order phase transition line between phase 1 and 2 is obtained when  $\Omega_1 = \Omega_2, \mu_1 = \mu_2 = \mu$ . Transitions between vacuum  $\leftrightarrow \chi$ S-QGP and  $\chi$ S-QGP  $\leftrightarrow$  nuclear phases are of this kind. On the other hand, phase transition between nuclear  $\leftrightarrow$  vacuum is second order in nature, at least for this case when there is no interaction between each D4. The second order phase transition line occurs when

$$\frac{\partial \mu}{\partial d} = \frac{\partial^2 \mathcal{F}_E}{\partial d^2} \tag{6.26}$$

has discontinuity at d = 0.

In the Sakai-Sugimoto model, there is a phase transition temperature above which gluons become deconfined. However, it does not necessarily imply that everything including quark and antiquark is totally free and chiral symmetry is completely restored above this temperature. When the baryon chemical potential is sufficiently high, baryons can exist even when the temperature is higher than the deconfinement temperature [19]. Only when the temperature increases even further that everything will be completely dissolved and the

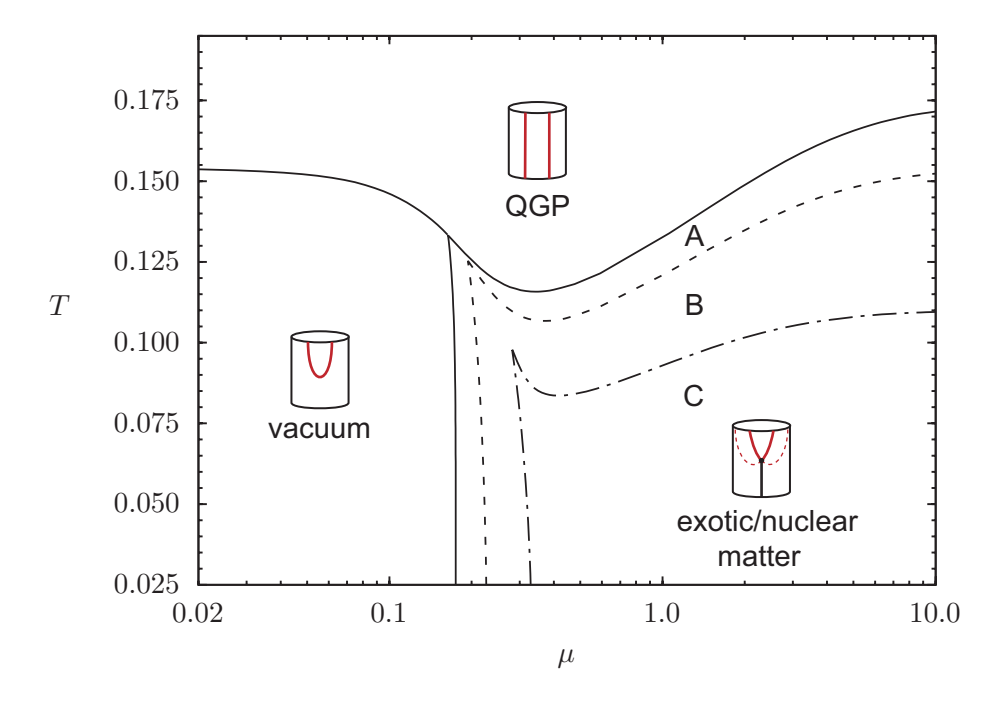


Figure 8. The phase diagram of exotic nuclear matters above the deconfinement temperature. Nuclear phase including exotics is shown as the region on the lower right corner where it is divided into 3 parts for representative purpose. A, B, C represents the region where exotic baryon phase with  $n_s = 0$  (N-baryon), 0.1, 0.3 is preferred over vacuum and  $\chi$ S-QGP respectively.

chiral symmetry is also restored. We also see this behavior in the phase diagram in figure 8 where we ignore the confined region at low temperature and present only the deconfined part of the phase diagram.

The phase diagram of vacuum with broken chiral symmetry,  $\chi$ S-QGP and phase of nuclear including exotic multi-quark states is shown in figure 8. The phase diagram involving vacuum and  $\chi$ S-QGP phases was first obtained in ref. [18] and the full phase diagram without the exotics was obtained in ref. [19]. Since the strings pull down the D4-D8 configuration towards the horizon, the configuration with  $n_s>0$  is less stable than the normal N-baryon ( $n_s=0$ ). This is shown in figure 8 where the region of  $n_s>0$  nuclear phase (B,C) is smaller than the region of N-baryon phase (A). They are actually less stable than the N-baryon since the grand canonical potential  $\Omega_{n_s>0}(T,\mu)>\Omega_{n_s=0}(T,\mu)$  for  $0.5>n_s>0$ . Above  $n_s>0.3$ , the exotic phase becomes unstable to density fluctuations ( $\frac{\partial \mu}{\partial d}<0$ ) at high temperatures in certain range of d but still remains stable in a region of parameter space. Numerical studies reveal that for approximately  $n_s>0.5$ , the multiquark states become unstable thermodynamically with respect to density fluctuations for most of the temperatures.

Addition of radial strings introduces extra source of the baryonic chemical potential. We can see from figure 8 that the value of  $\mu_{\text{onset}}$  for the exotic nuclear phase increases with the value of  $n_s$ . Nevertheless, once emerged (i.e.  $\mu > \mu_{\text{onset}}$ ), the exotic phases are more stable than the vacuum at any temperature, but less stable than  $\chi$ S-QGP at sufficiently high temperatures above which chiral symmetry is restored.

#### 7 Discussions

It is desirable to compare the binding energy of each multi-quark state in order to discuss the stability of each configuration as well as their relative abundances in the deconfined phase. At a fixed temperature T, we can compare numerically the binding energies E as functions of the size L of the configuration as is shown in figure 2, 3. For k-baryon and  $(N + \bar{k})$ -baryon, we compare the energy with N-baryon. For j-mesonance, we compare the energy with the energy of j mesons.

From figure 2, N-baryon is more energetically favoured than k-baryon and  $(N + \bar{k})$ -baryon for any value of  $k, \bar{k}$ . Since there are less hanging strings from the spacetime boundary and more radial strings pulled down into the horizon in the case of k-baryon, the vertex is located closer to the horizon and consequently becomes less energetically favoured comparing to the N-baryon. Similarly in the case of  $(N + \bar{k})$ , even though not as obvious, adding  $\bar{k}$  hanging and radial strings to the configuration of N-baryon results in positive energy increase in the binding potential, making this configuration less favoured energetically. An  $(N + \bar{k})$ -baryon naturally tends to decay into N-baryon plus  $\bar{k}$  free antiquark strings. A k-baryon also has the tendency to fuse with (N - k) quarks to form an N-baryon with lower energy.

The situation of j-mesonance is somewhat similar. Even though j mesons are always energetically preferred over j-mesonance for all value of j, j-mesonance with higher value of j has stronger binding force than the lower ones as is shown in figure 3. From the energy viewpoint, j-mesonance will prefer to split into a number of j mesons. It is notable that the screening length of j-mesonance will approach the value of meson,  $L_{\text{meson}}^*$ , but it will never exceed  $L_{\text{meson}}^*$ .

For the case of  $(N + \bar{k})$ -baryon and j-mesonance, there exist the limits  $\bar{k} \to \infty$  and  $j \to \infty$ . The first limit for  $(N + \bar{k})$ -baryon leads to the zero-size configuration which saturates the zero-force condition. The second limit for j-mesonance leads to the *mesonic* limit where the configuration is similar to the system of j mesons as we will see in the following.

From eq. (5.5), since  $A(n) \sim (j/N)^{-1}$ , A(n) becomes negligible for large j/N. Therefore, we can neglect A(n) and obtain that  $E_{F1}$  does not depend on j/N. Using asymptotic expansions, eq. (5.4) becomes

$$\mathcal{E} \simeq \left\{ \int_{1}^{\infty} dy \left[ \sqrt{\frac{y^{n} - x^{n}}{y^{n} - 1}} - 1 \right] - (1 - x) \right\}$$

$$= \left\{ u_{T} - \frac{\Gamma\left(\frac{1}{2}\right) \Gamma\left(1 - \frac{1}{n}\right)}{\Gamma\left(\frac{1}{2} - \frac{1}{n}\right)} \frac{C^{2/(n-2)}}{L^{2/(n-2)}} \right\} + \mathcal{O}(x^{n}), \tag{7.1}$$

where

$$C(n) \equiv \frac{R^{n/2}}{n} \frac{\Gamma(1 - \frac{1}{n})\Gamma(\frac{1}{2})}{\Gamma(\frac{3}{2} - \frac{1}{n})}.$$

Now, consider eq. (5.3), we find the screening length  $L_*$  (half the distance between quarks at which the binding energy is zero) by setting  $E_{\text{tot}} = 0$ . In the limit of j/N

becoming very large, we can obtain  $L_*$  from the condition

$$\mathcal{E}(L_*) = 0, \tag{7.2}$$

leading to

$$L_* \simeq \left[ \frac{\Gamma(\frac{1}{2})\Gamma(1-\frac{1}{n})}{u_T(n)\Gamma(\frac{1}{2}-\frac{1}{n})} \right]^{(n-2)/2} C(n).$$
 (7.3)

Again, the case n=3 and n=4 correspond to the Sakai-Sugimoto and the AdS-Schwarzschild gravity dual model respectively. This expression is exactly the same as the screening length of meson in the deconfined phase from ref. [20].³ It is no surprise since in the  $j\to\infty$  limit, the hanging strings from the boundary exert force overwhelmingly, therefore the "weight" of the baryon vertex plus the tension of radial strings become negligible. Effectively, the end of hanging string at the vertex will feel zero force down and thus the slope  $u'_c$  will be zero. As a result, the strings from the boundary will hang smoothly and appear similar to hanging strings in the case of the mesonic state.

Even in the deconfined phase, we therefore perceive that in addition to free quarks, antiquarks, and gluons, there will also be mesons and multi-quark states. Due to the lower energy, there are more N-baryons than  $(N+\bar{k})$ -baryons and k-baryons. The relative populations can be estimated using the Boltzmann factor

$$\exp\left(-\frac{E}{k_B T}\right),\tag{7.4}$$

determined by the corresponding binding energy E for each state.

A more precise way of considering the deconfined phase is to use the grand canonical potential as the indicator for the stable phase. Following Bergman, Lifschytz, and Lippert [19], we consider three phases of the deconfined soup, a vacuum phase and a nuclear phase with broken chiral symmetry, and a  $\chi$ S-QGP. For sufficiently high chemical potential and moderate temperature, the nuclear phase of the multiquark states is preferred over the vacuum and  $\chi$ S-QGP phase. Exotic nuclear states such as k-baryon,  $(N + \bar{k})$ -baryon, and j-mesonance are characterized by the number of radial strings  $n_s$  hanging down from the D4-branes to the horizon. It is found that the multiquark states with  $n_s > 0.5$  are unstable thermodynamically. However, all of these exotic states with  $0.5 \geq n_s > 0$  are less stable than the normal N-baryon with  $n_s = 0$ .

For each value of  $n_s$ , there exists a triple point where the grand canonical potentials of the three phases are equivalent. Varying  $n_s$ , this triple point will move along the phase transition line between vacuum and the  $\chi$ S-QGP as is shown in figure 8. The stable region of the nuclear phase shrinks as  $n_s$  increases. As  $n_s > 0.5$ , the nuclear phase becomes thermodynamically unstable with respect to the density fluctuations for most of the parameter space.

## 8 Conclusion

The gravity dual picture of the deconfined phase suggests that the binding energy or potential between quarks and antiquarks in this phase is nonzero due to the Coulombic

³Our definition of the screening length is one-half of the definition in ref. [20].

piece of the interaction. Since the colorless condition is not required in the deconfined phase, exotic configurations of the multiquark states are possible. We investigate three classes of these configurations, k-baryon,  $(N + \bar{k})$ -baryon, and j-mesonance. It is found that all of these configurations are less energetically favoured than the normal N-baryon as well as being less stable thermodynamically.

The dependence of the screening length on the parameters  $k, \bar{k}, j$  is studied and the results are shown in figure 4-6. The screening length of k-baryon and j-mesonance are notably increasing with the values of k and j whereas the screening length of  $(N + \bar{k})$ -baryon is a decreasing function of  $\bar{k}$ . Interestingly, j-mesonance has saturated value of screening length equal to the screening length of meson as  $j \to \infty$ .

The dependence on the quark mass of the binding potential at the leading order is derived and found to be  $\sim m^{1-n}$  (n=3,4 for the Sakai-Sugimoto, AdS-Schwarzschild model). The linear quark-mass dependence of the rest energy that we naturally expect is included in the regulator and therefore not present in the binding potential.

In order to consider phase diagram involving exotic nuclear phase, we consider the Sakai-Sugimoto model where the flavour branes D8 and  $\overline{D8}$  are introduced. The flavour D8-branes action is identified with the grand canonical potential of the relevant phase. The nuclear phase is considered in the limit when the D4-branes are pulled all the way up to the flavour branes. Exotic multiquark states with a number of strings stretched down to the horizon, i.e.  $n_s > 0$ , become less stable than normal N-baryon  $(n_s = 0)$  since radial strings attached to the D4-branes pull the D4-D8 configuration closer to the horizon. Nevertheless, comparing to the vacuum and  $\chi$ S-QGP phase, the nuclear phase of exotic multiquark states can be more stable in a region of phase diagram with high chemical potential and low temperature as is shown in figure 8. In this region, we expect to have a nuclear phase where N-baryons, k-baryons, and (N+k)-baryons coexist. For j-mesonance with  $n_s=1$ , our consideration of the grand canonical potential suggests that it is thermodynamically unstable to density fluctuations since  $\frac{\partial \mu}{\partial d} < 0$ . Generically, numerical studies reveal that exotic baryons with  $n_s > 0.5$  (namely k-baryon with k/N < 0.5,  $(N + \bar{k})$ -baryon with k/N > 0.5 and any j-mesonance) in the deconfined phase are thermodynamically unstable to density fluctuations.

### Acknowledgments

We would like to thank Wen-Yu Wen, Ahpisit Ungkitchanukit and Kazuyuki Furuuchi for valuable comments. E.H. is supported by the Commission on Higher Education (CHE), Thailand under the program Strategic Scholarships for Frontier Research Network for the Ph.D. Program Thai Doctoral Degree for this research. P.B. and A.C. is supported in part by the Thailand Research Fund (TRF) and Commission on Higher Education (CHE) under grant MRG5180227 and MRG5180225 respectively.

#### A Force condition at the D8-branes

There are three forces acting on a D4 locating inside the D8-branes, one from the D8, another from the radial strings pulling down towards horizon and lastly the force from its own "weight" in the background. The equilibrium can be sustained only when these three forces are balanced. As is shown in ref. [19], variation of the total action with respect to  $u_c$  and the constant of motion with respect to  $x_4(u)$  lead to

$$x_4'(u_c) = \left(\tilde{L}(u_c) - \frac{\partial S_{\text{source}}}{\partial u_c}\right) / \frac{\partial \tilde{S}_{D8}}{\partial x_4'} \bigg|_{u_c}, \tag{A.1}$$

$$= \frac{1}{d} \sqrt{\frac{9u_c^2(1 + \frac{d^2}{u_c^5})}{1 + \frac{1}{2}(\frac{u_T}{u_c})^3 + 3n_s\sqrt{f(u_c)}} - \frac{d^2u_c^{-3}}{f(u_c)}}$$
(A.2)

where the Legendre transformed action is

$$\tilde{S}_{D8} = \int_{u_c}^{\infty} \tilde{L}(x_4'(u), d) du,$$
(A.3)

$$= \mathcal{N} \int_{u_c}^{\infty} du \ u^4 \sqrt{f(u)(x_4'(u))^2 + u^{-3}} \sqrt{1 + \frac{d^2}{u^5}}, \tag{A.4}$$

and the source term is given by

$$S_{\text{source}} = \mathcal{N}d \left[ \frac{1}{3} u_c \sqrt{f(u_c)} + n_s (u_c - u_T) \right]. \tag{A.5}$$

There are two contributions from the D-branes and strings as the sources for the baryon chemical potential. Additional strings increase the baryonic chemical potential of the exotic multiquark states. Since the number of total charge on each D4 is N which is absorbed into  $\mathcal{N}$ , the number of radial strings stretched down to the horizon,  $n_s$ , is thus given in unit of 1/N.

#### References

- J.M. Maldacena, The large-N limit of superconformal field theories and supergravity, Adv. Theor. Math. Phys. 2 (1998) 231 [Int. J. Theor. Phys. 38 (1999) 1113] [hep-th/9711200]
   [SPIRES].
- [2] O. Aharony, S.S. Gubser, J.M. Maldacena, H. Ooguri and Y. Oz, *Large-N field theories*, string theory and gravity, *Phys. Rept.* **323** (2000) 183 [hep-th/9905111] [SPIRES].
- [3] E. Witten, Baryons and branes in Anti de Sitter space, JHEP 07 (1998) 006 [hep-th/9805112] [SPIRES].
- [4] D.J. Gross and H. Ooguri, Aspects of large-N gauge theory dynamics as seen by string theory, Phys. Rev. D 58 (1998) 106002 [hep-th/9805129] [SPIRES].
- [5] Y. Imamura, String junctions and their duals in heterotic string theory, Prog. Theor. Phys. 101 (1999) 1155 [hep-th/9901001] [SPIRES].

- [6] C.G. Callan, A. Guijosa and K.G. Savvidy, Baryons and string creation from the fivebrane worldvolume action, Nucl. Phys. B 547 (1999) 127 [hep-th/9810092] [SPIRES].
- [7] C.G. Callan Jr., A. Guijosa, K.G. Savvidy and O. Tafjord, Baryons and flux tubes in confining gauge theories from brane actions, Nucl. Phys. B 555 (1999) 183
   [hep-th/9902197] [SPIRES].
- [8] A. Brandhuber, N. Itzhaki, J. Sonnenschein and S. Yankielowicz, Baryons from supergravity, JHEP 07 (1998) 020 [hep-th/9806158] [SPIRES].
- [9] K. Ghoroku, M. Ishihara, A. Nakamura and F. Toyoda, Multi-quark baryons and color screening at finite temperature, Phys. Rev. D 79 (2009) 066009 [arXiv:0806.0195]
   [SPIRES].
- [10] K. Ghoroku and M. Ishihara, Baryons with D5 brane vertex and k-quarks, Phys. Rev. **D** 77 (2008) 086003 [arXiv:0801.4216] [SPIRES].
- [11] M.V. Carlucci, F. Giannuzzi, G. Nardulli, M. Pellicoro and S. Stramaglia, AdS-QCD quark-antiquark potential, meson spectrum and tetraquarks, Eur. Phys. J. C 57 (2008) 569 [arXiv:0711.2014] [SPIRES].
- [12] W.-Y. Wen, Multi-quark potential from AdS/QCD, Int. J. Mod. Phys. A 23 (2008) 4533 [arXiv:0708.2123] [SPIRES].
- [13] T. Sakai and S. Sugimoto, Low energy hadron physics in holographic QCD, Prog. Theor. Phys. 113 (2005) 843 [hep-th/0412141] [SPIRES].
- [14] T. Sakai and S. Sugimoto, More on a holographic dual of QCD, Prog. Theor. Phys. 114 (2005) 1083 [hep-th/0507073] [SPIRES].
- [15] E. Witten, Anti-de Sitter space, thermal phase transition, and confinement in gauge theories, Adv. Theor. Math. Phys. 2 (1998) 505 [hep-th/9803131] [SPIRES].
- [16] O. Aharony, J. Sonnenschein and S. Yankielowicz, A holographic model of deconfinement and chiral symmetry restoration, Annals Phys. 322 (2007) 1420 [hep-th/0604161] [SPIRES].
- [17] K.Y. Kim, S.J. Sin and I. Zahed, Dense hadronic matter in holographic QCD, hep-th/0608046 [SPIRES].
- [18] N. Horigome and Y. Tanii, *Holographic chiral phase transition with chemical potential*, JHEP **01** (2007) 072 [hep-th/0608198] [SPIRES].
- [19] O. Bergman, G. Lifschytz and M. Lippert, Holographic nuclear physics, JHEP 11 (2007) 056 [arXiv:0708.0326] [SPIRES].
- [20] O. Antipin, P. Burikham and J. Li, Effective quark antiquark potential in the quark gluon plasma from gravity dual models, JHEP 06 (2007) 046 [hep-ph/0703105] [SPIRES].
- [21] P. Burikham and J. Li, Aspects of the screening length and drag force in two alternative gravity duals of the quark-gluon plasma, JHEP 03 (2007) 067 [hep-ph/0701259] [SPIRES].



RECEIVED: September 7, 2009 REVISED: February 14, 2010 ACCEPTED: March 27, 2010 PUBLISHED: April 12, 2010

# Magnetic properties of holographic multiquarks in the quark-gluon plasma

#### Piyabut Burikham

Theoretical High-Energy Physics and Cosmology Group, Department of Physics, Faculty of Science, Chulalongkorn University, Bangkok 10330, Thailand

E-mail: piyabut@gmail.com

ABSTRACT: We study the magnetic properties of the coloured multiquark states in the quark-gluon plasma where the gluons are deconfined and the chiral symmetry is still broken, using the Sakai-Sugimoto model. There are two possible magnetized multiquark configurations. Both configurations converge to the same configuration at the critical field and temperature before they dissociate altogether either into less coloured multiquarks or into other phases for a fixed density. It is also found that the multiquarks with higher colour charges respond more to the external magnetic field in both the magnetization and the degree of chiral symmetry breaking. Magnetic field also makes it more difficult for multiquark states with large colour charges to satisfy the equilibrium condition of the configuration in the gravity dual picture. As long as the chemical potential  $\mu > \mu_{onset}$ , the magnetized multiquark phase is thermodynamically preferred over the magnetized vacuum. Pure pion gradient and the chiral-symmetric quark-gluon plasma ( $\chi_S$ -QGP) phase for the general Sakai-Sugimoto model are discussed and compared with the multiquark phase in the presence of the magnetic field. It is found that at large densities and moderate fields, the mixed phase of multiquarks and the pion gradient is thermodynamically preferred over the  $\chi_S$ -QGP.

Keywords: Brane Dynamics in Gauge Theories, D-branes

ARXIV EPRINT: 0909.0614

C	ontents	
1	Introduction	1
2	Exotic multiquark states in the Sakai-Sugimoto model	3
3	Magnetic properties of the coloured multiquarks in the nuclear phase	4
4	Comparison to other phases	13
	4.1 Pure pion gradient phase	13
	4.2 Multiquark-domain wall versus $\chi_S$ -QGP phase	14
5	Discussions and conclusion	18
A	Force condition of the multiquark configuration	19

#### 1 Introduction

There has been increasing interest in the study of nuclear phase structure as well as properties of a number of nuclear phases, especially the quark-gluon plasma in the recent few years. This is due to the new perspective in the nature of strongly interacting gauge theory from the holographic principle. Motivated by the AdS/CFT correspondence [1, 2], a number of gravity models was constructed to provide shadow gauge theories which share certain essential features with the QCD in the strong coupling regime. Sakai and Sugimoto [3, 4] proposed a toy holographic model of QCD where chiral symmetry breaking can be addressed. In Sakai-Sugimoto model, gluon deconfinement and chiral symmetry restoration are two distinct phase transitions. For non-antipodal case, the chiral symmetry restoration occurs at higher temperature than the gluon deconfinement [5], therefore it is possible to have a nuclear phase where gluons are deconfined while the quarks and antiquarks could still form colour bound states.

Bergman, Lifschytz, and Lippert [6] shows that when the baryon density is sufficiently large and the temperature is not too high, gluon-deconfined phase with broken chiral symmetry accommodates a nuclear phase where baryons can exist with thermodynamical stability. Even though the baryons can exist within the phase, the quark matters containing only free quarks or antiquarks do not share the same thermodynamical stability. This can be understood as a sign of chiral symmetry breaking, the quarks prefer to be bound together by gluon exchanges in this highly-densed thermal soup. Interestingly, further investigations into whether colour multiquark states in general could exist within this nuclear phase give positive results [7].

It was suggested quite a while ago in ref. [8] that it is possible to have k < N-baryons in  $\mathcal{N}_{SUSY} = 4$  background. In the gluon-deconfined phase, since free strings solution is

allowed in the corresponding gravity dual theories [9], the coloured states could also exist in the plasma. Various possibilities of exotic multiquark states are studied in ref. [10]–[13]. Colour multiquark states in the gluon-deconfined plasma are studied in ref. [7] where k > N-baryons as well as other classes of exotic multiquark states including  $N + \bar{k}$ -baryons and bound state of j mesons are investigated. The phase diagram of the colour multiquarks nuclear phase, chiral-symmetric ( $\chi$ S-QGP) phase, and the vacuum nuclear phase reveals that colour multiquarks are thermodynamically stable in the region where the temperature is not too high and the density is sufficiently large (figure 8 of ref. [7]).

In certain situations such as in the core of the neutron stars or other enormously densed astrophysical objects, exceptionally strong magnetic field is produced in addition to the high temperature and density. Under these fierce conditions, nuclear matters are pressed together so tightly that deconfinement phase transition could occur. As is shown in the phase diagram of ref. [7], coloured multiquark states can exist in the intermediate range of temperature and sufficiently high baryon chemical potential (implying high baryon density). They are thermodynamically preferred over the other phases such as the vacuum and the chiral-symmetric deconfined phase of quark-gluon plasma ( $\chi$ S-QGP). It is therefore interesting to explore magnetic properties of the nuclear phase where coloured exotic multiquarks exist under these extreme situations. It is possible that certain classes of densed stars are in the range of temperature and density suitable for the coloured multiquarks in the gluon-deconfined soup and the magnetic properties of these states thus significantly determine their stellar structures.

Responses of the holographic nuclear matter to the external magnetic field have been intensively investigated in ref. [14]–[19]. It was found in ref. [14] that the external magnetic field makes gluon-deconfined vacuum more stable thermodynamically than the case when there is no magnetic field, i.e. the transition temperature into the chiral-symmetric quarkgluon plasma increases with the magnetic field and saturates in the limit of an infinite field. Authors of ref. [19] found a phase transition induced by the external magnetic field in the  $\chi$ S-QGP phase. This could be traced back to the nonlinearity of the DBI action used to describe the holographic nuclear matter. Since this transition occurs when the magnetic field changes from small to large strength, the Yang-Mills approximation approach [17] is no longer valid and similar transition is not found without consideration of the full DBI action. We take the full DBI approach and investigate the magnetic responses of the multiquark nuclear phase with broken chiral symmetry in this article. We found that the magnetized multiquark phase are always thermodynamically preferred over the magnetized vacuum. At a fixed density, it is also found that the multiquark states can satisfy the scale fixing condition up to certain critical values beyond which they would change into multiquarks with smaller colour charges. For higher magnetic fields, all of the multiquarks cannot satisfy the scale fixing condition at the same density and we would expect other phases to set in or the density has to be increased for the multiquark configuration to be able to satisfy the scale fixing condition.

There are two multiquark configurations found below a critical field. The two configurations merge into one at the critical field and temperature for a fixed density. By comparing to the pure pion gradient and the  $\chi$ S-QGP phase, the multiquark phase is found to be preferred thermodynamically at large densities and moderate fields.

In section 2, the essential features of the multiquarks are reviewed. Magnetic responses and relevant magnetic phases of the colour multiquarks are studied in section 3 using the DBI action. Comparison to the pure pion gradient and the  $\chi$ S-QGP phase is discussed in section 4. We discuss the results and make some conclusions in section 5.

# 2 Exotic multiquark states in the Sakai-Sugimoto model

In the Sakai-Sugimoto model, gluon deconfinement and the chiral-symmetry restoration are two distinct phase transitions. Generically they occur at different temperatures. When the gluons become deconfined at the deconfinement phase transition, quarks could still be bound together by the free gluons due to the fact that the coupling is still strong (provided that the density is sufficiently high) and therefore the chiral symmetry could still be broken. Due to the deconfinement, the bound states of multiquarks are not colour singlet in general. Certain properties of the coloured multiquarks are studied in ref. [7] where it is demonstrated that the coloured states could exist with thermodynamical stability. When the temperature rises further, the bound states become less and less stable and finally completely dissolved into the quark-gluon plasma. The chiral symmetry is restored and everything becomes completely deconfined.

It was proposed by Witten [20], Gross and Ooguri [21] that a D-brane wrapping internal subspace of a holographic background could describe a colour-singlet bound state of N quarks in the dual  $\mathrm{U}(N)$  gauge theory. A wrapping D-brane sources  $\mathrm{U}(1)$  gauge field on its world volume and induces an N units of  $\mathrm{U}(1)$  charge upon itself. This charge needs to be cancelled by N external strings connecting to the wrapping brane. The wrapping brane with N strings attached is called a baryon vertex.

In the gluon-deconfined phase, more strings can be attached to the baryon vertex provided that there are equal number of strings stretching out and go to the background horizon. This configuration still conserves the U(1) charge of the brane and solve the equation of motion of the Nambu-Goto action [9]. We can parameterize the number of radial strings stretching from the vertex to the horizon as  $k_r$  and the number of strings connecting the vertex to the boundary of the background as  $k_h$ . For the k > N-baryon,  $k_h - k_r = N$  whilst for k < N-baryon,  $k_h + k_r = N$ . Other classes of exotic multiquark states can be constructed by adding more strings in and out of the vertex. Few examples are given in ref. [7] where some interesting properties are also discussed.

There could exist an interaction among the multiquarks in the form of connecting strings between each vertex very similar to the string connecting two end points of quark and antiquark in the holographic meson configuration. A multiquark can use one of the radial strings to merge with another radial string from neighbouring multiquark and form a colour binding interaction (while keeping  $k_h$  fixed). Therefore the number of radial strings represents the colour charges of the multiquark. When the gluons are deconfined, the "direct" colour interaction would be approximately the same as the meson and baryon binding potential of the Coulomb type plus some screening effect. Neglecting the direct interaction and considering only the DBI-induced collective behaviour of the gas of multiquarks [6, 7], an approximate phase diagram can be obtained showing exotic nuclear phase

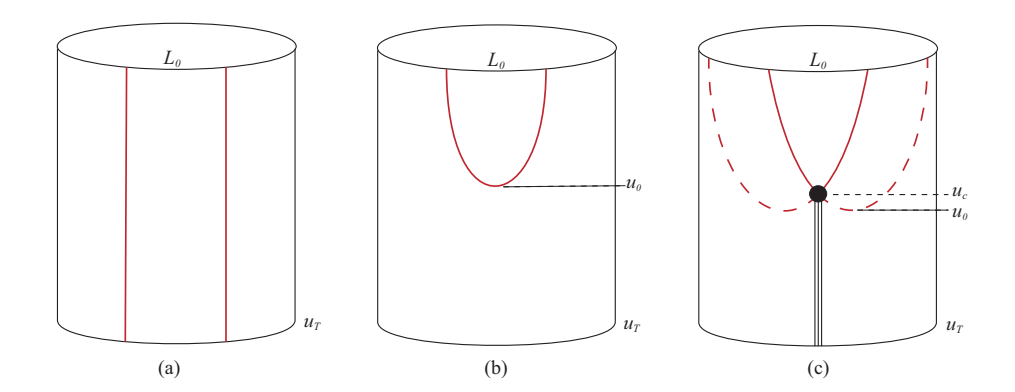


**Figure 1**. Configurations of  $\chi$ S-QGP (separate D8,  $\overline{D8}$ )(a), vacuum (merging D8 and  $\overline{D8}$ )(b) and exotic nuclear phase (vertex attached to the D8- $\overline{D8}$  with radial strings stretch down to horizon)(c).

where multiquarks can exist with thermodynamic stability. Schematic configurations of the three gluon-deconfined phases are given in figure 1 where the direction along the circle is the compactified coordinate  $x_4$  and the vertical direction is the radial coordinate u.

# 3 Magnetic properties of the coloured multiquarks in the nuclear phase

The setup we use is the Sakai-Sugimoto (SS) model with the source terms from the instanton embedded in the  $D8 - \overline{D8}$  configuration, and the radial strings similar to the configuration used in ref. [7]. The instanton (the baryon vertex being pulled up all the way to the position of the D8-branes by the strings connecting between the vertex and the flavour branes) is embedded within the D8-branes and acts as a source for the baryon density, d. The radial strings stretching from the instanton down to the horizon of the background act as another source. The number of radial strings is parameterized by  $n_s = (\text{number of radial strings})/N$ . It also tells us how much colour charges a multiquark has.

The baryon chemical potential is also generated on the D8-branes by the vector part,  $a_0^V$ , of the U(1) subgroup of the U( $n_f$ ) flavour group of the D8-branes. The magnetic field is then turned on by another part of the U(1). We choose the direction of the magnetic field so that the vector potential is

$$a_3^V = Bx_2. (3.1)$$

The vector part  $a_0^V$  is related to the baryon chemical potential  $\mu$  by

$$\mu = a_0^V(u \to \infty),$$

$$a_0^V(u_c) = \mu_{\text{source}},$$

$$\mu_{\text{source}} = \frac{1}{N} \frac{\partial S_{\text{source}}}{\partial d}.$$
(3.2)

The contributions from the sources,  $\mu_{\text{source}}$ , are from the baryon vertex and the radial strings. The full expressions are given in the appendix. The contribution from the U(1) vector gauge field in the D8-branes,  $\mu$ , corresponds to the baryon chemical potential from

the content of the plasma. The five-dimensional Chern-Simon term of the D8-branes generates another axial part of the U(1),  $a_1^A$ , by coupling it with B and  $a_0^V$ . In this way, the external magnetic field induces the axial current  $j_A$  associated with the axial field  $a_1^A$ .

The background metric of the Sakai-Sugimoto model is

$$ds^{2} = \left(\frac{u}{R_{\rm D4}}\right)^{3/2} \left(f(u)dt^{2} + \delta_{ij}dx^{i}dx^{j} + dx_{4}^{2}\right) + \left(\frac{R_{\rm D4}}{u}\right)^{3/2} \left(u^{2}d\Omega_{4}^{2} + \frac{du^{2}}{f(u)}\right)$$
$$F_{(4)} = \frac{2\pi N}{V_{4}}\epsilon_{4}, \qquad e^{\phi} = g_{s}\left(\frac{u}{R_{\rm D4}}\right)^{3/4}, \qquad R_{\rm D4}^{3} \equiv \pi g_{s}Nl_{s}^{3},$$

where  $f(u) \equiv 1 - u_T^3/u^3$ ,  $u_T = 16\pi^2 R_{\rm D4}^3 T^2/9$ . The volume of the unit four-sphere  $\Omega_4$  is denoted by  $V_4$  and the corresponding volume 4-form by  $\epsilon_4$ .  $l_s$  and  $g_s$  are the string length scale and the string coupling. The  $x_4$  coordinate is compactified with radius R which is generically different from the curvature  $R_{D4}$  of the background.

The DBI and the Chern-Simon actions of the D8-branes in this background can be computed to be

$$S_{D8} = \mathcal{N} \int_{u_0}^{\infty} du \ u^{5/2} \sqrt{1 + \frac{B^2}{u^3}} \sqrt{1 + f(u)(a_1'^A)^2 - (a_0'^V)^2 + f(u)u^3 x_4'^2}$$
 (3.3)

$$S_{\rm CS} = -\frac{3}{2} \mathcal{N} \int_{u_0}^{\infty} du \, \left( \partial_2 a_3^V a_0^V a_1^{A\prime} - \partial_2 a_3^V a_0^{V\prime} a_1^A \right). \tag{3.4}$$

The normalization factor,  $\mathcal{N}=NR_{D4}^2/(6\pi^2(2\pi\alpha')^3)$ , represents the brane tension. The explanation of the factor 3/2 is given in ref. [16] where it could be understood as representing the edge effect of the finite region with uniform magnetic field. The equations of motion with respect to  $a_0^V$ ,  $a_1^A$  are

$$\frac{\sqrt{u^5 + B^2 u^2} f(u) a_1^{\prime A}}{\sqrt{1 + f(u)(a_1^{\prime A})^2 - (a_0^{\prime V})^2 + f(u)u^3 x_4^{\prime 2}}} = j_A - \frac{3}{2} B\mu + 3Ba_0^V, \tag{3.5}$$

$$\frac{\sqrt{u^5 + B^2 u^2} \ a_0^{\prime V}}{\sqrt{1 + f(u)(a_1^{\prime A})^2 - (a_0^{\prime V})^2 + f(u)u^3 x_4^{\prime 2}}} = d - \frac{3}{2} B a_1^A(\infty) + 3B a_1^A. \tag{3.6}$$

The quantities  $d, j_A$  are the corresponding density and current density at the boundary of the background  $(u \to \infty)$ , they are defined to be

$$j^{\mu}(x, u \to \infty) = \frac{\delta S_{\text{eom}}}{\delta A_{\mu}} \bigg|_{u \to \infty}$$
 (3.7)

$$= (d, \vec{j_A}). \tag{3.8}$$

Explicitly, they are

$$d = \frac{\sqrt{u^5 + B^2 u^2} \ a_0^{\prime V}}{\sqrt{1 + f(u)(a_1^{\prime A})^2 - (a_0^{\prime V})^2 + f(u)u^3 x_4^{\prime 2}}} \bigg|_{\infty} - \frac{3}{2} B a_1^A(\infty), \tag{3.9}$$

$$j_A = \frac{\sqrt{u^5 + B^2 u^2} f(u) a_1^{\prime A}}{\sqrt{1 + f(u)(a_1^{\prime A})^2 - (a_0^{\prime V})^2 + f(u)u^3 x_4^{\prime 2}}} \bigg|_{\infty} - \frac{3}{2} B\mu.$$
 (3.10)

For our multiquark configuration, the D8-branes starts from  $u = u_c$  and extends to  $u \to \infty$ . At the boundary  $(u \to \infty)$ , the chiral symmetry is broken and therefore the value of  $a_1^A(\infty)$  is taken to be a physical field,  $\nabla \varphi$  [16], describing the degree of chiral symmetry breaking. The total action is minimized with respect to  $a_1^A(\infty)$  if the axial current  $j_A$  (also defined at the boundary) is zero.

The total action does not depend on  $x_4(u)$  explicitly, therefore the constant of motion leads to

$$(x_4'(u))^2 = \frac{1}{u^3 f(u)} \left[ \frac{u^3 \left[ f(u)(C(u) + D(u)^2) - \left( j_A - \frac{3}{2}B\mu + 3Ba_0^V \right)^2 \right]}{F^2} - 1 \right]^{-1}, (3.11)$$

where

$$F = \frac{u_c^3 \sqrt{f(u_c)} \sqrt{f(u_c)(C(u_c) + D(u_c)^2) - (j_A - \frac{3}{2}B\mu + 3Ba_0^V(u_c))^2} x_4'(u_c)}{\sqrt{1 + f(u_c)u_c^3 x_4'^2(u_c)}}$$
(3.12)

and  $C(u) \equiv u^5 + B^2 u^2$ ,  $D(u) \equiv d + 3Ba_1^A(u) - 3B\nabla\varphi/2$ . The expression of  $x_4'(u_c)$  is given in the appendix. It is determined from the force condition and the scale fixing condition

$$L_0 = 2 \int_{u_c}^{\infty} x_4'(u) \ du = 1. \tag{3.13}$$

Since  $x_4'(u)$  depends on both  $a_0^V(u), a_1^A(u)$ , we need to solve the differential equations (3.5) and (3.6) with  $x_4'(u)$  substituted into the equations of motion and check whether the solutions satisfy the scale fixing condition eq. (3.13). The values of the vector and axial field at the vertex are also chosen so that  $a_0^V(u_c) = \mu_{source}, a_1^A(u_c) = 0$ . We basically perform the shooting algorithm by choosing the value of  $\mu$  and  $\nabla \varphi$  in the expression for  $x_4'(u_c)$  until we hit  $a_0^V(\infty) = \mu$  and  $a_1^A(\infty) = \nabla \varphi$ . If the resulted solution satisfies the scale fixing condition  $L_0 = 1$ , we keep the solution. If not, we adjust the value of  $u_c$  and perform the shooting procedure again. The position  $u_c$  for  $n_s = 0$  is given as a function of the density, the magnetic field, and the temperature in figure 2.

From the solutions of the equations of motion, the relations between baryon chemical potential  $(\mu)$  and the baryon density (d), the magnetic field (B), and the temperature (T) are obtained for the choice of parameters  $n_s = 0$  (normal baryon),  $j_A = 0$ , as are shown in figure 3. There are two types of solution corresponding to the two holographic multiquark configurations. One is the configuration with  $u_c$  close to  $u_T$  (configuration- $\mathbf{A}$ ) and another is the configuration with a large separation between  $u_c$  and  $u_T$  (configuration- $\mathbf{B}$ ).

The baryon chemical potential is found to be an increasing function of the density for most range of d for both configuration  $\mathbf{A}$ , $\mathbf{B}$ . As is shown in figure 2, configuration- $\mathbf{A}$  has the position of vertex  $u_c$  closer to the horizon  $u_T$  than configuration- $\mathbf{B}$ . At very small d, the two configurations emerge separately as two distinct configurations. Interestingly, as the magnetic field and temperature increase, the two configurations converge into a single configuration as we can see the position  $u_c$  approaches the same value at the critical field and temperature (see figure 2). However, when the two configurations merge, the configuration no longer satisfies the scale fixing condition  $L_0 = 1$  and we expect it to change into other

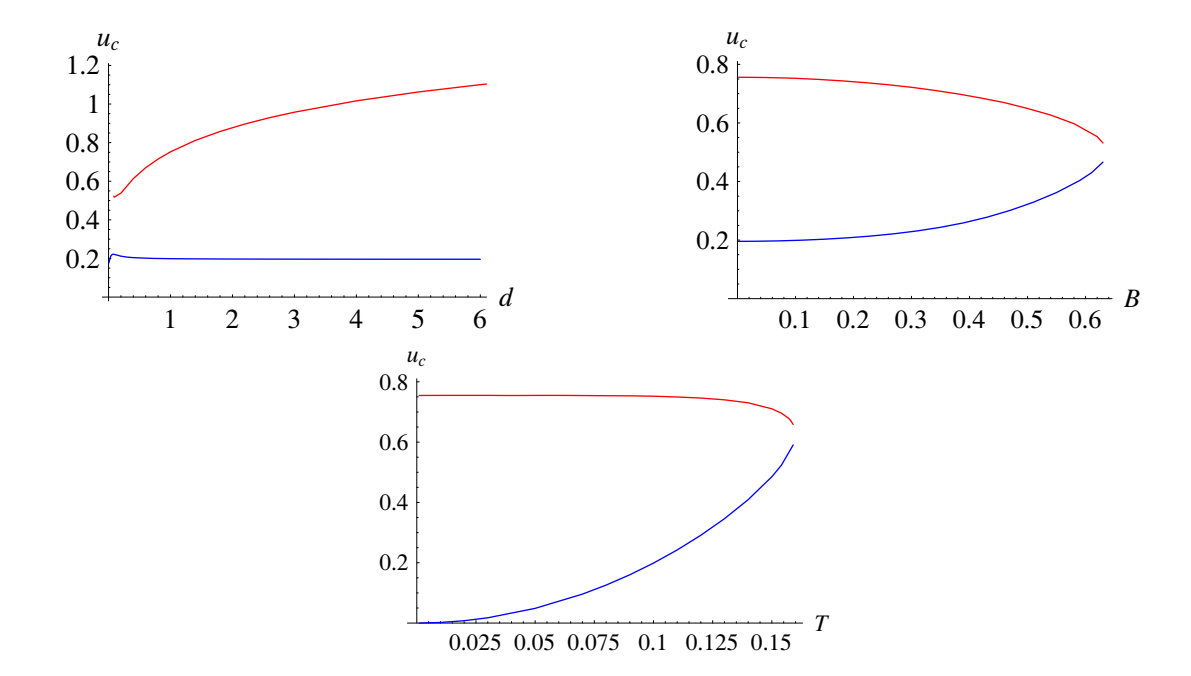


Figure 2. Position  $u_c$  of the vertex for  $n_s = 0$  (normal baryon) and fixed  $j_A = 0$  as a function of (a) d with fixed B = 0.10, T = 0.10,(b) B with fixed d = 1, T = 0.10,(c) T with fixed B = 0.10, d = 1. The lower (blue) line is the configuration-A with  $u_c$  close to  $u_T$  and the upper (red) line is the configuration-B with large separation between  $u_c$  and  $u_T$ .

phases such as the chiral-symmetric quark-gluon plasma for a fixed density. It turns out that if the density is allowed to change, the multiquark configuration can continue to satisfy the scale fixing condition at higher fields provided that the density is sufficiently large. This will be discussed more in section 4.

In figure 3, the baryon chemical potential is an increasing function of d, this is true for both configuration-A and B. It is roughly a linear function of the density, showing that the DBI-induced collective interaction between the multiquarks are negligible. As d gets larger, the DBI-induced effect sets in and the negative binding interaction makes  $\mu$  grows with d less quickly than the linear progression. Note that this DBI-induced interaction occurs even when the baryon is colour singlet due to the nonlinear nature of the DBI action. The origin of this DBI-induced interaction is the "tidal weight" of the DBI action contributed from both the branes' worldsheet metric and the background gauge field strength. Naturally, any form of energy contributes to the tidal weight even the colour singlets.

For configuration-**B**, there seems to be minimal density  $d_{\min}$  below which the shooting algorithm could not find other valid solutions. We are not certain what happens below these values. It is possible that when the field is turned on, the D8-branes acquire higher tension and therefore the configuration requires minimal density to pull it down in order for the distance between D8 and  $\overline{D8}$  to reach  $L_0 = 1$ . For  $T = 0.10, B = 0.10, n_s = 0$ , the value of  $d_{\min}$  for multiquark configuration **B** is approximately 0.086.

Figure 3 shows that the chemical potential is a decreasing function with respect to the magnetic field. This is similar to the behaviour of baryons in chiral-symmetric quark-gluon

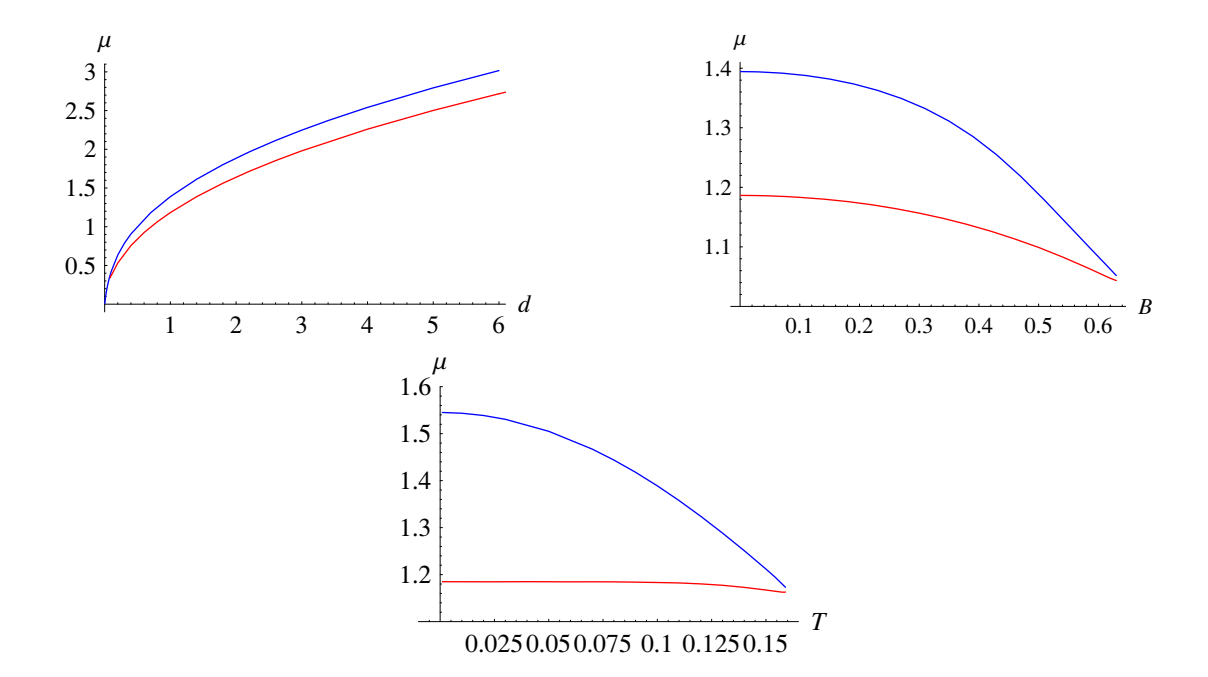


**Figure 3**. The baryon chemical potential  $\mu$  for  $n_s = 0$  (normal baryon) and fixed  $j_A = 0$  as a function of (a) d with fixed B = 0.10, T = 0.10,(b) B with fixed d = 1, T = 0.10,(c) T with fixed B = 0.10, d = 1. The upper (blue) line is the configuration-**A** with  $u_c$  close to  $u_T$  and the lower (red) line is the configuration-**B** with large separation between  $u_c$  and  $u_T$ .

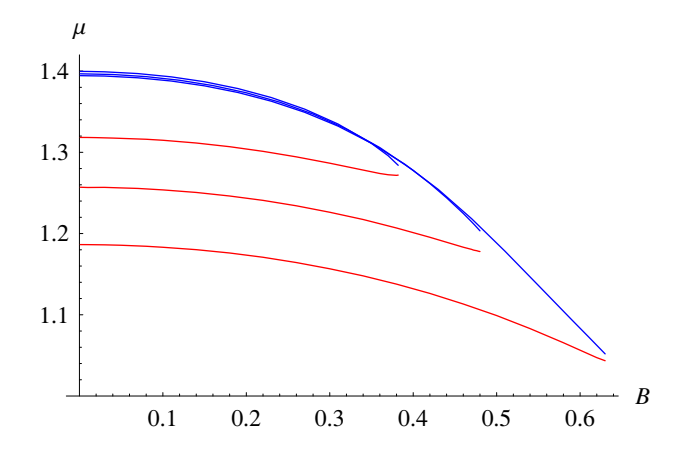


**Figure 4.** Comparison between the baryon chemical potential as a function of B at fixed  $j_A = 0$ , d = 1, T = 0.10 and (a)  $n_s = 0$  (normal baryon), the bottom graph,(b)  $n_s = 0.10$ , the middle graph, (c)  $n_s = 0.20$ , the top graph. The upper (blue) lines are the configuration-**A** with  $u_c$  close to  $u_T$  and the lower (red) lines are the configuration-**B** with large separation between  $u_c$  and  $u_T$ .

plasma studied in ref. [16]. When the field gets stronger up to certain values, the field becomes too strong for the force condition to hold at the scale fixing  $L_0 = 1$ . This strange behaviour is shown in figure 4 where multiquarks with smaller  $n_s$  are shown to be able to exist up to stronger fields.

As is also shown in figure 3, the relationship between  $\mu$  and T is as we expect, a

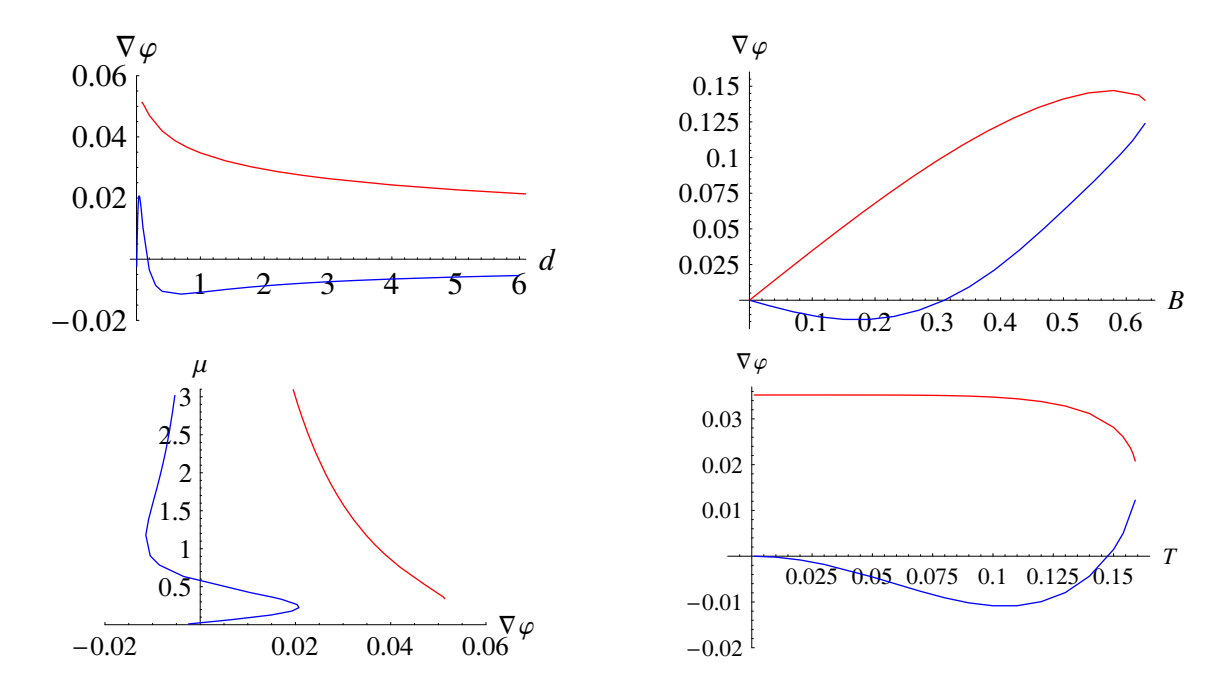


Figure 5. The gradient of the scalar field  $\nabla \varphi \equiv a_1^A(\infty)$  for  $n_s = 0$  (normal baryon) and fixed  $j_A = 0$  as a function of (a) d with fixed B = 0.10, T = 0.10,(b) B with fixed d = 1, T = 0.10,(c)  $\mu$  with fixed B = 0.10, T = 0.10,(d) T with fixed B = 0.10, d = 1. The lower (blue) line is the configuration- $\mathbf{A}$  with  $u_c$  close to  $u_T$  and the upper (red) line is the configuration- $\mathbf{B}$  with large separation between  $u_c$  and  $u_T$ .

decreasing function of T for fixed density d since higher temperature will melt the multiquarks away. For fixed d and B, the multiquark configuration satisfies the scale fixing condition up to a maximum temperature above which we expect it to melt into the plasma. For  $n_s = 0$ , this critical temperature is about 0.159 for d = 1.

It is interesting to note that the baryon chemical potential of  $n_s = 0$  multiquarks for both configurations converge to the same value at critical field ( $\simeq 0.63$ ) and temperature ( $\simeq 0.159$ ) for d = 1. This behaviour also shows up in the gradient scalar field as is shown in figure 5.

Figure 5 shows the relations between the field  $\nabla \varphi$  and the density, the magnetic field, the baryon chemical potential, and the temperature. The pion gradient  $\nabla \varphi$  represents the domain wall of the scalar field induced by the magnetic field on the nuclear vacuum [22]. Roughly speaking, it quantifies the degree of chiral symmetry breaking. The domain wall carries baryon charge and thus contributes to the baryon density. For multiquark configuration-**B**, it increases with B for a fixed density. From figure 5, the pion gradient field increases linearly with respect to the field for small fields. Then it starts to saturate closed to the critical field. This is somewhat similar to the behaviour of the pion gradient in the confined phase studied in ref. [16]. For configuration-**B**, the pion gradient field is a decreasing function of the density when the field is fixed. This implies that for a fixed magnetic field, the population of the domain wall becomes lesser as the density of the baryon (including multiquarks and other bound states) increases. We will see this

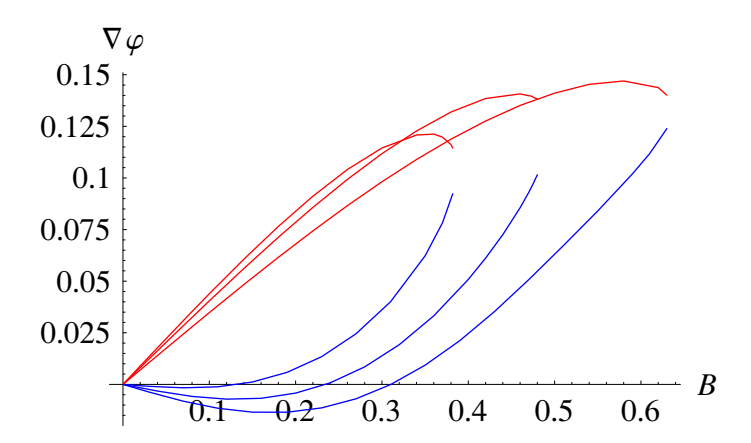


Figure 6. Comparison between the gradient of the scalar field  $\nabla \varphi$  as a function of B at fixed  $j_A = 0, d = 1, T = 0.10$  and (a)  $n_s = 0$  (normal baryon), the bottom graph,(b)  $n_s = 0.10$ , the middle graph, (c)  $n_s = 0.20$ , the top graph. The lower (blue) lines are the configuration-**A** with  $u_c$  close to  $u_T$  and the upper (red) lines are the configuration-**B** with large separation between  $u_c$  and  $u_T$ .

behaviour again in section 4 when we consider the pure pion gradient phase. Finally from figure 5, the degree of chiral symmetry breaking  $\nabla \varphi$  decreases as temperature rises for multiquark configuration-**B**.

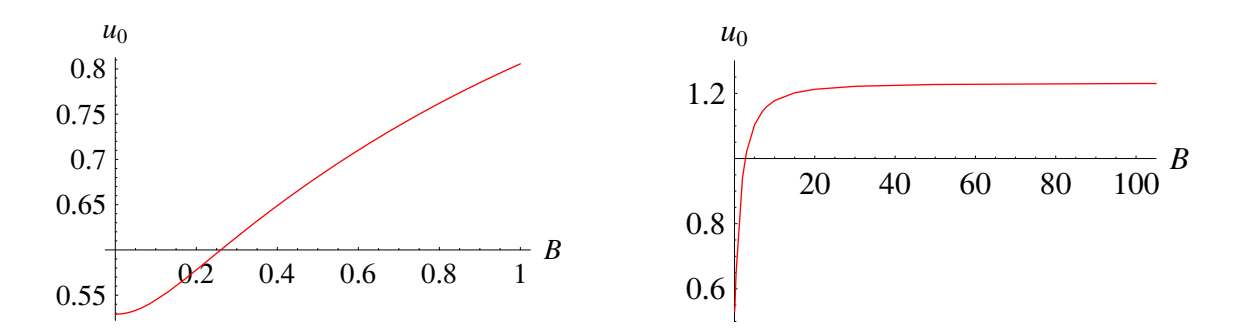
For configuration- $\bf A$ , the pion gradient field decreases at first for small magnetic fields, but turns to rise with the field around  $B\approx 0.16$  until it converges to configuration- $\bf B$  at the critical field. The dependence of the field  $\nabla \varphi$  on the density at a fixed B=0.10, T=0.10 shows a minimum at  $d\approx 0.7$ , corresponding to  $\mu\approx 1.18$ . Then as the density grows, the pion gradient increases and saturates, implying limited contribution of the domain wall for large baryon density. The temperature dependence of the pion gradient field for multiquark configuration- $\bf A$  shows some peculiar behaviour. First, it becomes more negative at low temperatures then turns to rise and converge to configuration- $\bf B$  at the critical temperature.

Figure 6 shows how the pion gradient field  $\nabla \varphi$  varies with the magnetic field B for  $n_s = 0, 0.10, 0.20$ . For the same B, multiquarks with higher  $n_s$  responds more to the magnetic field by inducing larger  $\nabla \varphi$ , implying higher degree of chiral symmetry breaking. The pion gradient field for both multiquark configuration- $\mathbf{A}$ , $\mathbf{B}$  forms a butterfly-wing shape graph for each  $n_s$ . The edge of the wing is at the critical field where the configuration converges and barely satisfies the scale fixing condition.

The magnetization of the multiquarks nuclear matter can be defined using the regulated free energy,  $\mathcal{F}_{E} = \Omega(\mu, B) + \mu d$ , in the canonical ensemble as

$$M(d,B) = -\frac{\partial \mathcal{F}_{E}(d,B)}{\partial B}\Big|_{d},$$
 (3.14)

where  $\Omega(\mu, B) = S[a_0(u), a_1(u)](e.o.m.) - S[\text{magnetized vacuum}]$ . The action with  $a_0^{\prime V}, a_1^{\prime A}$ 



**Figure 7**. Relation between  $u_0$  and external magnetic field B of the vacuum for the temperature T = 0.10,  $u_0$  saturates to the approximate value of 1.23 at large field.

eliminated is given by  $S[a_0(u), a_1(u)](e.o.m.) = S_{D8} + S_{CS}$  where

$$S_{D8} = \mathcal{N} \int_{u_c}^{\infty} du \ C(u) \sqrt{\frac{f(u)(1 + f(u)u^3 x_4'^2)}{f(u)(C(u) + D(u)^2) - (j_A - \frac{3}{2}B\mu + 3Ba_0^V)^2}},$$

and  $S_{\text{CS}}$  is given in the appendix. The grand canonical potential is regulated with respect to the magnetized vacuum. The action of the magnetized vacuum with non-vanishing  $x'_4$  is

$$S[\text{magnetized vacuum}] = \int_{u_0}^{\infty} \sqrt{C(u)(1 + f(u)u^3 x_4^{\prime 2})} \bigg|_{\text{vac}} du,$$

where

$$x_4'(u)|_{\text{vac}} = \frac{1}{\sqrt{f(u)u^3 \left(\frac{f(u)u^3C(u)}{f(u_0)u_0^3C(u_0)} - 1\right)}}.$$
(3.15)

The position  $u_0$  where  $x'_4(u_0) = \infty$  of the magnetized vacuum can be solved numerically from  $L_0 = 1$  (with  $u_0$  replacing  $u_c$  in the limit of integration). The relation between  $u_0$  and the magnetic field is shown in figure 7 for T = 0.10. As the magnetic field gets stronger, the position of the lowest position of the D8- $\overline{D8}$  configuration,  $u_0$ , becomes larger, in order to satisfy the condition  $L_0 = 1$  (implying heavier branes due to magnetic field energy). At T = 0.10, position of  $u_0$  saturates to the value of about 1.23 (The number changes with temperature, of course) in the limit of an infinite field.

The magnetization of the multiquark nuclear matter is shown in figure 8 for  $n_s = 0$  (red), 0.10 (green), 0.20 (blue). The magnetization is positive and increases as B increases until the field is close to the critical value then it starts to drop. Generically, configuration- $\mathbf{A}$  of multiquarks has larger magnetization than configuration- $\mathbf{B}$ . For the configuration- $\mathbf{B}$  ( $\mathbf{A}$ ), multiquarks with higher (lower)  $n_s$  have higher magnetizations. As the magnetic field gets stronger beyond the critical field for each  $n_s$ , the multiquarks will undergo a transition into the ones with smaller  $n_s$ . For even larger fields, even the  $n_s = 0$  multiquarks cannot satisfy the scale fixing condition if the density is not allowed to change.

Interestingly, numerical studies reveal that the grand canonical potential of the multiquark phase is always lower than the grand canonical potential of the magnetized vacuum,

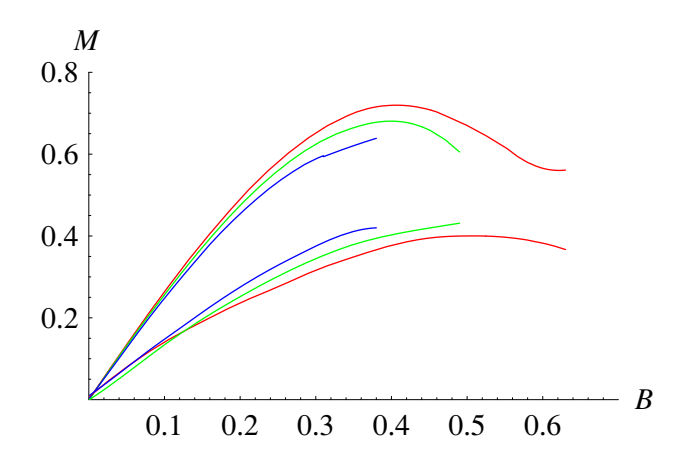


**Figure 8.** The magnetization of the multiquarks nuclear matter at fixed  $j_A = 0, d = 1$ , and T = 0.10 for  $n_s = 0$  (red), 0.10 (green), 0.20 (blue). The upper lines are the configuration-**A** with  $u_c$  close to  $u_T$  and the lower lines are the configuration-**B** with large separation between  $u_c$  and  $u_T$ .

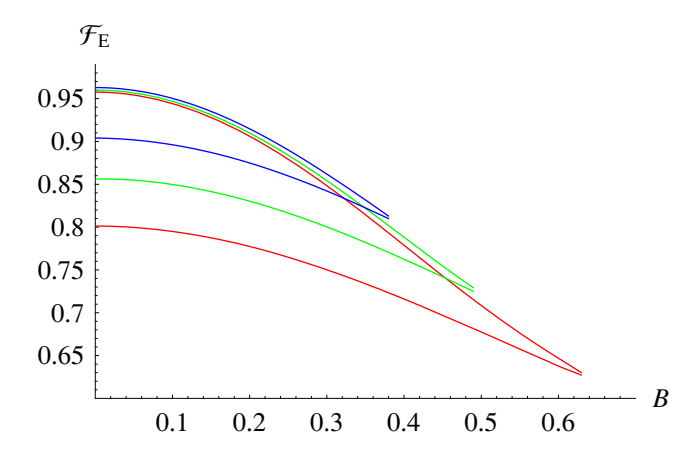


**Figure 9.** The free energy of the multiquarks nuclear matter at fixed  $j_A = 0, d = 1$ , and T = 0.10 for  $n_s = 0$  (red), 0.10 (green), 0.20 (blue). The upper lines are the configuration-**A** with  $u_c$  close to  $u_T$  and the lower lines are the configuration-**B** with large separation between  $u_c$  and  $u_T$ .

i.e.  $S[a_0(u), a_1(u)](e.o.m.) - S[\text{magnetized vacuum}] < 0$ , for the entire range of B. This suggests that once  $\mu > \mu_{\text{onset}}$ , the magnetized multiquark phase is always thermodynamically preferred over the magnetized vacuum, the situation similar to the case when there is no magnetic field investigated in ref. [7]. Among the two configurations, we found from figure 9 that the free energy of configuration- $\mathbf{B}$  is always lower than configuration- $\mathbf{A}$  and thus more stable thermodynamically. These two multiquark configurations- $\mathbf{A}$ , $\mathbf{B}$  are the long and short cusp configurations discussed in ref. [6], being extended to the general case with nonzero magnetic fields. It is found here that for a fixed density, strong field and/or high temperature (see figure 3 and 5) converge the two into a single configuration right before dissociating them altogether.

Figure 9 shows how the free energy changes with the magnetic field for  $n_s = 0$  (red), 0.10 (green), 0.20 (blue) at the temperature T = 0.10 and the density d = 1. For each  $n_s$ ,

both configurations converge to the same configuration (with the same baryon chemical potential, degree of chiral symmetry breaking and free energy) at the critical fields. The critical fields for  $n_s = 0, 0.1, 0.2$  are roughly 0.63, 0.48, 0.38 respectively.

# 4 Comparison to other phases

In this section we compare the baryon chemical potential and free energy of the magnetized multiquarks to the pure pion gradient phase and the chiral symmetric quark-gluon plasma ( $\chi_S$ -QGP) phase, both under the external magnetic field with gluons deconfined. The pure pion gradient phase is defined to be the phase with  $\mu_{\text{source}} = 0$  (sourceless case) and the baryon chemical potential comes purely from the induced gradient field,  $\nabla \varphi$ , in response to the external field. The baryon density also comes purely from the pion gradient field ( $d = 3B\nabla \varphi/2$ ). A similar situation in the confined phase of the antipodal SS model has been studied in ref. [16]. The  $\chi_S$ -QGP under the presence of the external magnetic field has been explored in ref. [16, 19] but again only limited to the antipodal case of the SS model. In this section we explore some of their magnetic properties in more general case where  $x'_4(u)$  is not zero and the scale is fixed to  $L_0 = 1$ . Even though the extra constraints are irrelevant to the  $\chi_S$ -QGP (since  $x'_4 = 0$  for this configuration), it makes crucial difference in the case of pure pion gradient phase. The scale fixing condition is found to be very difficult for the pure pion gradient configuration to satisfy for most of the density as we will discuss below.

All three phases under consideration obey the same set of equations of motion, eq. (3.5), (3.6) with each specific set of the boundary conditions and parameters as the following,

multiquark phase: 
$$j_A = 0, \mu_{\text{source}} = a_0^V(u_c), \nabla \varphi = a_1^A(\infty), a_1^A(u_c) = 0,$$

pure pion gradient phase: all the same with the multiquark phase with the following exceptions,  $\mu_{\text{source}} = 0$ ,  $a_0^V(u_c) \neq 0$ ,  $d = \frac{3}{2}B \nabla \varphi$ ,

$$\chi_S$$
-QGP:  $x_4'(u) = 0$  and  $\nabla \varphi = a_1^A(\infty) = 0$ ,  $\mu_{\text{source}} = a_0^V(u_c = u_T) = 0$ ,  $j_A = \frac{3}{2}B\mu$  (since the configuration extends to  $u_T$  and  $f(u_T) = 0$  so that eq. (3.5) is zero).

First, we will explore certain properties of the pure pion gradient phase and show that it does not exist in the range of parameters  $(d \ge 1, B \le 1-2)$  under consideration. Then comparison between the multiquark and the  $\chi_{S}$ -QGP phases will be discussed.

### 4.1 Pure pion gradient phase

For pure pion gradient configuration, the contribution of the sources, the vertex and strings, is set to zero. Effectively, we set  $\mu_{\text{source}} = 0, d = 3B \nabla \varphi/2$ . This is because when  $\nabla \varphi$  is zero, the density d should represent the density of the sources, i.e. the pure multiquark or pure baryon configuration, therefore the source density should be given by  $d - \frac{3}{2}B\nabla \varphi$  on the right-hand side of eq. (3.6). When we fix the value of the density at a fixed magnetic field,  $\nabla \varphi$  is also fixed. For example, when  $d = 1, B = 0.1, \nabla \varphi \simeq 6.667$ , a relatively large value. This large value of  $\nabla \varphi = a_1^A(\infty)$  leads to a generically large value of  $a_1^A(u)$  for

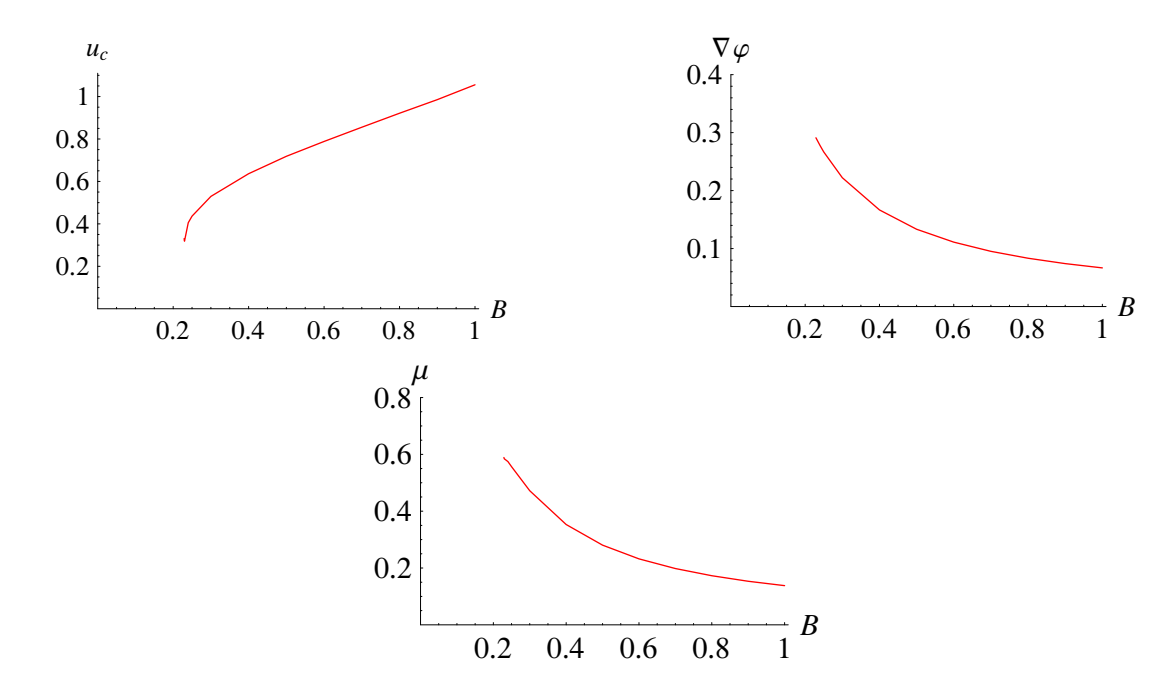


**Figure 10**. The position  $u_c$ , the pion gradient field, and the baryon chemical potential of the pure pion gradient phase at d = 0.10, T = 0.10 as a function of the magnetic field.

the most range of u. From eq. (3.11) and (3.12), we see that for the pure pion phase,  $D(u) = 3Ba_1^A(u)$  and thus it must be large for the most range of u as well. In the multiquark configuration, the d dependence of  $D(u_c)$  in the expression of F, eq. (3.12), will compensate the largeness of D(u) and  $x'_4$  can be made sufficiently large so that  $L_0 = 1$  could still be satisfied. However, in pure pion phase,  $D(u_c)$  is simply zero. This makes  $x'_4$  getting smaller as the density gets larger and the scale fixing condition  $L_0 = 1$  would not be satisfied above certain value of the density for a fixed B.

As a result, we wish to keep  $\nabla \varphi$  sufficiently small in order to satisfy the scale fixing condition. This implies that higher densities require larger magnetic fields. To demonstrate this, we fix baryon density to d=0.1 and plot the position  $u_c$  of the vertex and the baryon chemical potential as a function of the magnetic field in figure 10. The graph of  $u_c$  shows a minimal field at about  $B\approx 0.229$  below which  $L_0<1$  for all solutions. For a larger density  $d\geq 1$ , the required field strengths are B>>1 in order for the scale fixing condition to be satisfied. For the range of parameters  $d=1.0, B\leq 1.0$ , we therefore need to consider only the two phases of the multiquark and the  $\chi_S$ -QGP. The same situation occurs for the range of parameters  $d=10, B\leq 1-2$  where the pure pion gradient phase does NOT satisfy the scale fixing condition and therefore does not exist as well.

# 4.2 Multiquark-domain wall versus $\chi_S$ -QGP phase

The baryon chemical potential  $\mu$  is to be found by shooting algorithm for a fixed d, B, T, for each phase. For d = 1, B = 0.10, T = 0.10, they are shown in figure 11. Observe that there are two possible solutions for the  $\chi_{S}$ -QGP phase. As the magnetic field increases beyond a certain value (in this case around  $B \approx 0.25$ ), there will be phase transition to another

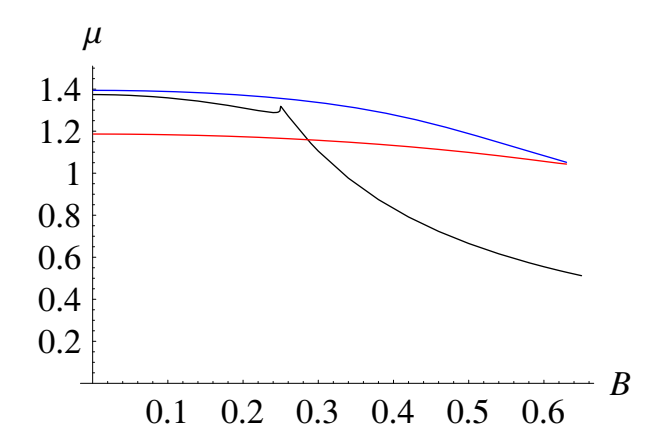


**Figure 11.** Comparison between the baryon chemical potential for T = 0.10 at a fixed density d = 1 of (a)  $n_s = 0$  (normal baryon) multiquark configuration-**A**, the top (blue) graph,(b)  $\chi_S$ -QGP, the middle (black) graph,(c)  $n_s = 0$  (normal baryon) multiquark configuration-**B**, the bottom (red) graph.

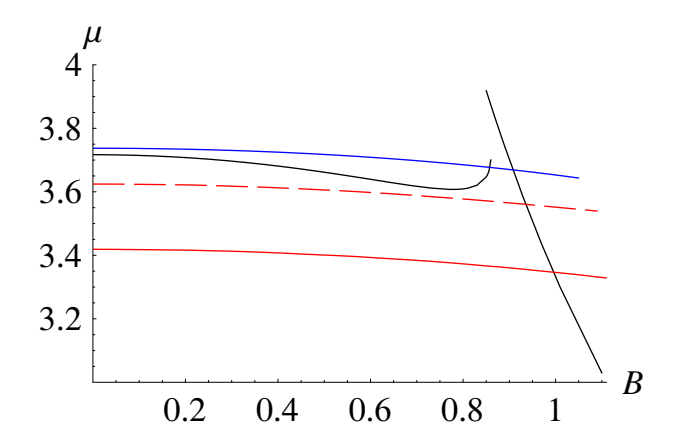


**Figure 12.** Comparison between the baryon chemical potential for T = 0.10 at a fixed density d = 10 of (a)  $n_s = 0$  (normal baryon) multiquark configuration-**A**, the top (blue) curve,(b)  $\chi_S$ -QGP, the black curve,(c)  $n_s = 0.2$  multiquark configuration-**B**, the dashed red curve,(d)  $n_s = 0$  (normal baryon) multiquark configuration-**B**, the red curve.

solution within this phase. This behaviour is explored in details in ref. [19]. When the density is raised to d = 10, the transition occurs at higher field around  $B \approx 0.86$  (figure 12). The transitions can also be seen in the plots of the free energy, figure 13, 14, where the slopes of the graphs change abruptly around the critical fields. For d = 1, this is quite small and somewhat hard to see but it becomes apparent for d = 10.

From the plots of the free energy, figure 14, the multiquark configuration-**A** is the least preferred phase when the density is small (d=1). Its free energy is larger than the  $\chi_S$ -QGP phase for all fields. For  $B \leq 0.196$ , the most preferred phase is the multiquark configuration-**B** phase with the lower free energy. The  $\chi_S$ -QGP phase is more stable for d=1, B>0.196. Nevertheless, the multiquark configurations can exist up to only

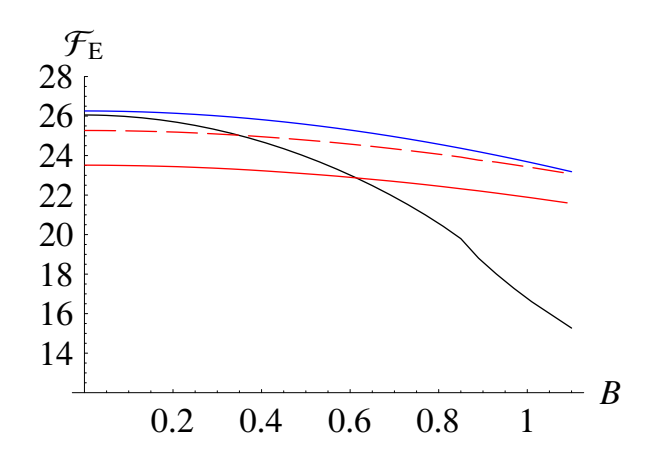


**Figure 13**. Comparison between the free energy for T = 0.10 at a fixed density d = 10 of (a)  $n_s = 0$  (normal baryon) multiquark configuration-**A**, the top (blue) curve,(b)  $\chi_S$ -QGP, the black curve,(c)  $n_s = 0.2$  multiquark configuration-**B**, the dashed red curve,(d)  $n_s = 0$  (normal baryon) multiquark configuration-**B**, the red curve.

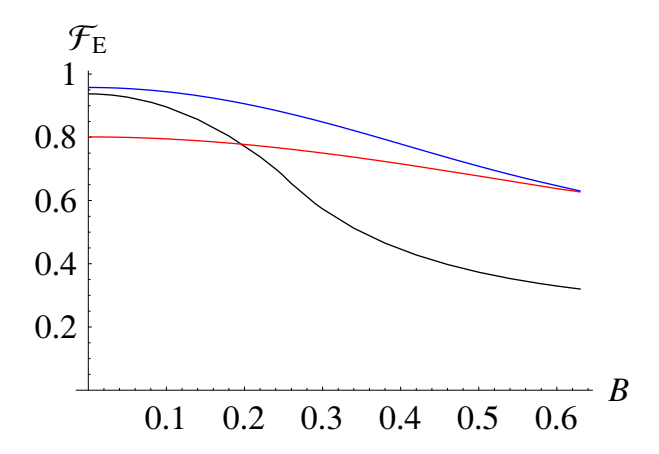
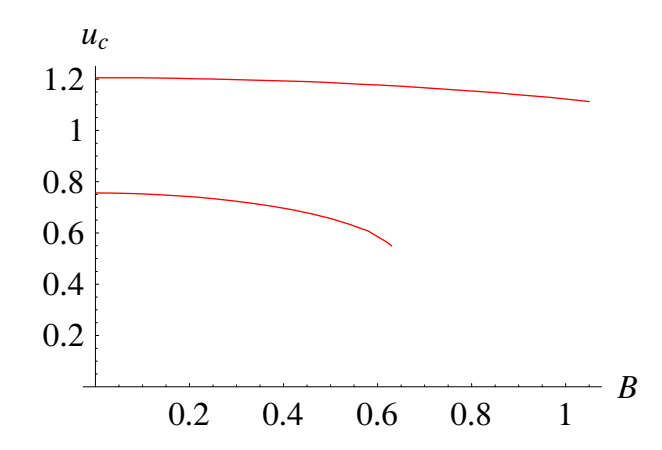


Figure 14. Comparison between the free energy for T=0.10 at a fixed density d=1 of (a)  $n_s=0$  (normal baryon) multiquark configuration-**A**, the top (blue) graph,(b)  $\chi_S$ -QGP, the middle (black) graph,(c)  $n_s=0$  (normal baryon) multiquark configuration-**B**, the bottom (red) graph.

about the critical fields beyond which they cannot satisfy the scale fixing condition at that particular density.

However, this does not mean that the multiquarks phase cannot exist in the range of field larger than the critical value. Stronger field gives the D8-branes larger tension and thus it requires sufficiently heavier vertex and strings to pull it down in order for the distance between D8 and  $\overline{D8}$  to reach  $L_0=1$ . This implies that we need larger d in order to make the configuration satisfy the scale fixing condition at stronger fields. Figures 12, 13, 15 confirm this insight. They show the plots of the multiquarks configurations when the density is large (d=10). Multiquark configurations can exist far beyond the critical field  $B\approx 0.63$  of the small d case (d=1). In particular, figure 13 demonstrates that at d=10, the multiquark configurations  $(n_s=0,0.2)$ , with lower free energies, are thermodynamically preferred over the  $\chi_S$ -QGP for B<0.61 and B<0.348 respectively.



**Figure 15**. The position of the vertex  $u_c$  as a function of B at a fixed density d = 1 (lower) and d = 10 (upper) for T = 0.10 of  $n_s = 0$  (normal baryon) multiquark configuration-**B** phase.

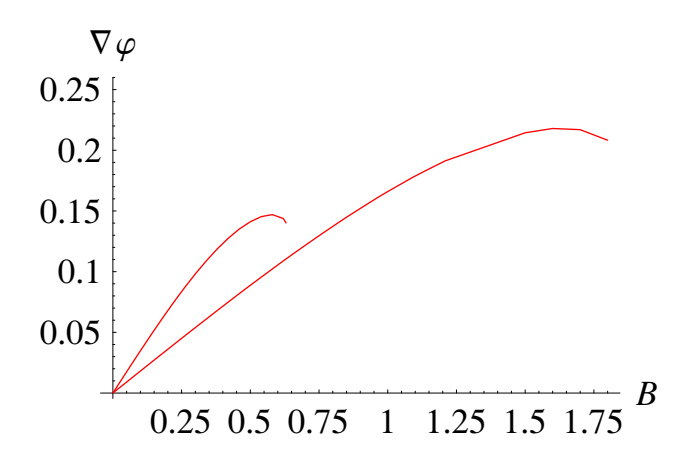


**Figure 16**. Plots between the pion gradient field of the multiquark phase and the magnetic field for  $T = 0.10, n_s = 0$  at d = 1 (shorter) and d = 10 (longer).

It is thus reasonable to conclude that for larger densities, the multiquarks phase will be more and more preferred over the  $\chi_{S}$ -QGP phase, in a larger and larger range of the field. Magnetized multiquarks and the induced pion gradient field are thus stable thermodynamically and they will mix together in the magnetized nuclear (multiquark-domain wall) phase provided that the density is sufficiently large and the temperature is not too high.

Finally for completeness, we present the plots of the pion gradient field of the multiquark phase (figure 16), the pion gradient field becomes smaller for a given B as the density increases. However, it extends to larger range of fields for larger density. We can therefore conclude that at the large densities (and baryon chemical potential), contribution of the pion gradient becomes lesser and the multiquarks contribute dominantly to the baryon density and chemical potential. This is also shown in figure 5.

# 5 Discussions and conclusion

In Sakai-Sugimoto model, chiral symmetry restoration and gluon deconfinement are two distinct phase transitions. Generically, with an exception of the antipodal case with  $x'_4 = 0$ , gluon deconfinement occurs at lower temperature than the chiral symmetry restoration. For the region of the phase diagram between the two transitions, coloured multiquarks can exist with thermodynamical stability (the phase diagram is shown in figure 8 of ref. [7]).

Magnetic responses of the nuclear phase with colour multiquarks are studied here by using one component of the U(1) subgroup of U( $N_f$ ) as the vector potential of the external magnetic field. The Chern-Simon action of the D8-branes couples the magnetic field to an axial vector component,  $a_1^A$ , of the U(1), inducing axial current  $j_A$ . When the chiral symmetry is broken, we effectively set  $j_A$  to zero. The value of  $a_1^A(\infty)$  then describes the degree of chiral symmetry breaking of the phase.

There are two possible multiquark configurations **A** and **B**. Configuration-**A** is the configuration where the baryon vertex is close to the horizon. Configuration-**B**, on the other hand, has the baryon vertex more separated from the horizon. By comparing the free energy of the two configurations in figure 9, we found that configuration-**B** is more stable themodynamically. We establish relations between the baryon chemical potential and the baryon density, the external magnetic field, and the temperature for both configurations as are shown in figure 3. Baryon chemical potential is an increasing function of the density when the field is turned on. This is the same behaviour to the case when there is no field.

On the other hand, the relation between chemical potential and the magnetic field is rather interesting. The baryon chemical potential is a decreasing function of the field. For multiquarks with high value of  $n_s$  (number of radial strings), the configuration finds it more difficult to satisfy the scale fixing condition at large fields. There is a maximum field strength for each  $n_s$  above which the multiquark configuration cannot exist (figure 4). This is in contrast to the behaviour of the chiral-symmetric quark-gluon plasma (in the antipodal case of the Sakai-Sugimoto model with no instantons, i.e.  $x'_4(u) = 0$  case) studied in ref. [16] where chemical potential is always a decreasing function with respect to B and the configuration continues to exist at arbitrarily large fields. This is due to the fixation of the density. Stronger field gives the flavour branes more tension and when the field is too strong, a fixed density source would not be sufficiently heavy to pull the branes down for the distance between D8 and  $\overline{D8}$  to reach  $L_0 = 1$ . Temperature also has effect on the multiquarks, sufficiently high temperature will melt away the multiquarks even in the presence of an external field.

The gradient of the scalar field representing the chiral symmetry breaking,  $\nabla \varphi = a_1^A(\infty)$ , is found to roughly increase in magnitude with the field. For the same field strength and fixed density, multiquarks with higher  $n_s$  (i.e. larger colour charges) show higher degree of chiral symmetry breaking (larger magnitude of  $a_1^A(\infty)$ ), but can only sustain the force condition up to smaller fields as is shown in figure 6.

The mixing of pion gradient with the miltiquark in the multiquark phase decreases as the density increases (figure 5). It is found that the pure pion gradient phase (no multiquark contribution) does not satisfy the scale fixing condition for large densities and moderate fields.

What would happen if the magnetic field increases beyond the point where the multiquarks can satisfy the scale fixing condition  $L_0 = 1$ ? We would expect the multiquarks to change into the multiquarks with lower  $n_s$  as is shown in figure 4 for a fixed d and T since they can still satisfy the scale fixing condition. This induces a sudden drop in the baryon chemical potential. Also in the situation where  $\mu$  is kept fixed instead of d, the multiquarks are forced to jump to the larger d in order to change into the multiquarks with lower  $n_s$  as the field increases beyond the critical point. For even larger fields, all of the multiquarks cannot satisfy the scale fixing condition for a fixed density. There would be phase transition to other phase. For a fixed density, the phase will change into the  $\chi_S$ -QGP. However, if we allow the density to change (in a more realistic situation), the system could change into the multiquark (with pion gradient mixing) phase for a sufficiently large density. The phase of multiquark with pion gradient mixing is found to be more preferred than the  $\chi_S$ -QGP at large densities (implying large baryon chemical potentials) and moderate fields. This is shown in figure 13.

For configuration-**B** multiquarks, The magnetization of the multiquark nuclear matter is found to be an increasing function of B for  $n_s = 0, 0.10, 0.20$  except when the fields get close to the critical points. Close to the critical fields, the magnetizations saturate and even start to decrease. The magnetized multiquarks phases are thermodynamically preferred over the magnetized vacuum once the baryon chemical potential is higher than the onset value ( $\mu > \mu_{\rm onset}$ ). This is similar to the case when there is no magnetic field investigated in ref. [7].

# Acknowledgments

I would like to thank Ekapong Hirunsirisawat for help with the first illustration. P.B. is supported in part by the Thailand Research Fund (TRF) and Commission on Higher Education (CHE) under grant MRG5180227.

# A Force condition of the multiquark configuration

The forces on the D4-brane in the flavour D8-branes are balanced among three forces from the tidal weight of the D4-brane, the force from the strings attached to the D4, and the force from the D8-branes. Varying the total action with respect to  $u_c$  gives the surface term. Together with the scale-fixing condition  $2\int_{u_c}^{\infty} du x_4'(u) = L_0 = 1$ , we obtain [6]

$$x_4'(u_c) = \left(\tilde{L}(u_c) - \frac{\partial S_{\text{source}}}{\partial u_c}\right) / \frac{\partial \tilde{S}}{\partial x_4'}\Big|_{u_c},$$
 (A.1)

as the condition on  $u_c$ .

The Legendre transformed action is given by

$$\tilde{S} = \int_{u_c}^{\infty} \tilde{L}(x_4'(u), d) du, 
= \mathcal{N} \int_{u_c}^{\infty} du \sqrt{\frac{1}{f(u)} + u^3 x_4'^2} 
\times \sqrt{f(u)(C(u) + D(u)^2) - \left(j_A - \frac{3}{2}B\mu + 3Ba_0^V\right)^2},$$
(A.2)

where  $C(u) \equiv u^5 + B^2 u^2$ ,  $D(u) \equiv d + 3Ba_1^A(u) - 3B\nabla\varphi/2$ . It is calculated by performing Legendre transformation with respect to  $a_0^{V\prime}$  and  $a_1^{A\prime}$  respectively. Note that the Chern-Simon action is also included in the total action during the transformations.

The Chern-Simon term with the derivatives  $a^{V\prime}, a^{A\prime}$  eliminated is

$$S_{\rm CS} = -\mathcal{N} \frac{3}{2} B \int_{u_c}^{\infty} du \; \frac{\left(a_0^V \left(j_A - \frac{3}{2} B \mu + 3 B a_0^V\right) - f(u) D(u) a_1^A\right) \sqrt{\frac{1}{f(u)} + u^3 x_4'^2}}{\sqrt{f(u) (C(u) + D(u)^2) - \left(j_A - \frac{3}{2} B \mu + 3 B a_0^V\right)^2}}.$$
(A.3)

Lastly, in order to compute  $x'_4(u_c)$  we consider the source term [7]

$$S_{\text{source}} = \mathcal{N}d\left[\frac{1}{3}u_c\sqrt{f(u_c)} + n_s(u_c - u_T)\right],$$

$$= \mathcal{N}d\mu_{\text{source}}$$
(A.4)

where  $n_s = k_r/N$  is the number of radial strings in the unit of 1/N.

From eq. (A.1), (A.2), (A.3), (A.5), and setting  $a_0^V(u_c) = \mu_{\text{source}}, a_1^A(u_c) = 0$  we can solve to obtain

$$(x_4'(u_c))^2 = \frac{1}{f_c u_c^3} \left[ \frac{9}{d^2} \frac{\left( f_c (C_c + D_c^2) - \left( j_A - \frac{3}{2} B \mu + 3 B a_0^V (u_c) \right)^2 \right)}{\left( 1 + \frac{1}{2} \left( \frac{u_T}{u_c} \right)^3 + 3 n_s \sqrt{f_c} \right)^2} - 1 \right]$$

where  $f_c \equiv f(u_c), C_c \equiv C(u_c), D_c \equiv D(u_c)$ .

When we fix the parameter  $n_s$ , the temperature T, the baryon density d, the axial current  $j_A = 0$  (by minimizing the action with respect to  $a_1^A(\infty)$ ), and setting  $a_1^A(u_c) = 0$ ,  $a_0^V(u_c) = \mu_{\text{source}}$ , then the position  $u_c$  of the D4-brane is completely determined as a function of the magnetic field B. Once the equations of motion are solved, the value of  $\mu = a_0^V(\infty)$  and  $a_1^A(\infty)$  are determined.

# References

- J.M. Maldacena, The large-N limit of superconformal field theories and supergravity, Adv. Theor. Math. Phys. 2 (1998) 231 [Int. J. Theor. Phys. 38 (1999) 1113] [hep-th/9711200] [SPIRES].
- [2] O. Aharony, S.S. Gubser, J.M. Maldacena, H. Ooguri and Y. Oz, *Large-N field theories*, string theory and gravity, *Phys. Rept.* **323** (2000) 183 [hep-th/9905111] [SPIRES].

- [3] T. Sakai and S. Sugimoto, Low Energy Hadron Physics in Holographic QCD Prog. Theor. Phys. 113 (2005) 843 [hep-th/0412141] [SPIRES].
- [4] T. Sakai and S. Sugimoto, More on a Holographic Dual of QCD, Prog. Theor. Phys. 114 (2005) 1083 [hep-th/0507073] [SPIRES].
- [5] O. Aharony, J. Sonnenschein and S. Yankielowicz, A holographic model of deconfinement and chiral symmetry restoration, Annals Phys. 322 (2007) 1420 [hep-th/0604161] [SPIRES].
- [6] O. Bergman, G. Lifschytz and M. Lippert, Holographic Nuclear Physics, JHEP 11 (2007) 056 [arXiv:0708.0326] [SPIRES].
- P. Burikham, A. Chatrabhuti and E. Hirunsirisawat, Exotic Multi-quark States in the Deconfined Phase from Gravity Dual Models, JHEP 05 (2009) 006 [arXiv:0811.0243]
   [SPIRES].
- [8] A. Brandhuber, N. Itzhaki, J. Sonnenschein and S. Yankielowicz, Baryons from supergravity, JHEP 07 (1998) 020 [hep-th/9806158] [SPIRES].
- [9] O. Antipin, P. Burikham and J. Li, Effective Quark Antiquark Potential in the Quark Gluon Plasma from Gravity Dual Models, JHEP **06** (2007) 046 [hep-ph/0703105] [SPIRES].
- [10] K. Ghoroku, M. Ishihara, A. Nakamura and F. Toyoda, Multi-quark baryons and color screening at finite temperature, Phys. Rev. D 79 (2009) 066009 [arXiv:0806.0195] [SPIRES].
- [11] K. Ghoroku and M. Ishihara, *Baryons with D5 Brane Vertex and k-Quarks*, *Phys. Rev.* **D 77** (2008) 086003 [arXiv:0801.4216] [SPIRES].
- [12] M.V. Carlucci, F. Giannuzzi, G. Nardulli, M. Pellicoro and S. Stramaglia, AdS-QCD quark-antiquark potential, meson spectrum and tetraquarks, Eur. Phys. J. C 57 (2008) 569 [arXiv:0711.2014] [SPIRES].
- [13] W.-Y. Wen, Multi-quark potential from AdS/QCD, Int. J. Mod. Phys. A 23 (2008) 4533 [arXiv:0708.2123] [SPIRES].
- [14] O. Bergman, G. Lifschytz and M. Lippert, Response of Holographic QCD to Electric and Magnetic Fields, JHEP 05 (2008) 007 [arXiv:0802.3720] [SPIRES].
- [15] C.V. Johnson and A. Kundu, External Fields and Chiral Symmetry Breaking in the Sakai-Sugimoto Model, JHEP 12 (2008) 053 [arXiv:0803.0038] [SPIRES].
- [16] O. Bergman, G. Lifschytz and M. Lippert, Magnetic properties of dense holographic QCD, Phys. Rev. D 79 (2009) 105024 [arXiv:0806.0366] [SPIRES].
- [17] E.G. Thompson and D.T. Son, Magnetized baryonic matter in holographic QCD, Phys. Rev. D 78 (2008) 066007 [arXiv:0806.0367] [SPIRES].
- [18] C.V. Johnson and A. Kundu, Meson Spectra and Magnetic Fields in the Sakai-Sugimoto Model, JHEP 07 (2009) 103 [arXiv:0904.4320] [SPIRES].
- [19] G. Lifschytz and M. Lippert, *Holographic Magnetic Phase Transition*, *Phys. Rev.* **D 80** (2009) 066007 [arXiv:0906.3892] [SPIRES].
- [20] E. Witten, Baryons and branes in anti de Sitter space, JHEP 07 (1998) 006 [hep-th/9805112] [SPIRES].
- [21] D.J. Gross and H. Ooguri, Aspects of large-N gauge theory dynamics as seen by string theory, Phys. Rev. D 58 (1998) 106002 [hep-th/9805129] [SPIRES].
- [22] D.T. Son and M.A. Stephanov, Axial anomaly and magnetism of nuclear and quark matter, Phys. Rev. D 77 (2008) 014021 [arXiv:0710.1084] [SPIRES].

# REPORT JHEP_043P_0410

# REPORT ON JHEP_043P_0410

DATE: MAY 21, 2010

AUTHOR(S): P. BURIKHAM, E. HIRUNSIRISAWAT, S. PINKANJANAROD

 $\mathrm{TiTLE}$ : Thermodynamic Properties of Holographic Multiquark and the Multiquark St

RECEIVED: 2010-04-08 07:44:36.0

# Referee report

Dear Editor:

I accepted the second and corrected version of the authors. Sincerely the referee

# Thermodynamic Properties of Holographic Multiquark and the Multiquark Star

P. Burikham^{1,2}*, E. Hirunsirisawat¹†S. Pinkanjanarod^{1,3}‡

- Theoretical High-Energy Physics and Cosmology Group, Department of Physics, Faculty of Science, Chulalongkorn University, Bangkok 10330, Thailand
- ² Thailand Center of Excellence in Physics, Ministry of Education, Bangkok, Thailand
- ³ Department of Physics, Faculty of Science, Kasetsart University, Bangkok 10900, Thailand

April 21, 2010

## Abstract

We study thermodynamic properties of the multiquark nuclear matter. The dependence of the equation of state on the colour charges is explored both analytically and numerically in the limits where the baryon density is small and large at fixed temperature between the gluon deconfinement and chiral symmetry restoration. The gravitational stability of the hypothetical multiquark stars are discussed using the Tolman-Oppenheimer-Volkoff equation. Since the equations of state of the multiquarks can be well approximated by different power laws for small and large density, the content of the multiquark stars has the core and crust structure. We found that most of the mass of the star comes from the crust region where the density is relatively small. The mass limit of the multiquark star is determined as well as its relation to the star radius. For typical energy density scale of 10 GeV/fm³, the converging mass and radius of the hypothetical multiquark star in the limit of large central density are approximately 2.6-3.9 solar mass and 15-27 km. The adiabatic index and sound speed distributions of the multiquark matter in the star are also calculated and discussed. The sound speed never exceeds the speed of light and the multiquark matters are thus compressible even at high density and pressure.

^{*}Email:piyabut@gmail.com, piyabut.b@chula.ac.th

[†]Email:ekapong.hirun@gmail.com, ekapong.h@student.chula.ac.th

[‡]Email:quazact@gmail.com, Sitthichai.P@student.chula.ac.th

# 1 Introduction

All of the high energy experiments which fail to produce a free quark are strong evidences that the coupling constant of the strong interaction becomes nonperturbatively large at low energy and large distance. Quarks and gluons are said to be confined within hadrons and the colourless condition becomes a requirement of an assembly of quarks at low energy. However, when the energy or temperature scale of a system of quarks and gluons increases, the coupling of the strong interaction tends to be weaker and finally we expect the deconfinement to occur. In addition, if the quarks and gluons are compressed extremely tightly together, quarks could interact with neighbouring quarks and gluons equally and become effectively deconfined from the mesonic or baryonic bound state. In the latter case, the coupling could still be strong despite of the deconfinement. Nevertheless, we could also have the situation where gluons are deconfined but the quarks are not completely free due to the remaining Coulomb-type potential from gluon exchanges between quarks.

Recently, the experimental results from collision of heavy ions suggested that the nuclear deconfinement phase might have been created in the laboratory and we might have produced the quark-gluon plasma (QGP). The RHIC experiment revealed that the produced QGP behaves like fluid with very small viscosity. However, this property of small viscosity fluid is hard to be understood in the picture of QGP as the gas of free quarks and gluons. Additionally, lattice simulations show that QGP has relatively high pressure right above the deconfinement temperature  $T_c$  which is again difficult to explain using the weakly coupled quarks and gluons gas [1, 2]. It is possible that various coloured and colour-singlet bound states of quarks and gluons could exist in the plasma at the temperature  $(1-3)T_c$  [3, 2, 4]. The existence of the coloured bound states could explain the problems of high pressure, small viscosity, and the jet quenching of the QGP at once.

Due to the large coupling of the strong interaction at low energies, a perturbative method has limited applicability to the high energy processes and phenomena. The development of the holographic principle and AdS/CFT correspondence [5] provides us with a new method to investigate the physics of strongly coupled nuclear matter both in the low energy regime and in the energy scale close to the deconfinement temperature. Holographic models of meson were proposed by Juan Maldacena, Soo-Jong Rey, Stefan Theisen, Jung-Tay Yee [6, 7, 8]. The Coulomb potential plus screening effect of quark and antiquark are calculated from the Nambu-Goto action of the string in the bulk spacetime at zero and finite temperature. For baryons, Witten, Gross and Ooguri [9, 10] proposed a holographic baryon to be a D-brane wrapping internal subspace of the background spacetime with  $N_c$  strings connected and stretching out to the boundary. For  $AdS_5 \times S^5$ , the baryon vertex is a D5-brane wrapping the  $S^5$ . The basic requirement is that a total of  $N_c$  charges from the endpoint of the strings cancel with the charge of the vertex itself. A generalization of this condition allows more strings to go in and come out of the vertex, as long as the total charges from all of the string endpoints add up to  $N_c$  [11, 12, 13, 14, 15, 16]. Baryon vertex plus strings configuration in this case represent the holographic multiquark states. Generically they have colour charges but because of the confinement, they can only exist in the deconfined phase.

The coloured multiquark phase can be studied in the general Sakai-Sugimoto model (SS)[17.

18] in the intermediate temperature above the gluon deconfinement but below the chiral symmetry restoration temperature [19]. It was found that the multiquark phase is thermodynamically stable and preferred over the other phases in the gluon-deconfined plasma provided that the density is sufficiently large [16]. The situation of high density and moderate temperature could exist inside certain classes of compact stars and it is thus interesting to investigate the thermodynamical properties of the multiquark nuclear matter as well as their contributions to the stability of the dense stars. In this article, we will consider the hypothetical multiquark star which obeys the equation of state derived from the holographic multiquarks in the SS model. With the power-law approximation of the equations of state, we study its gravitational stability using the Tolman-Oppenheimer-Volkoff equation (TOV)[20]. The mass, density and pressure distributions are obtained numerically. The mass-radius relation and the mass limit are also discussed. Corresponding hydrodynamical properties such as the sound speed of the multiquark nuclear matter are explored within the star. The multiquark matters are found to be compressible throughout the entire multiquark star.

This article is organized as the following. Section 2 describes the holographic setup for the multiquarks and the multiquark phase in the gluon-deconfined SS model. The thermodynamic relations and the equations of state of the multiquark nuclear matter are calculated and discussed in Section 3 and 4. In Section 5, the Einstein field equation for the spherically symmetric star is solved to obtain the TOV equation. Assuming the equations of state derived in Section 3 and 4 for the multiquark nuclear matter, we explore the gravitational physics of a hypothetical multiquark star. A mass-radius relation is derived and some discussion on the more realistic situation is commented. The adiabatic index and the sound speed of the multiquark nuclear matter within the star are studied. Section 6 concludes the article.

# 2 Holographic multiquark configuration

Since string theories in the bulk spacetime correspond to certain gauge theories on the boundary of that space, it is natural to find construction of the bound states of quarks in the form of strings and branes. While the meson is proposed to be the string hanging in the bulk with both ends locating at the boundary of the AdS space [6], the baryon is proposed to be the Dp-brane wrapped on the  $S^p$  with  $N_c$  strings attached and extending to the boundary of the bulk space [9, 10].

On the gauge theory side, hadrons exist in the confined phase as a result of the linear part of the binding potential. However, the bound states of quarks can actually exist in the deconfined phase at the intermediate temperatures above the deconfinement as well. Even though gluons are free to propagate and the linear potential is absent, the quarks can form bound state through the remaining Coulomb-type potential due to the colour charges of the quarks.

The holographic model of non-singlet bound state was also proposed. As is demonstrated in Ref. [16], we can modify the Witten's baryon vertex by attaching more strings to the vertex provided that the total number of charges of all of the strings are preserved to  $N_c$ . Some

strings may extend along radial direction of the AdS space down to the horizon and some can extend to the boundary. We define the number of strings that extend to the boundary to be  $k_h$  and the number of strings extending radially to the horizon to be  $k_r$ . The restriction of  $k_h$  and  $k_r$  is due to the force condition of the string configuration (see Ref. [16] for details).

In this article, we consider the holographic model of multiquarks in the Sakai-Sugimoto (SS) model [17, 18] similar to the configurations considered in Ref. [16]. The background metric of the bulk spacetime in the SS model in a deconfined phase at finite temperature is given by

$$ds^{2} = \left(\frac{u}{R_{D4}}\right)^{3/2} \left(f(u)dt^{2} + \delta_{ij}dx^{i}dx^{j} + dx_{4}^{2}\right) + \left(\frac{R_{D4}}{u}\right)^{3/2} \left(u^{2}d\Omega_{4}^{2} + \frac{du^{2}}{f(u)}\right).$$

The four-form field strength, the dilaton, and the curvature radius of the spacetime are

$$F_{(4)} = \frac{2\pi N}{V_4} \epsilon_4, \qquad e^{\phi} = g_s \left(\frac{u}{R_{D4}}\right)^{3/4}, \qquad R_{D4}^3 \equiv \pi g_s N l_s^3,$$

respectively, where  $f(u) \equiv 1 - u_T^3/u^3$ ,  $u_T = 16\pi^2 R_{\rm D4}^3 T^2/9$ .  $x_4$  is the compactified coordinate transverse to the probe D8/ $\overline{\rm D8}$  branes with arbitrary periodicity  $2\pi R$ . The volume of the unit four-sphere  $\Omega_4$  is denoted by  $V_4$  and the corresponding volume 4-form by  $\epsilon_4$ .  $F_{(4)}$  is the 4-form field strength,  $l_s$  is the string length and  $g_s$  is the string coupling.

In the SS model, the chiral symmetry dynamics is taken into account, by construction, in the form of the dynamics of the flavour branes, D8 and  $\overline{D8}$ . The DBI action of D8- $\overline{D8}$  is

$$S_{D8} = -\mu_8 \int d^9 X e^{-\phi} Tr \sqrt{-\det(g_{MN} + 2\pi\alpha' F_{MN})}$$
 (1)

where  $F_{MN}$  is the field strength of the flavour group  $U(N_f)$  on the branes. It is given by

$$F = d\mathcal{A} + i\mathcal{A} \wedge \mathcal{A}. \tag{2}$$

The  $U(N_f)$  gauge field  $\mathcal{A}$  can be decomposed into  $SU(N_f)$  part A and U(1) part  $\hat{A}$ :

$$\mathcal{A} = A + \frac{1}{\sqrt{2N_f}}\hat{A},\tag{3}$$

where only the diagonal U(1) will be turned on here. Lastly,  $g_{MN}$  is the induced metric on the D8-branes world volume.

In the deconfined phase, the equation of motion from the action of D8- $\overline{D8}$  provides 3 possible configurations: (i) connected D8- $\overline{D8}$  without sources in the bulk representing the vacuum state and (ii) the parallel configuration of both D8-branes and  $\overline{D8}$  representing the  $\chi_{S}$ -QGP. Another stable configuration (iii) is the connected D8- $\overline{D8}$  branes with the D4-brane as the baryon vertex submerged and localized in the middle of the D8 and  $\overline{D8}$ . In

 $^{^{1}}$ Actually, the quark matter, represented by the connected D8- $\overline{D8}$  branes with radial strings stretching out to the horizon, is another possible configuration satisfying the equation of motion. However, it was found that this phase is thermodynamically unstable to density fluctuations by Bergman, Lifschytz, and Lippert [21].

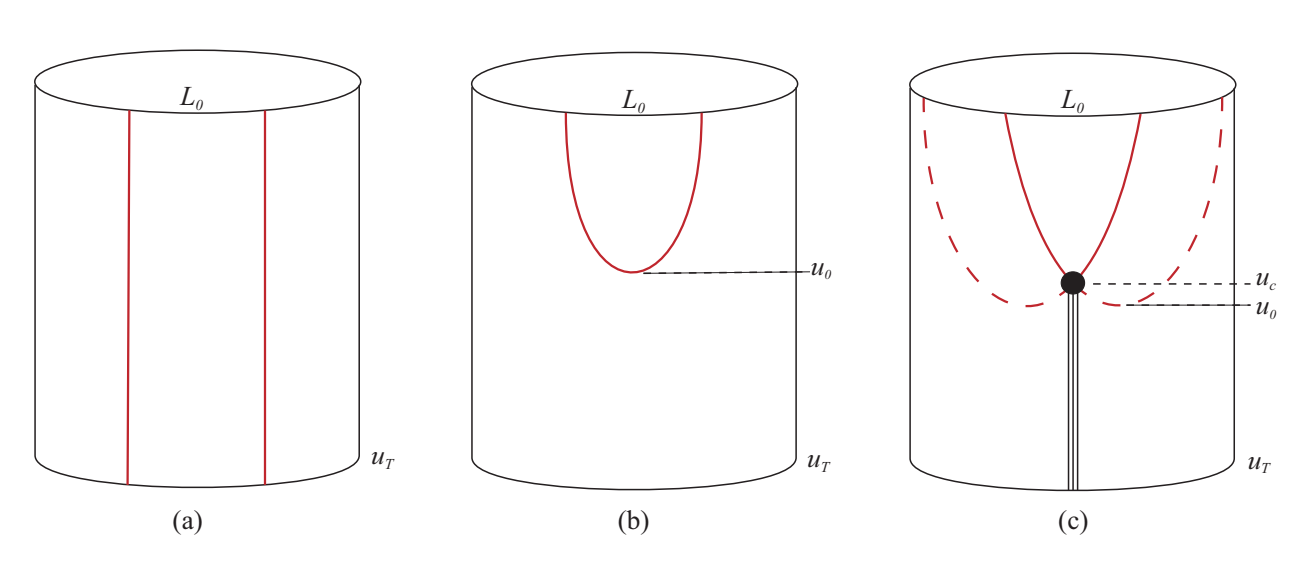


Figure 1: Different configurations of D8 and  $\overline{D8}$ -branes in the background field following the Sakai-Sugimoto model that are dual to the phases of (a)  $\chi_S$ -QGP, (b) vacuum and (c) multiquark phase.

this model, we assume that the hanging strings shrink to approximately zero and the only apparent strings are the  $k_r$  radial strings. The three configurations are shown in Fig. 1. We will consider the thermodynamic properties of only the last multiquark configuration. The action of the exotic multiquark phase is given by

$$S = S_{D8} + S_{D4} + \tilde{S}_{F1},\tag{4}$$

where  $S_{D8}$  is the DBI action of the connected D8-branes,  $S_{D4}$  represents the DBI action of the D4-brane wrapped on  $S^4$  and  $\tilde{S}_{F1}$  is the action of  $k_r$  radial strings extending from the baryon vertex down to the horizon. For simplicity, we ignore the distortion of the baryon vertex due to the Chern-Simon term [22, 23].

The DBI action of the D8- $\overline{D8}$ -brane coupled to the diagonal U(1) gauge field is given by

$$S_{D8} = \mathcal{N} \int_{u_c}^{\infty} du \ u^4 \sqrt{f(u)(x_4'(u))^2 + u^{-3}(1 - (\hat{a}_0'(u))^2)}, \tag{5}$$

where the constant  $\mathcal{N} = (\mu_8 \tau N_f \Omega_4 V_3 R^5)/g_s$ , and the rescaled U(1) diagonal field  $\hat{a} = 2\pi\alpha'\hat{A}/(R\sqrt{2N_f})$ . Position of the vertex is denoted by  $u_c$ , it is determined from the equilibrium condition of the D8-D4-strings configuration (see Appendix A of Ref. [16]). The source action of the D4 and strings,  $S_{D4} + \tilde{S}_{F1}$ , are given by

$$S_{source} = \mathcal{N}d \left[ \frac{1}{3} u_c \sqrt{f(u_c)} + n_s (u_c - u_T) \right], \tag{6}$$

where  $n_s$  is the number of radial strings  $k_r$  in the unit of  $N_c$ . The number of radial strings  $n_s$  represents the colour charges of a multiquark. For a fixed number of  $k_h$ , one of the radial

strings can merge with another radial string from another multiquark and form a colour-binding potential between the two in a similar way holographic meson is formed between a quark and an antiquark.

The  $U_B(1)$  symmetry corresponds to the U(1)-diagonal part of the global flavor symmetry,  $U(N_f)$ , which is provided by the  $N_f$  flavor branes. Naturally, the baryon chemical potential, conjugating to the  $U_B(1)$  charge, in the gauge theory side can be identified with the boundary value of the zero component of the gauge field in the flavor branes, i.e.  $A_0$ , conjugating to the U(1) "electric" charge. For convenience, our normalized baryon chemical potential is [24]

$$\mu = \hat{a}_0(\infty). \tag{7}$$

In gauge-gravity duality, we identify the grand canonical potential density in the gauge theory side in the form of the D8-branes action evaluated with the classical solution [25]:

$$\Omega(\mu) = \frac{1}{N} S_{D8}[T, x_4'(u), \hat{a}_0(u)]_{cl}$$
(8)

With the additional source term, the free energy is in the form of the combination of the Legendre-transform of the grand potential and the source action, Eqn. (6). The baryon chemical potential is simply the derivative of the free energy with respect to its conjugate, i.e. the baryon number density, at a particular temperature:

$$\mu = \frac{\partial}{\partial d} \frac{1}{\mathcal{N}} \left( \tilde{S}_{D8}[T, x_4'(u), d(u)]_{cl} + S_{\text{source}}(d, u_c) \right)$$
(9)

where the Legendre-transformed action  $\tilde{S}_{\mathrm{D8}}$  is given by

$$\tilde{S}_{D8}[T, x_4'(u), d(u)] = S_{D8}[T, x_4'(u), \hat{a}_0(u)] + \mathcal{N} \int_{u_0}^{\infty} d(u)\hat{a}_0' du$$
(10)

$$= \int_{u_c}^{\infty} du u^4 \sqrt{f(u)(x_4'(u))^2 + u^{-3}} \sqrt{1 + \frac{d(u)^2}{u^5}}, \tag{11}$$

where d(u) is the electric displacement. It is a constant of the configuration given by

$$d(u) = -\frac{1}{N} \frac{\delta S_{D8}}{\delta \hat{a}'_0(u)} = \frac{u \hat{a}'_0(u)}{\sqrt{f(u)(x'_4(u))^2 + u^{-3}(1 - (\hat{a}'_0(u))^2)}} = \text{const.}$$
 (12)

Note that the Legendre transformation changes the dependence on the variable  $\hat{a}_0(u)$  in  $S_{D8}$  to d(u) in  $\tilde{S}_{D8}$ . As a result, the grand potential as a function of the baryon chemical potential is transformed into the free energy as a function of the baryon number density. Another constant of the configuration is

$$(x_4'(u))^2 = \frac{1}{u^3 f(u)} \left[ \frac{f(u)(u^8 + u^3 d^2)}{F^2} - 1 \right]^{-1} = \text{const.},$$
 (13)

where F is a function of  $u_c$ , d, T and  $n_s$ , given by

$$F^{2} = u_{c}^{3} f_{c} \left( u_{c}^{5} + d^{2} - \frac{d^{2} \eta_{c}^{2}}{9 f_{c}} \right), \tag{14}$$

where  $\eta_c \equiv 1 + \frac{1}{2} \left(\frac{u_T}{u_c}\right)^3 + 3n_s \sqrt{f_c}$ . For convenience, here and henceforth, f,  $f_c$  and  $f_0$  are used to represent f(u),  $f(u_c)$  and  $f(u_0)$ , respectively. Note that this form of F is derived from the force condition at the cusp  $u_c$ . The detailed calculations are given in the Appendix of Ref. [16].

With the equation of motion for  $x_4$ , Eqn. (13), and the separation between D8- and  $\overline{D8}$ -branes  $L_0$  being fixed to  $L_0 = 2 \int_{uc}^{\infty} x_4'(u) du = 1$ , we obtain [21]

$$\mu = \int_{u_c}^{\infty} \hat{a}_0'(u) + \frac{1}{\mathcal{N}} \frac{\partial S_{source}}{\partial d} \bigg|_{T, L_0, u_c}, \tag{15}$$

where the second term is the contribution from the sources,  $\mu_{source}$ . From these relations, we can then study the thermodynamic properties of the multiquark phase. The phase diagram of the multiquark nuclear phase is studied in Ref. [16] when the colour-binding interaction is neglected. It is found that multiquarks are preferred thermodynamically over the other gluon-deconfined phases for the large density and intermediate temperature below the chiral symmetry restoration temperature.

# 3 Calculations of the equation of state

Thermodynamic properties of the nuclear/exotic matter phase can be described by the equation of state. First, we will investigate the relations between the pressure and the number density. From the previous section (see also Ref. [16]), the grand potential density and the chemical potential of the nuclear/exotic matters are given by

$$\Omega = \int_{u_c}^{\infty} du \left[ 1 - \frac{F^2}{f(u)(u^8 + u^3 d^2)} \right]^{-1/2} \frac{u^5}{\sqrt{u^5 + d^2}}, \tag{16}$$

$$\mu = \int_{u_c}^{\infty} du \left[ 1 - \frac{F^2}{f(u)(u^8 + u^3 d^2)} \right]^{-1/2} \frac{d}{\sqrt{u^5 + d^2}} + \frac{1}{3} u_c \sqrt{f(u_c)} + n_s (u_c - u_T) \quad (17)$$

respectively.

Since the differential of the grand potential  $G_{\Omega}$  can be written as

$$dG_{\Omega} = -PdV - SdT - Nd\mu \tag{18}$$

where the state parameters describing the system P, V, S, T, N are the pressure, volume, entropy, temperature, the total number of particles of the system respectively. Since the change of volume is not our concern, we define the volume density of  $G_{\Omega}$ , S and N to be  $\Omega$ , s and d, respectively. Therefore, we have, at a particular T and  $\mu$ ,

$$P = -G_{\Omega}/V \equiv -\Omega(T, \mu). \tag{19}$$

By assuming that the multi-quark states are spatially uniform, we obtain

$$d = \frac{\partial P}{\partial \mu}(T, \mu). \tag{20}$$

Using the chain rule,

$$\left. \frac{\partial P}{\partial d} \right|_{T} = \left. \frac{\partial \mu}{\partial d} \right|_{T} d,\tag{21}$$

so that

$$P(d, T, n_s) = \mu(d, T, n_s) \ d - \int_0^d \mu(d', T, n_s) \ d(d'), \tag{22}$$

where we have assumed that the regulated pressure is zero when there is no nuclear matter, i.e. d = 0.

In the limit of very small d,  $u_c$  approaches  $u_0$ ,  $\eta_c$  becomes  $\eta_0 + \mathcal{O}(d)$ , where  $\eta_0$  is defined to be  $\eta_c$  with  $u_c$  replaced by  $u_0$ . From Eqn. (17), the baryon chemical potential can then be approximated to be

$$\mu - \mu_{source} \simeq d \left\{ \int_{u_c}^{\infty} du \left[ 1 - \frac{u_0^8 f_0}{f u^8} - \frac{f_0 u_0^3 \left( 1 - \frac{\eta_0^2}{9 f_0} - \frac{u_0^5}{u^5} \right) d^2}{f u^8} \right]^{-1/2} u^{-5/2} \left( 1 - \frac{d^2}{2u^5} \right) \right\}, (23)$$

where  $\mu_{source} = \frac{1}{3}u_c\sqrt{f(u_c)} + n_s(u_c - u_T)$ , and we have neglected the higher order terms of d. By using the binomial expansion, the above equation becomes

$$\mu - \mu_{source} \simeq d \left\{ \int_{u_0}^{\infty} du \frac{u^{-5/2}}{\sqrt{1 - \frac{f_0 u_0^8}{f u^8}}} \left[ 1 + \left( \frac{f_0 u_0^3}{f u^8 - f_0 u_0^8} \left( 1 - \frac{\eta_0^2}{9 f_0} - \frac{u_0^5}{u^5} \right) - \frac{1}{u^5} \right) \frac{d^2}{2} \right] \right\}$$

$$= \alpha_0 d - \beta_0(n_s) d^3, \tag{24}$$

where

$$\alpha_0 \equiv \int_{u_0}^{\infty} du \frac{u^{-5/2}}{1 - \frac{f_0 u_0^8}{f u^8}} \,, \tag{25}$$

$$\beta_0(n_s) \equiv \int_{u_0}^{\infty} du \frac{u^{-5/2}}{2\sqrt{1 - \frac{f_0 u_0^8}{f_0 u^8}}} \left( \frac{f_0 u_0^3}{f u^8 - f_0 u_0^8} \left( 1 - \frac{\eta_0^2}{9f_0} - \frac{u_0^5}{u^5} \right) + \frac{1}{u^5} \right). \tag{26}$$

By substituting Eqn.(24) into Eqn.(22), we can determine the pressure in the limit of very small d as

$$P \simeq \frac{\alpha_0}{2} d^2 - \frac{3\beta_0(n_s)}{4} d^4.$$
 (27)

In the limit of very large d and relatively small T,

$$\mu - \mu_{source} = \int_{u_c}^{\infty} du \left[ 1 - \frac{f_c u_c^3}{f u^3} \left( \frac{u_c^5 + d^2 - \frac{d^2 \eta_c^2}{9f_c}}{u^5 + d^2} \right) \right]^{-1/2} \frac{d}{\sqrt{u^5 + d^2}}$$
 (28)

$$\approx \int_{u_c}^{\infty} du \frac{d}{\sqrt{u^5 + d^2}} + \frac{1}{2} u_c^3 f_c d^2 \left( 1 - \frac{\eta_c^2}{9f_c} \right) \int_{u_c}^{\infty} du \frac{d}{f u^3 (u^5 + d^2)^{3/2}}$$
(29)

$$\approx \frac{d^{2/5}}{5} \frac{\Gamma\left(\frac{1}{5}\right) \Gamma\left(\frac{3}{10}\right)}{\Gamma\left(\frac{1}{2}\right)} + \frac{u_c^3 f_c}{10} \left(1 - \frac{\eta_c^2}{9f_c}\right) d^{-4/5} \frac{\Gamma\left(-\frac{2}{5}\right) \Gamma\left(\frac{19}{10}\right)}{\Gamma\left(\frac{3}{2}\right)}$$
(30)

where we have used the fact that the lower limit of integration  $u_c^5/d^2$  is approximately zero as d is very large. Again by using Eqn. (22), we obtain

$$P \simeq \frac{2}{35} \left( \frac{\Gamma\left(\frac{1}{5}\right) \Gamma\left(\frac{3}{10}\right)}{\Gamma\left(\frac{1}{2}\right)} \right) d^{7/5}. \tag{31}$$

And the energy density can then be found via the relation  $d\rho = \mu d(d)$ .

Next we consider the entropy of the multiquarks phase. From the differential of the free energy,

$$dF_E = -PdV - SdT + \mu dN, (32)$$

the entropy is given by

$$S = -\frac{\partial F_E}{\partial T}. (33)$$

The entropy density can then be written as

$$s = -\frac{\partial \mathcal{F}_E}{\partial T},\tag{34}$$

where  $\mathcal{F}_E$  is the free energy density which relates to the grand potential density as  $\mathcal{F}_E = \Omega + \mu d$ . Since we have the pressure  $P = -\Omega$ , we can write

$$s = \frac{\partial P}{\partial T} - \left(\frac{\partial \mu}{\partial T}\right) d. \tag{35}$$

For both small d and large d, we can see from the formula of the pressure (see Eqn. (27), (31), noting that  $\alpha_0$ ,  $\beta_0$  is insensitive to temperature) and the chemical potential (see Eqn.(24),(30)), that the dominant contribution comes only from  $\mu_{source}$ , thus  $s \simeq -\left(\frac{\partial \mu_{source}}{\partial T}\right) d. \tag{36}$ 

$$s \simeq -\left(\frac{\partial \mu_{source}}{\partial T}\right) d. \tag{36}$$

The baryon chemical potential from the D8-branes is insensitive to the changes of temperature. This implies that the main contribution to the entropy density of the multiquark nuclear phase comes from the source term namely the vertex and strings.

Since

$$\frac{\partial \mu_{source}}{\partial T} = \frac{\partial}{\partial T} \left( \frac{1}{3} u_c \sqrt{f(u_c)} + n_s (u_c - u_T) \right), \tag{37}$$

$$\frac{\partial \mu_{source}}{\partial T} \approx -\frac{\left(\frac{16\pi^2}{9}\right)^3 T^5}{u_0^2 \sqrt{1 - \left(\frac{u_T}{u_0}\right)^3}} - n_s \frac{32\pi^2 T}{9},\tag{38}$$

where we have used the fact that  $u_c$  is approximately constant with respect to the temperature in the range between the gluon deconfinement and the chiral symmetry restoration (see

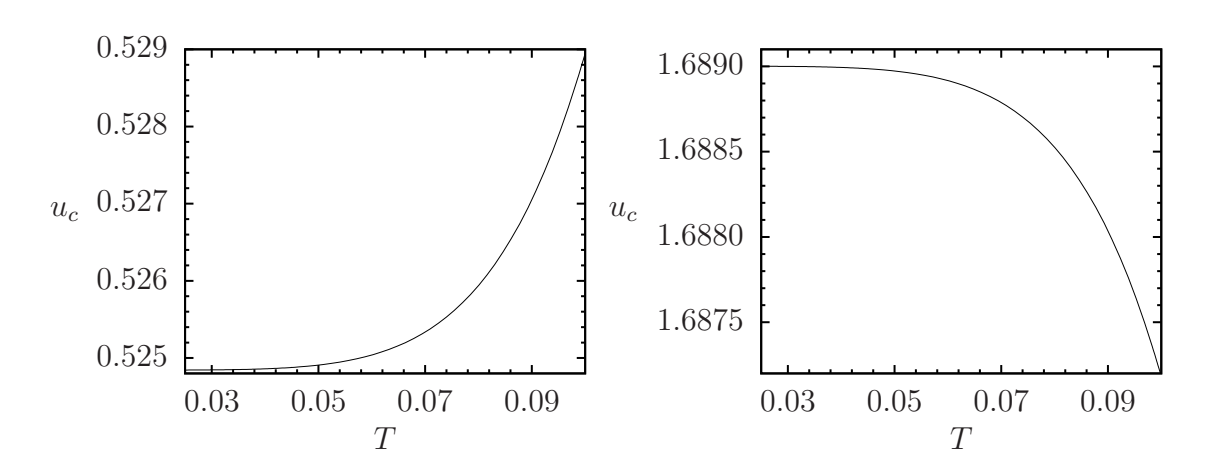


Figure 2: The graphs show the relations between  $u_c$  and T at small density (left) and at large density (right).

Fig. 2). Therefore, we obtain

$$s \approx \frac{\left(\frac{16\pi^2}{9}\right)^3 T^5 d}{u_0^2 \sqrt{1 - \left(\frac{u_T}{u_0}\right)^3}} + n_s \frac{32\pi^2 T d}{9}.$$
 (39)

For small  $n_s$ , the entropy density is proportional to  $T^5$ . When  $n_s$  gets larger (carrying colour charge), the entropy density becomes dominated by the colour term  $s \propto n_s T$ . This is confirmed numerically in Section 4. It has been found that the entropy density of the  $\chi_S$ -QGP scales as  $T^6$  [21] corresponding to the fluid of mostly free quarks and gluons. We can see that the effect of the colour charge of the multiquarks as quasi-particles is to make them less like free particles with the temperature dependence  $\sim n_s T$ , i.e. much less sensitive to the temperature.

It is interesting to compare the dependence of pressure on the number density, Eqn. (27) and (31), to the confined case at zero temperature studied in Ref. [27]. The power-law relations for both small and large density of the confined and deconfined multiquark phases are in the same form (for  $n_s = 0$ ). The reason is that the main contributions to the pressure for both phases are given by the D8-branes parts and they have similar dependence on the density for both phases. For the deconfined multiquark phase, the additional contributions from the source terms in Eqn. (17),  $\mu_{source}$ , are mostly constant with respect to the density (this is because  $u_c$  becomes approximately independent of d for small and large d limits).

Consequently, when we substitute into Eqn. (22), the constant contributions cancel out and affect nothing on the pressure.

On the contrary, the entropy density for the deconfined phase is dominated by the contributions from the sources namely the vertex and strings. The contribution of the D8-branes is insensitive to the change of temperature and therefore does not affect the entropy density significantly. The additional source terms, however, depend on the temperature and thus contribute dominantly to the entropy density. Once the temperature rises beyond the gluon-deconfined temperature, entropy density will rise abruptly (for sufficiently large density d) and become sensitive to the temperature according to Eqn. (39), due to the release of quarks from colourless confinement appearing as the sources. However, we will see later on using the numerical study in Section 4 that for low densities and for small  $n_s$ , the numerical value of the entropy density is yet relatively small.

# 4 Numerical studies of the thermodynamic relations

From the analytic approximations in the previous section, we expect the pressure to appear as straight line in the logarithmic scale for small and large d with the slope approximately 2 and 7/5 respectively. The relation between pressure and density of the multiquarks from the full expressions can be plotted numerically as are shown in Fig. 3-5. The pressure does not really depend much on the temperature and we therefore present only the plots at T=0.03. Remarkably, the transition from small to large d is clearly visible in the logarithmic-scale plots. The transition occurs around  $d_c \simeq 0.072$ . Interestingly, as is shown in Fig. 5, the multiquarks with larger  $n_s$  has lower pressure than the ones with smaller  $n_s$  for  $d < d_c$  and vice versa. The dependence on  $n_s$  remains to be seen for small d as we can see from Eqn. (27). For large d, the  $n_s$ -dependence is highly suppressed as predicted by Eqn. (31).

The entropy density as a function of the temperature for various ranges of the density is shown in Fig. 6. The temperature dependence for both small and large d are the same,  $\simeq T^5$  at the leading order. The d-dependence is linear and thus appears as separation of straight lines in the logarithmic-scale plot. For  $n_s > 0$ , we can see from Eqn. (39) that the linear term in T should become increasingly important. This is confirmed numerically as is shown in Fig. 6. The slope of the graph between the entropy density s and s in the double-log scale for s = 0 (the left plot) and s = 0.3 (the right plot) is approximately 5 and 1 respectively. Regardless of the temperature dependence, it should be noted that the numerical value of the entropy density for small densities and low s in Fig. 6 is quite small.

Lastly, the relations between the baryon number density and chemical potential are shown in Fig. 7. Temperature has very small effect on these curves and negligible for the range of temperature between the gluon deconfinement and the chiral-symmetry restoration. The baryon chemical potential depends linearly on the number density for small d. For large d, the relation between the chemical potential and number density becomes  $\mu \approx d^{2/5}$ . Interestingly, the multiquark quasi-particles behave more like fermions as a result of being the electric response of the DBI action [21].

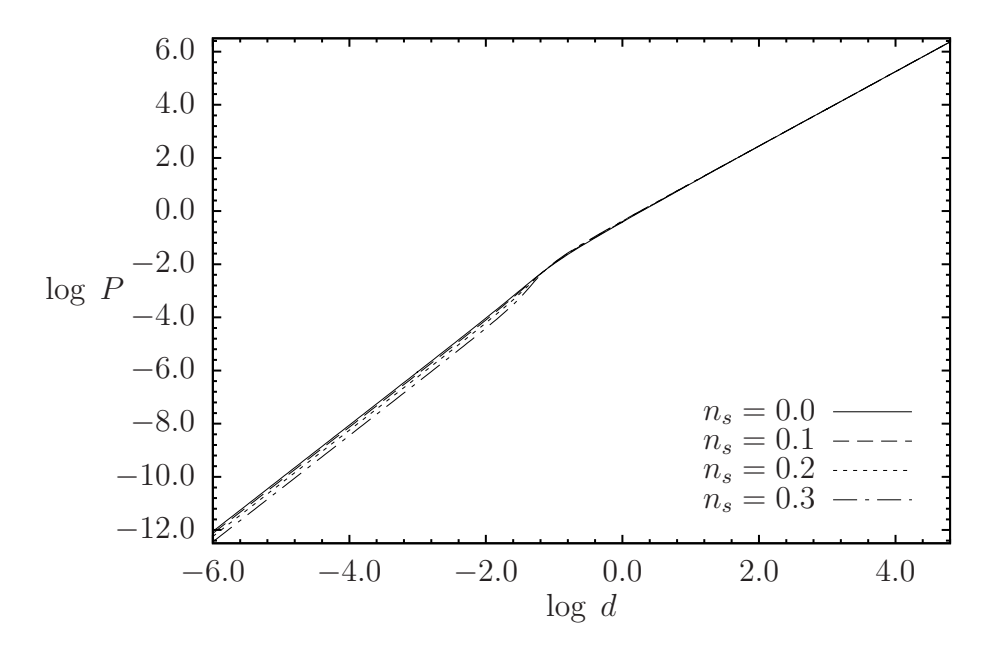


Figure 3: Pressure and density in logarithmic scale at T = 0.03.

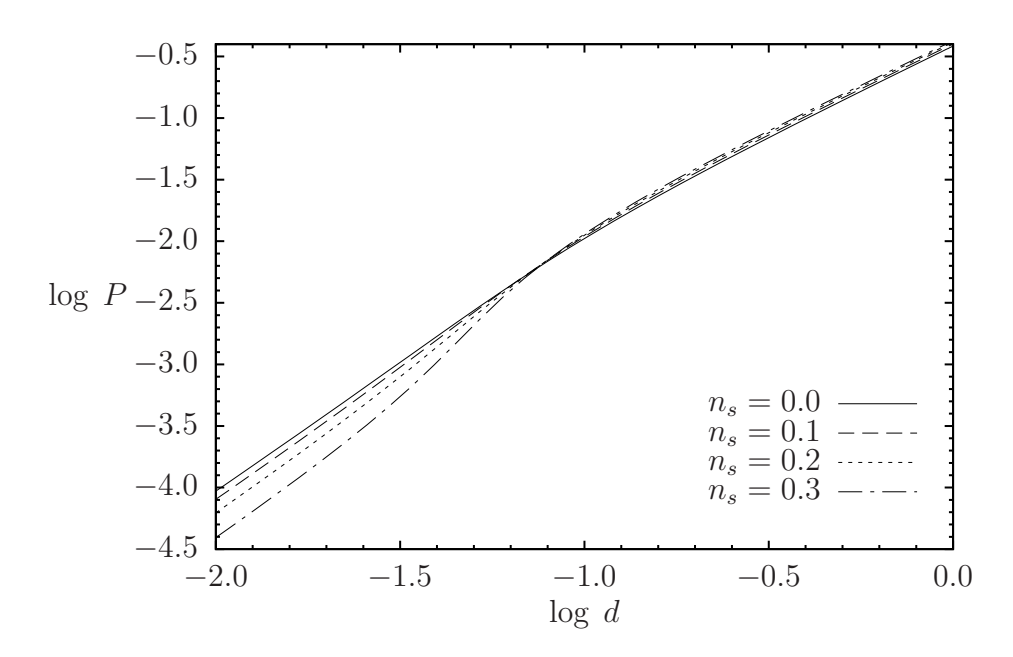


Figure 4: Pressure and density in logarithmic scale at T=0.03, zoomed in around the transition region.

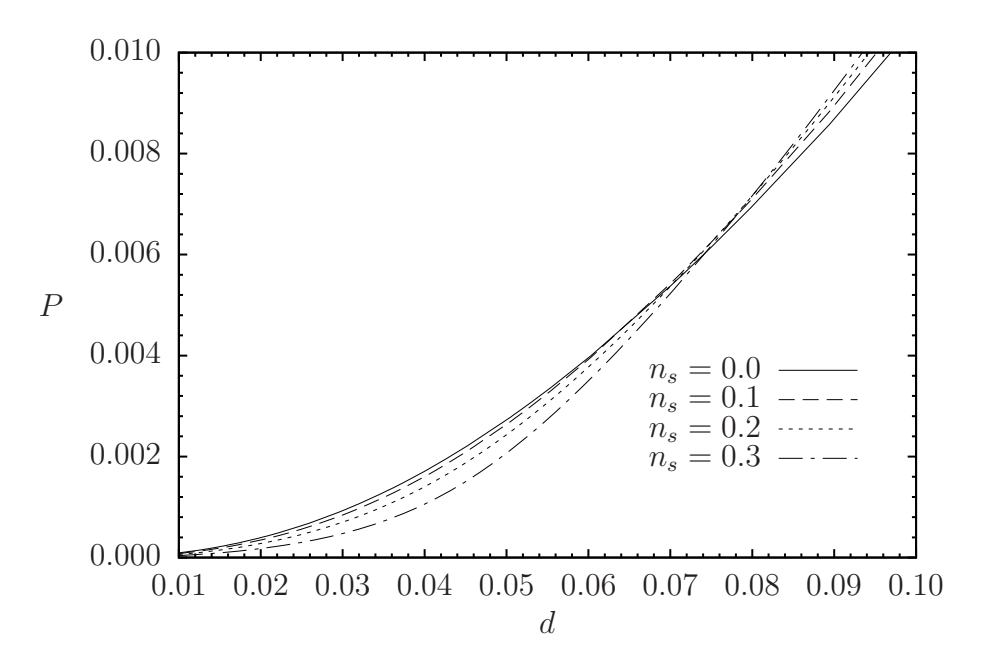


Figure 5: Pressure and density in linear scale.

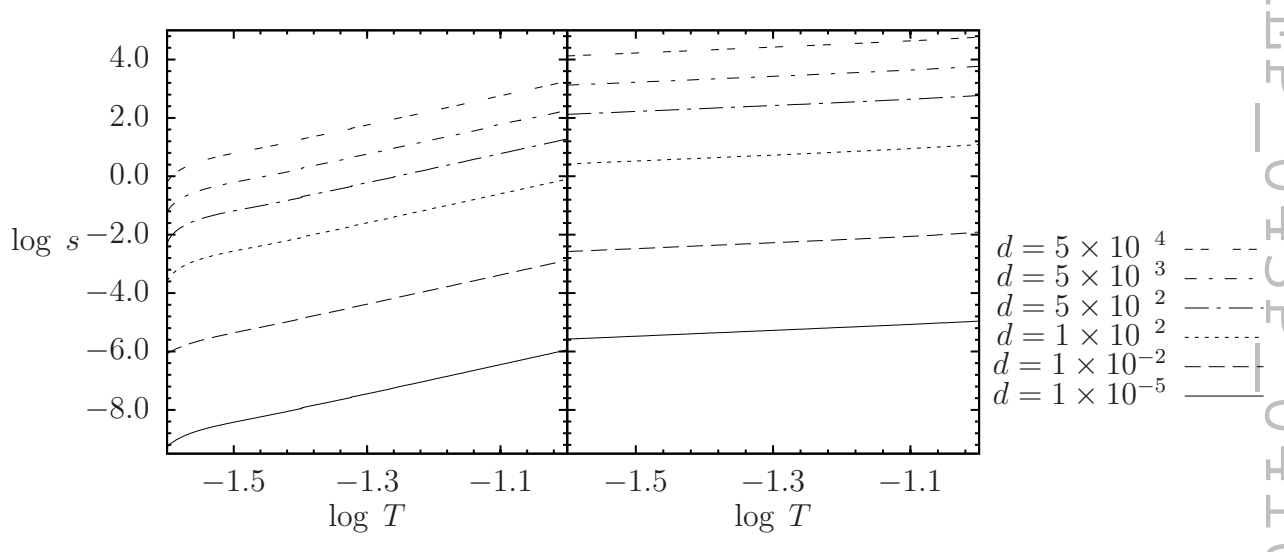


Figure 6: Entropy and temperature in logarithmic scale for  $n_s = 0$  (left), 0.3 (right).

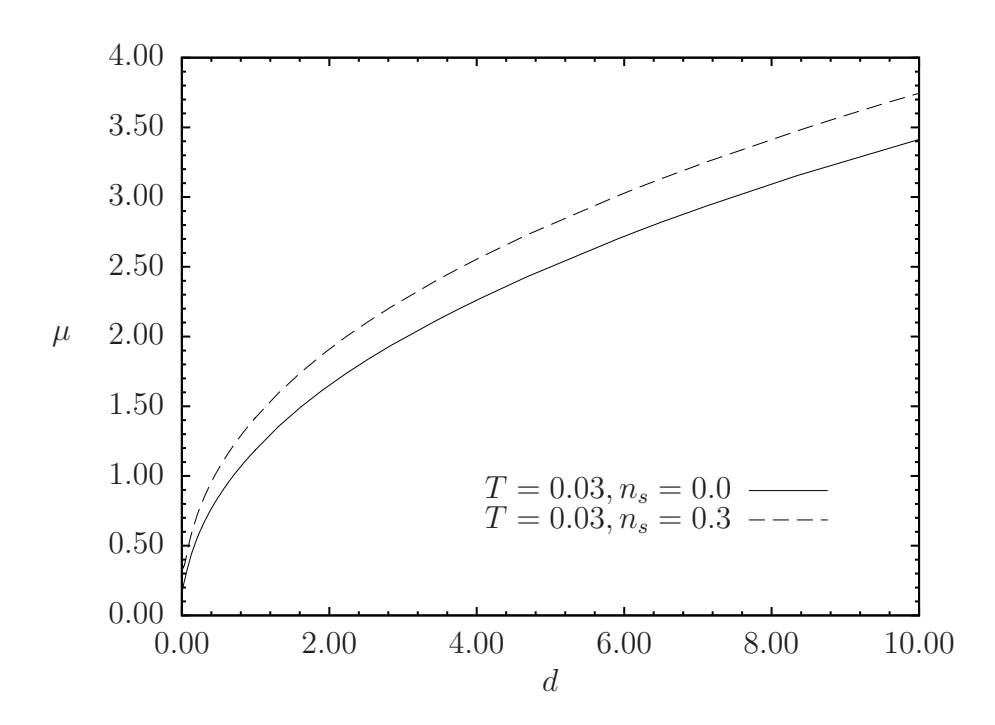


Figure 7: The baryon chemical potential and number density in logarithmic scale at T = 0.03.

# 5 Gravitational stability of the dense multiquark star

When a dying star collapses under its own gravity, it is generically believed that the degeneracy pressure of either electrons or neutrons would be able to stop the collapse to form a white dwarf or a neutron star. If the star is more massive than the upper mass limit of the neutron star, it would collapse into a black hole eventually. The mass limit of the neutron star is sensitive to the physics of warm dense nuclear matter but little is known about the equation of state of nuclear matter under high temperature and large density. Even though the original mass limit of the neutron star estimated by Oppenheimer, and Volkoff was only 0.7 solar mass [20], the new limit when the nuclear interactions are included could be as large as 2.5 solar mass [26]. Under extreme pressure and density, the quarks within hadrons could be freed and wander around the interior of the star. In other words, quarks are effectively deconfined from the localized hadrons but confined by gravity within the star. Using the bag model to describe the state of being confined by gravity but possibly deconfined from the hadrons, it turns out that quark matter phase, e.g. strange star, is possible under extreme pressure and density.

However, physics of the deconfinement is largely unknown due to the non-perturbative nature of the strong interaction and the difficulty of lattice approach to deal with finite baryon density situation. The bag model are not always served as a reliable theoretical tool to explore the behaviour of quarks in the dense star when the deconfinement exists. It is therefore interesting to use the equation of state of the deconfined nuclear matter from the holographic model to investigate the behaviour of the dense star as a complementary tool

to the bag model and other approaches.

In this section, we will consider a hypothetical multiquark star containing only the multiquark matter with uniform constant temperature. The relations between pressure and density will be adopted directly from the holographic model as the equations of state of the quasi-particles. Since the pressure and density have very small temperature dependence for the range of temperatures under consideration, the results are valid generically.

A study into the gravitational stability of a spherically symmetric dense star can be performed using the Tolman-Oppenheimer-Volkoff equation [20]. It is known that the spherically symmetric dense star has metric in a form

$$ds^{2} = A(r)dt^{2} - B(r)dr^{2} - r^{2}d\Omega_{2}.$$
(40)

After substituting into the Einstein field equation, we obtain the following relations,

$$B(r) = \left(1 - \frac{A^*(r)}{r}\right)^{-1},\tag{41}$$

$$\frac{dA^*(r)}{dr} = 8\pi\rho r^2,\tag{42}$$

and

$$\frac{dP(r)}{dr} = -\frac{(\rho+P)}{2} \frac{A'(r)}{A(r)} = -\frac{(\rho+P)}{2} \frac{8\pi P r^3 + A^*(r)}{r(r-A^*(r))}.$$
 (43)

The last equation is known as the Tolman-Oppenheimer-Volkoff (TOV) equation. The accumulated mass of the star, M(r), is given by  $A^*(r) = 2M(r)$ . It has been shown in Ref. [28] that the chemical potential can be defined through the background metric in the form of  $\mu(r) = \frac{\epsilon_F}{\sqrt{A(r)}}$ . It will automatically solve the TOV equation. Note that the constant  $\epsilon_F$  is arbitrary. Since

$$\frac{\mu'(r)}{\mu(r)} = -\frac{1}{2} \frac{A'(r)}{A(r)},\tag{44}$$

the TOV equation becomes

$$\frac{dP(r)}{dr} = (\rho + P)\frac{\mu'(r)}{\mu(r)}. (45)$$

Together with the first law of thermodynamics  $\rho + P = \mu d$ , the TOV equation then takes the following form,

$$d\mu = \frac{1}{d} \left( \frac{\partial P}{\partial d} \right) d(d). \tag{46}$$

Obviously, the chemical potential can be determined, as a function of the number density:

$$\mu(d) = \int_0^d \frac{1}{\eta} \left(\frac{\partial P}{\partial \eta}\right) d\eta + \mu_{onset},\tag{47}$$

where  $\mu_{onset} \equiv \mu(d=0)$ . Additionally, considering from the TOV equation together with the first law of thermodynamics, the density  $d\rho = \mu d(d)$  can be integrated to

$$\rho(d) = \int_0^d \left[ \int_0^{\eta} \frac{1}{\eta'} \left( \frac{\partial P}{\partial \eta'} \right) d\eta' + \mu_{onset} \right] d\eta. \tag{48}$$

For a power-law equation of state,  $P = kd^{\lambda}$ , the chemical potential, Eqn. (47), becomes

$$\mu(d) = \frac{\lambda k}{\lambda - 1} d^{\lambda - 1} + \mu_{onset},\tag{49}$$

and eventually the equation of state is given by

$$\rho = \frac{1}{\lambda - 1} P + \mu_{onset} \left(\frac{P}{k}\right)^{1/\lambda}.$$
 (50)

In our holographic model of multiquarks, the relation between pressure and density has a unique power-law behaviour, as is also found in Ref. [21] for the case of normal baryon ( $n_s = 0$ ). This is shown in Fig. 3-4. For small d,  $P \propto d^2$  ( $n_s = 0$ ) and for large d,  $P \propto d^{7/5}$ . The dependence on  $n_s$  becomes significant when the density d is small and the equation of state can be approximated by  $P \simeq \alpha d^2 + \beta d^4$ . Since there are two power-laws governing, we need to match the solutions from the two regions together (i.e. core and crust). The number density where the equation of state changes from the large-d to the small-d is denoted by  $d_c$ .

For  $n_s = 0$ , at the transition point  $d = d_c$ , the energy density is given by Eqn. (50),

$$\rho_c = \frac{k' d_c^{\lambda'}}{\lambda' - 1} + \mu_{onset} d_c, \tag{51}$$

where  $P = k'd^{\lambda'}$  (Eqn. (27) suggests that  $\lambda' = 2$ ) is the equation of state of the small d region. We recalculate the relation Eqn. (47), (48) for the large d region which match with this  $\rho_c$  to be

$$\mu = \mu_c + \lambda k \left( \frac{d^{\lambda - 1}}{\lambda - 1} - \frac{d_c^{\lambda - 1}}{\lambda - 1} \right), \tag{52}$$

$$\rho = \rho_c + \frac{1}{\lambda - 1}P + \mu_c \left[ \left( \frac{P}{k} \right)^{1/\lambda} - d_c \right] + kd_c^{\lambda} - \frac{\lambda k}{\lambda - 1}d_c^{\lambda - 1} \left( \frac{P}{k} \right)^{1/\lambda}. \tag{53}$$

Numerical results and Eqn. (31) suggest that  $\lambda = 7/5$  for the large d region.

For  $n_s > 0$ , assume the equation of state for small d is in the form of  $P = ad^{\lambda_1} + bd^{\lambda_2}$  (Eqn. (27) suggests that  $\lambda_{1,2} = 2, 4$ ), the chemical potential and energy density for the small d region become

$$\mu = \mu_{onset} + \frac{\lambda_1 a d^{\lambda_1 - 1}}{\lambda_1 - 1} + \frac{\lambda_2 b d^{\lambda_2 - 1}}{\lambda_2 - 1},\tag{54}$$

$$\rho = \mu_{onset}d + \frac{ad^{\lambda_1}}{\lambda_1 - 1} + \frac{bd^{\lambda_2}}{\lambda_2 - 1}.$$
 (55)

We obtain the transition density in the similar fashion,

$$\rho_c = \mu_{onset} d_c + \frac{a d_c^{\lambda_1}}{\lambda_1 - 1} + \frac{b d_c^{\lambda_2}}{\lambda_2 - 1}.$$
 (56)

Numerical results show that for large d, the effect of  $n_s$  is negligible. Therefore, the baryon chemical potential and the density for the large d region are again given by Eqn. (52) and (53). The equations of state, Eqn. (50),(53) as well as the corresponding relations for  $n_s > 0$  case, are in the mixed form containing both the quasi-particle nonlinear terms and the linear term. The linear term is roughly  $\rho_{linear} \approx 2.5P$  and the quasi-particle term is approximately  $\rho_{quasi} \approx P^{5/7}$ .

We can solve the TOV equation when the equations of state are given as above by starting from the core of the star out to the surface. As we go from the center towards the surface of the star, the density decreases until it reaches a critical value  $\rho_c$ . This density corresponds to the number density  $d_c$  where the power-law changes from  $P \simeq d^{7/5}$  to  $P \simeq d^2$  (see Fig. 3-4). For the crust region where the density  $\rho < \rho_c$ , multiquarks obey a different equation of state given by Eqn. (50). The radius of the core is defined to be the distance  $R_{core}$  where  $\rho(R_{core}) = \rho_c$  and the surface of the star is defined to be the radial distance R where  $\rho(R) = 0$ .

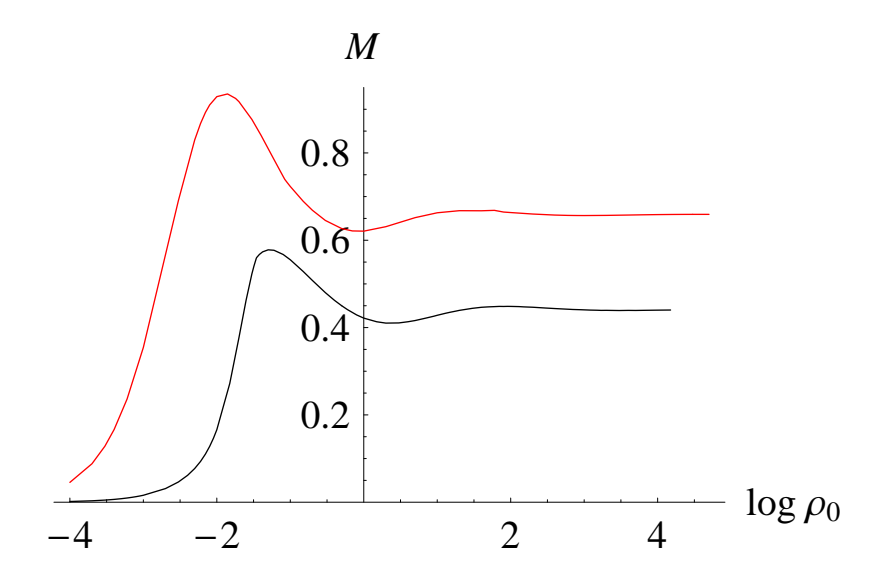


Figure 8: The relation between mass and central density of the multiquark star for multiquarks with  $n_s = 0$  (upper), 0.3 (lower).

For  $n_s=0$ , numerical fittings suggest that  $k=10^{-0.4}, \lambda=7/5, d_c=0.215443, \mu_c=0.564374$  (core) and  $k'=1, \lambda'=2, \mu_{onset}=0.17495$  (crust). For  $n_s=0.3$ , good fit parameters are  $k=10^{-0.4}, \lambda=7/5, d_c=0.086666, \mu_c=0.490069$  (core) and a,b=0.375,180.0,;  $\lambda_{1,2}=2,4$ ;  $\mu_{onset}=0.32767$  (crust). Varying the central density  $\rho_0$  of the star, we obtain the mass-density relation in Fig. 8. Each curve has two maxima, a larger one in the small density region and a smaller one in the large density region. Each maximum corresponds to each power-law of the equation of state, the low density to the crust and the large density to the core. Interestingly, the contribution to the total mass of the multiquark star comes dominantly from the crust. This is shown in Fig. 9. Even though the density is much lower, the volume of the crust is proportional to the second power of the radius and thus makes the contribution of the crust to the total mass larger than the core's.

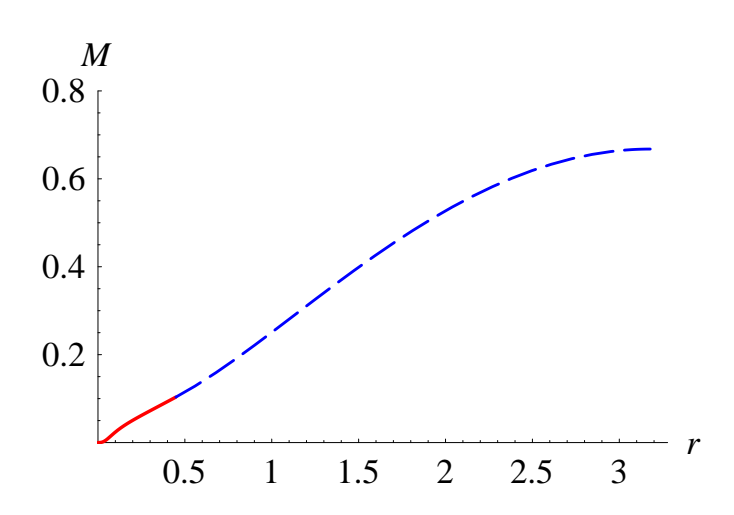


Figure 9: The accumulated mass distribution in the hypothetical multiquark star for the central density  $\rho_0 = 20$  and  $n_s = 0$ . The inner (outer) red (dashed-blue) line represents the core (crust) region.

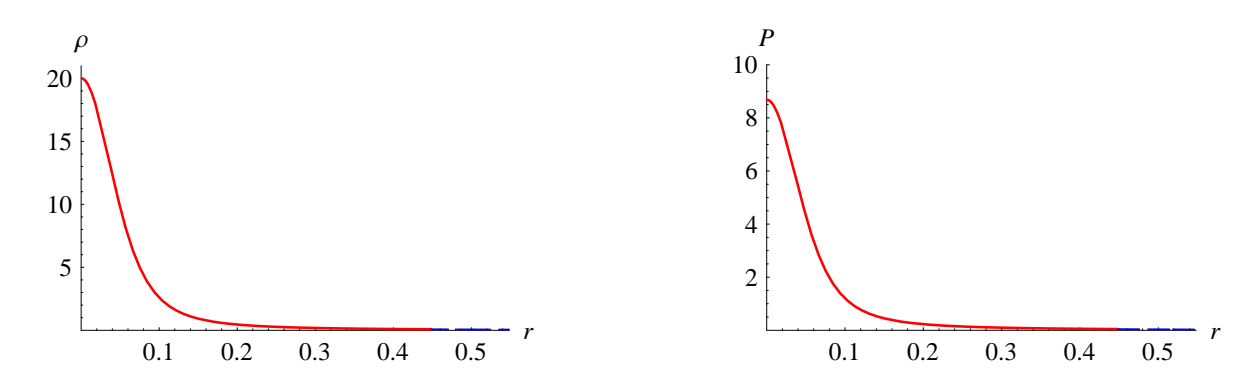


Figure 10: The density, and pressure distribution in the hypothetical multiquark star for the central density  $\rho_0 = 20$  and  $n_s = 0$ . The inner (outer) red (dashed-blue) line represents the core (crust) region.

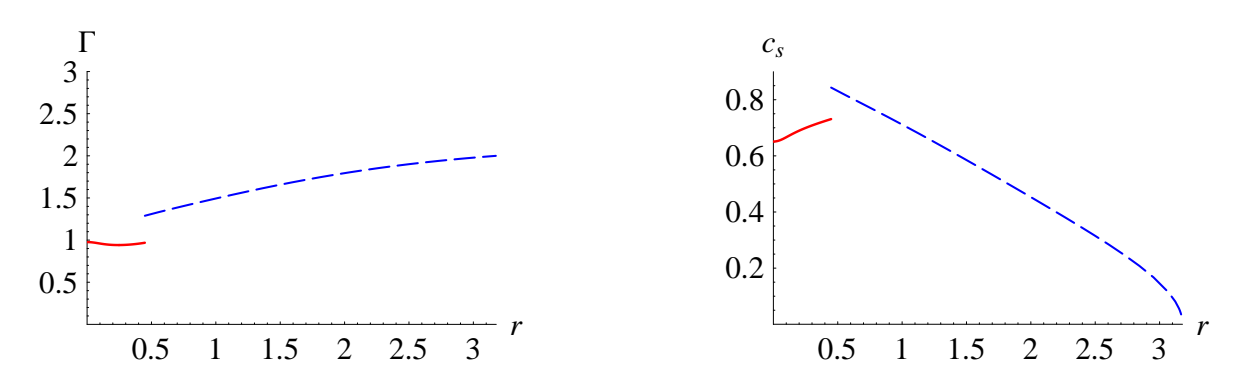


Figure 11: The adiabatic index at constant entropy ( $\Gamma$ ) and the sound speed ( $c_s$ ) distribution in the hypothetical multiquark star for the central density  $\rho_0 = 20$  and  $n_s = 0$ . The inner (outer) red (dashed-blue) line represents the core (crust) region.

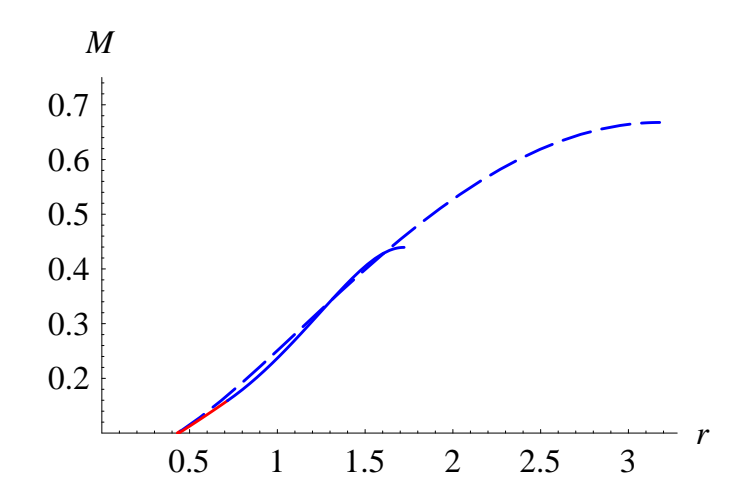


Figure 12: Comparison of the accumulated mass distribution in the hypothetical multiquark star for the central density  $\rho_0 = 20$  between  $n_s = 0$  and 0.3. The (dashed) blue line represents the crust region of multiquark star with  $n_s = 0.3$  (0). The red lines represent the core region of which both cases are almost the same.

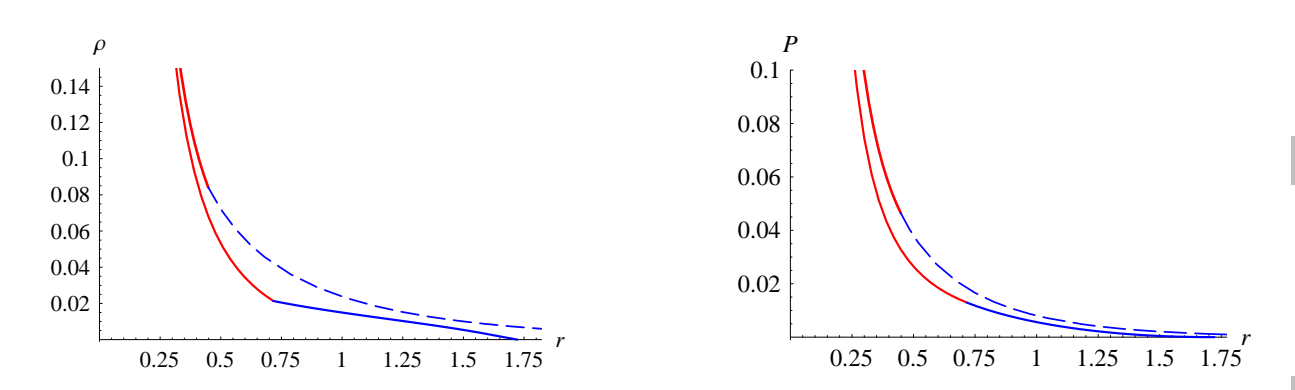
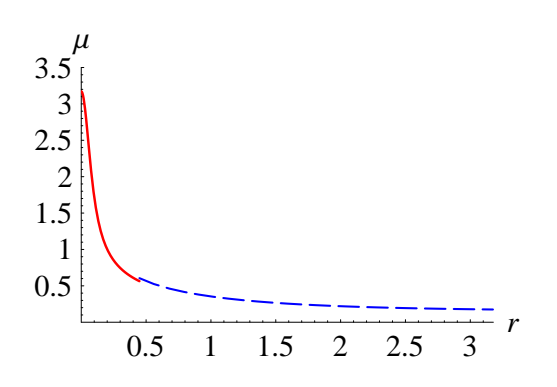


Figure 13: Comparison of the density, and pressure distribution in the hypothetical multiquark star for the central density  $\rho_0 = 20$  between  $n_s = 0$  and 0.3. The (dashed) blue line represents the crust region of multiquark star with  $n_s = 0.3$  (0). The red lines represent the core region of which both cases are almost the same.



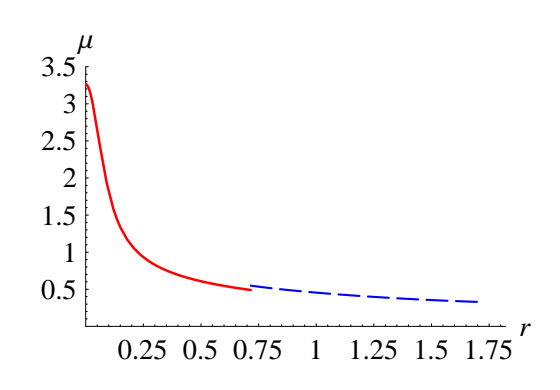
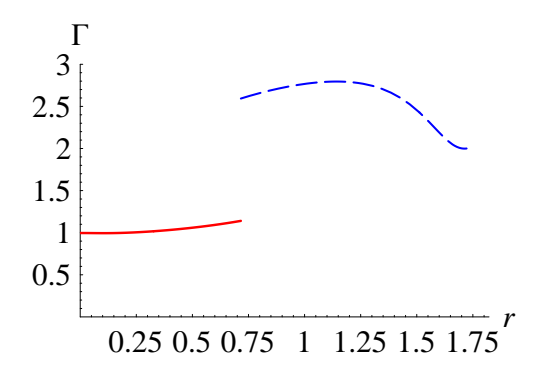


Figure 14: Comparison of the baryon chemical distributions in the hypothetical multiquark star for the central density  $\rho_0 = 20$  between  $n_s = 0$  (left) and 0.3 (right). The solid (dashed) red (blue) line represents the core (crust) region.



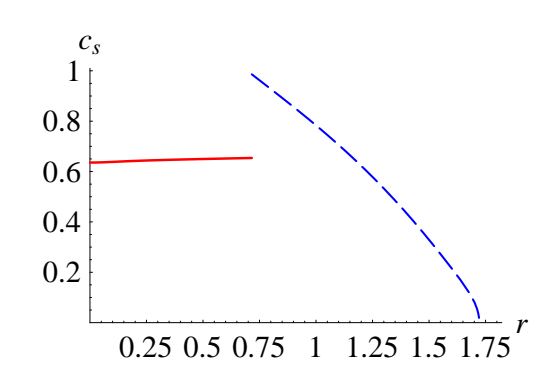


Figure 15: The adiabatic index at constant entropy ( $\Gamma$ ) and the sound speed ( $c_s$ ) distribution in the hypothetical multiquark star for the central density  $\rho_0 = 20$  and  $n_s = 0.3$ . The inner (outer) red (dashed-blue) line represents the core (crust) region.

Figure 10 shows the pressure and density distribution within the multiquark star for the case of  $n_s = 0$  for the central density  $\rho_0 = 20$ . Even though the density and pressure decrease rapidly with respect to the radius of the star, they never quite reach zero. It turns out that when the density and pressure reach the critical values where the equation of state changes into the different power-law for small d, the crust region continues for a large fraction of the total radius of the star. This makes the crust mass contribution to the total mass of the star dominant as is shown in Fig. 9.

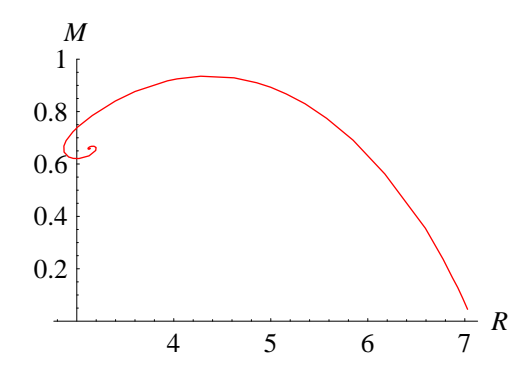
Some remarks should be made regarding the hydrodynamic properties of the multiquark phase (taken as nuclear liquid). At constant temperature and entropy, we can define the adiabatic index

$$\Gamma \equiv \frac{\rho}{P} \frac{\partial P}{\partial \rho},\tag{57}$$

$$= \frac{\rho}{P}c_s^2 \tag{58}$$

where  $c_s$  is the sound speed in the multiquark liquid. They depend on the equation of state of the multiquark and their distributions within the multiquark star are shown in Fig. 11 for  $n_s = 0$ . The sound speed never exceeds the speed of light in vacuum. It is also found that the adiabatic index and the sound speed change within a small fraction as the central densities are varied for a given  $n_s$ .

The multiquark star with  $n_s = 0.3$  (having colour charges) converge to a smaller mass and radius at high central density (Fig. 12). Multiquarks with colour charges has lower pressure (and therefore smaller density) than the colourless ones for small density (Fig. 13). This smaller pressure makes the coloured multiquark star smaller and thus less massive than the colourless one. In more realistic situations, all of the possible multiquarks with varying  $n_s$  coexist in the multiquark phase. The mass limit and mass radius relation will vary between the two typical cases we consider here. Since the equations of state are found NOT to be sensitive to the temperature within the range between the gluon deconfinement and the chiral symmetry restoration, our results should also be valid even when the temperature varies within the star (but not too high and too low, of course).



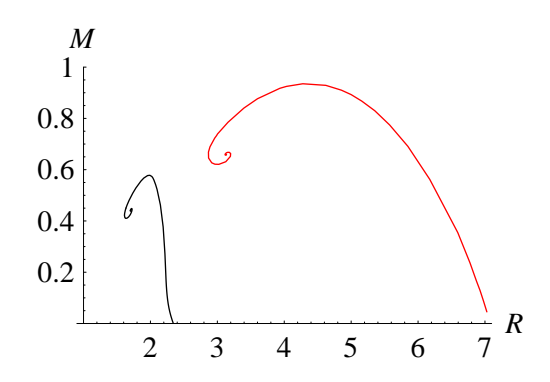
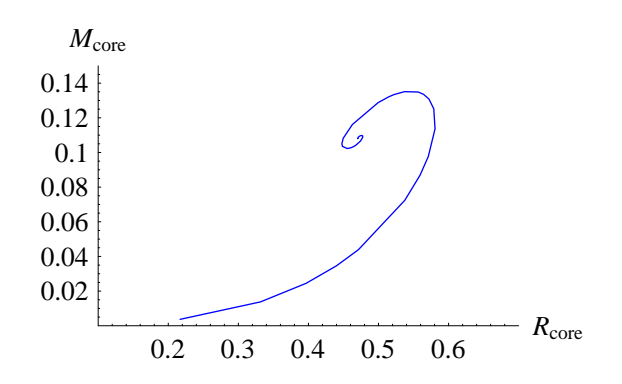


Figure 16: The relation between mass and radius of the multiquark star with (a)  $n_s = 0$ , (b)  $n_s = 0$  (red) and  $n_s = 0.3$  (black).



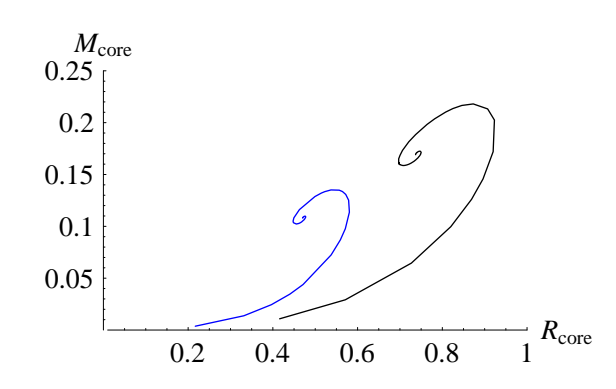


Figure 17: The relation between mass and radius of the core of the multiquark star with (a)  $n_s = 0$ , (b)  $n_s = 0$  (blue) and  $n_s = 0.3$  (black).

The baryon chemical potential distributions in the multiquark star for  $n_s = 0, 0.3$  are shown in Fig. 14. In the core region, the chemical potential distributions of both cases are similar due to the similarity of the equations of state for large density. A small jump of the chemical potential at the transition radius between core and crust region is the artifact from the power-law approximation. The value of the chemical potential at the transition radius from the full expression which we used in the numerical simulations is slightly different from the approximated value using the power-law.

The adiabatic index and sound speed of the multiquark phase for  $n_s = 0.3$  are shown in Fig. 15. The adiabatic index is higher than  $n_s = 0$  case but the sound speed in the low density region is distinctively higher. Around the transition density, the sound speed reaches the maximum value of about 0.986 of the speed of light in vacuum. For both  $n_s = 0, 0.3$  cases, it is obvious that the adiabatic index is closer to 1 in the core reflecting the fact that the density distribution is more condensed in the core region. The adiabatic index reaches  $\lambda' = 2$  at the star surface since the the equation of state at zero density is  $P \propto \rho^{\lambda'}$  (i.e.  $\Gamma(\rho \to 0) = \lambda'$  for Eqn. (50)).

The spiral relation between mass and radius of the multiquark star is shown in Fig. 16. As the central density is increasing, the mass and radius of the  $n_s = 0$  (0.3) multiquark star converge to the value of 0.659 (0.440) and 3.132 (1.704) respectively. For the core, the mass and radius of the core for  $n_s = 0$  (0.3) converge to the value of 0.108 (0.169) and 0.471 (0.737).

Finally, we would like to estimate these limits of mass and radius in the physical units. Since our dimensionless quantities are related to the physical quantities through conversion factors given in Table 1 (Appendix A), both physical mass and radius vary with the energy density of the nuclear matter phase as  $\propto 1/\sqrt{\rm energy}$  density scale. For a multiquark nuclear phase with energy density scale 10 GeV/fm³, the conversion factor of the mass and radius are  $5.91 M_{solar}$  and 8.71 km respectively. This would correspond to the converging mass and radius (in the limit of very large central density) of  $3.89~(2.60) M_{solar}$  and 27.29~(14.85) km for  $n_s = 0~(0.3)$  multiquark star respectively.

In realistic situation, the nuclear phase in the outer region could lose heat out to the space in the form of radiation. The nuclear matter in the outer region of the crust will cool

down and mostly become confined into neutrons and hadrons (e.g. hyperons, pions). This would make the multiquark crust to end at shorter radius than the estimated value and render the multiquark star to be smaller and less massive than the estimated values in the hypothetical prototype. For example, for the energy density scale 10 GeV/fm³, the critical density is  $\rho_c \approx 1.5 \times 10^{18} \text{ kg/m}^3$  ( $n_s = 0$ ). This is still a sufficiently large density for the neutron layer to be formed. If the temperature of the nuclear matter in the crust region falls below the deconfinement temperature, the multiquarks will be confined into extremely dense neutrons and hadrons instead. For a typical neutron star, the distance of the neutron layer out to the star surface is roughly 5-6 km [29]. If we add this number to the radius of the multiquark core,  $0.471 \times 8.71 \simeq 4.10$  km, we end up with a more realistic estimation for the multiquark star with radius  $\sim 10$  km. Regardless of the name, only the core region is in the deconfined multiquark phase and the content of the outer layers are the confined nucleons.

# 6 Discussions and conclusion

In the gluon-deconfined phase of the general Sakai-Sugimoto model, multiquark states can exist in the intermediate temperatures below the chiral symmetry restoration temperature provided that the density is sufficiently large. They are stable and preferred thermodynamically over other phases and thus they can play important role in the physics of compact warm stars. By analytic and numerical methods, we demonstrate that the equation of state of the multiquark nuclear matter can be approximated by two power-laws in the small and large density region. Roughly speaking, the pressure is proportional to  $d^2$  and  $d^{7/5}$  for the small and large number density (d) regions respectively.

It is also found that the effect of the colour charges of the multiquark is to reduce the pressure of the multiquarks when the density is small. At higher densities, multiquarks with colour charges exert slightly larger pressure than the colourless ones. The temperature dependence of the entropy density shows an  $s \propto T^5$  relation and the colour charge dependence  $s_{colour} \propto n_s T$  (see Fig. 6 and Eqn. (39)). This implies that the multiquarks with colour charges have larger entropy but their number of degrees of freedom depend less sensitively on the temperature. Multiquarks in the deconfined phase behave like quasi-particles with the entropy density being less sensitive to the temperature than the gas of mostly free gluons and quarks in the  $\chi_{S}$ -QGP phase.

Using the power-law equations of state for both small and large density regions, a spherically symmetric Einstein field equation is solved to obtain the Tolman-Oppenheimer-Volkoff equation. By solving this equation numerically, we establish the mass, density and pressure distribution of the hypothetical multiquark star. It turns out that the multiquark star is separated into two layers, a core with higher density and a crust with lower density. Mass limit curve is also obtained as well as the mass sequence plot between the mass and radius of the multiquark star. They show typical spiral behaviour of the star sequence plots. The mass limit curve shows two peaks corresponding to the equation of state of the small and the large density. Analyses show that the most contribution to the total mass is mainly

from the crust. The adiabatic index at constant entropy,  $\Gamma$ , and the sound speed,  $c_s$ , of the multiquark nuclear phase within the star are calculated numerically. For large density,  $\Gamma$  is approximately close to 1 and  $c_s$  is roughly within range 0.6-0.7 of the speed of light. For small density,  $\Gamma$  is in the range 1.3-2.0 (2.0-3.0) and  $c_s$  is roughly 0-0.85 (0-0.99) for multiquark with  $n_s=0$  (0.3).

# Acknowledgments

P.B. is supported in part by the Thailand Research Fund (TRF) and the Commission on Higher Education (CHE) under grant MRG5180227. E.H. is supported by the Commission on Higher Education (CHE), Thailand under the program Strategic Scholarships for Frontier Research Network for the Ph.D. Program Thai Doctoral Degree for this research.

# A Dimensional translation table

quantity	dimensionless variable	physical variable
pressure	P	$\frac{c^4}{Gr_0^2}P$
density	ho	$\frac{c^2}{Gr_0^2}\rho$
mass	M	$\frac{r_0c^2}{G}M$
radius	r	$r_0r$

Table 1: Dimensional translation table of relevant physical quantities,  $r_0 \equiv \left(\frac{G\mathcal{N}}{c^4\tau V_3}\right)^{-1/2} = \left(\frac{G}{c^4}(\text{energy density scale})\right)^{-1/2}$ .

# References

- [1] F. Karsch, "Lattice QCD at finite temperature," AIP Conf. Proc. 631 (2003) 112.
- [2] E. V. Shuryak, I. Zahed, "Towards a theory of binary bound states in the quark gluon plasma," *Phys. Rev.* **D70** (2004) 054507, [arXiv:hep-ph/0403127].
- [3] E. V. Shuryak, I. Zahed, "Rethinking the properties of the quark gluon plasma at  $T \sim T_c$ ", Phys. Rev. C70 (2004) 021901, [arXiv:hep-ph/0307267].
- [4] J. Liao, E.V. Shuryak, "Polymer chains and baryons in a strongly coupled quark-gluon plasma," Nuc. Phys. A775 (2006) 224, [arXiv:hep-th/0508035].
- [5] J. M. Maldacena, "The Large N Limit of Superconformal Field Theories and Supergravity," Adv. Theor. Math. Phys. 2 (1998) 231-252 [Int. J. Theor. Phys. 38 (1998) 1113-1133], [arXiv:hep-th/9711200].
- [6] Juan M. Maldacena, "Wilson loops in large N field theories," *Phys. Rev. Lett.* **80** (1998) 4859-4862, [arXiv:hep-th/9803002].
- [7] Soo-Jong Rey, Jung-Tay Yee, "Macroscopic strings as heavy quarks in large N gauge theory and anti-de Sitter supergravity," Eur. Phys. J. C 22 (2001) 379-394, [arXiv:hep-th/9803001].
- [8] Soo-Jong Rey, Stefan Theisen, Jung-Tay Yee, "Wilson-Polyakov loop at finite temperature in large N gauge theory and anti-de Sitter supergravity," *Nucl. Phys.* **B 527** (1998) 171-186, [arXiv:hep-th/9803135].
- [9] E. Witten, "Baryons and Branes in Anti-de Sitter Space," *JHEP* **07** (1998) 006, [arXiv:hep-th/9805112].
- [10] D. J. Gross and H. Ooguri, "Aspects of large N gauge theory dynamics as seen by string theory," Phys. Rev. D58 (1998) 106002, [arXiv:hep-th/9805129].
- [11] A. Brandhuber, N. Itzhaki, J. Sonnenschein and S. Yankielowicz, "Baryon from supergravity," *JHEP* **07** (1998) 046, [arXiv:hep-th/9806158].
- [12] K. Ghoroku, M. Ishihara, A. Nakamura and F. Toyoda, "Multi-Quark Baryons and Color Screening at Finite Temperature," *Phys. Rev.* **D79** (2009) 066009, [arXiv:0806.0195 [hep-th]].
- [13] K. Ghoroku and M. Ishihara, "Baryons with D5 Brane Vertex and k-Quarks States," *Phys. Rev.* **D77** (2008) 086003, [arXiv:0801.4216 [hep-th]].
- [14] M.V. Carlucci, F. Giannuzzi, G. Nardulli, M. Pellicoro and S. Stramaglia, "AdS-QCD quark-antiquark potential, meson spectrum and tetraquarks," *Eur. Phys. J.* C57 (2008) 569, [arXiv:0711.2014 [hep-ph]].

- [15] W-Y. Wen, "Multi-quark potential from AdS/QCD," Int. J. Mod. Phys. A23 (2008) 4533, [arXiv:0708.2123 [hep-th]].
- [16] P. Burikham, A. Chatrabhuti and E. Hirunsirisawat, "Exotic multi-quark states in the deconfined phase from gravity dual models," *JHEP* **05** (2009) 006, [arXiv:0811.0243 [hep-ph]].
- [17] T. Sakai and S. Sugimoto, "Low Energy Hadron Physics in Holographic QCD," *Prog. Theor. Phys.* **113** (2005) 843, [arXiv:hep-th/0412141].
- [18] T. Sakai and S. Sugimoto, "More on a Holographic Dual of QCD," *Prog. Theor. Phys.* **114** (2005) 1083, [arXiv:hep-th/0507073].
- [19] O. Aharony, J. Sonnenschein and S. Yankielowicz, "A Holographic Model of Deconfinement and Chiral Symmetry Restoration," *Annals Phys.* **322** (2007) 1420, [arXiv:hep-th/0604161].
- [20] J.R. Oppenheimer and G.M. Volkoff, "On Massive Neutron Cores," Phys. Rev. 55 (1939) 374, R.C. Tolman, "Static solutions of Einstein's field equations for spheres of fluid," Phys. Rev. 55 (1939) 364.
- [21] Oren Bergman, Gilad Lifschytz, Matthew Lippert, "Holographic Nuclear Physics," *JHEP* **11** (2007) 056, [arXiv:hep-th/0708.0326].
- [22] C. G. Callan, A. Guijosa and K. G. Savvidy, "Baryons and String Creation from the Fivebrane Worldvolume Action," *Nucl. Phys.* B 547 (1999) 127 [arXiv:hep-th/9810092].
- [23] C. G. Callan, A. Guijosa, K. G. Savvidy and O. Tafjord, "Baryons and Flux Tubes in Confining Gauge Theories from Brane Actions," *Nucl. Phys.* B 555 (1999) 183 [arXiv:hep-th/9902197].
- [24] N. Horigome and Y. Tanii, "Holographic chiral phase transition with chemical potential," *JHEP* **01** (2007) 072, [arXiv:hep-th/0608198].
- [25] K. Y. Kim, S. J. Sin and I. Zahed, "Dense hadronic matter in holographic QCD," [arXiv:hep-th/0608046].
- [26] A. Akmal, V.R. Pandharipande, and D.G. Ravenhall, "The equation of state of nucleon matter and neutron star structure", Phys. Rev. C58 (1998) 1804, [arXiv:nucl-th/9804027].
- [27] Keun-Young Kim, Sang-Jin Sin, Ismail Zahed, "The Chiral Model of Sakai-Sugimoto at Finite Baryon Density", *JHEP* **01** (2008) 002, [arXiv:0708.1469 [hep-th]].
- [28] J. de Boer, K. Papadodimas and E. Verlinde, "Holographic Neutron Stars," [arXiv:0907.2695 [hep-th]].
- [29] F. Weber, "Strange Quark Matter and Compact Stars", *Prog. Part. Nucl. Phys.* **54** (2005) 193, [arXiv:astro-ph/0407155].